

POLITECNICO DI TORINO

**CORSO DI LAUREA IN INGEGNERIA ENERGETICA E
NUCLEARE**

TESI DI LAUREA MAGISTRALE



**ANALYSIS OF MARINE CURRENTS
AS RENEWABLE SOURCES**

Relatore

Bracco Giovanni (DIMEAS)

Correlatori

Mattiazzo Giuliana (DIMEAS)

Cervelli Giulia (Docente esterno)

Candidato

Mattia Parodi (244051)

Marzo 2021

Abstract

The world is going towards the decarbonization of the production of energy, developing new technologies for a better exploitation of the existing sources. It leads to explore the renewable ones, such as solar, thermal, wind and even the ocean; first ones have been developed for years, earning a lot of achievements, but the main drawback is their unpredictability and irregularity. The exploitation of the ocean's kinetic energy partially resolves these problems since tidal are much more predictable over longtime scales since they follow the Moon cycle, being caused by gravitational interactions between the Moon itself, the Sun, and the Earth. Furthermore, to harness tidal power it is used the same technology as wind turbines, but with the main advantage of the high-water density compared to the air, which leads to a significant reduction of the blades' size.

The Thesis, after a general introduction about ocean energy, just focuses on marine currents, particularly the state-of-the-art technologies that use this resource: devices, existing machines, operational, maintenance and economical aspects. The Mediterranean Sea situation is then analyzed, to understand its real possibilities of exploitation, with a detailed study of Italian coast. In this respect, a reference mapping is outlined and the energy production of a potential site in a suitably chosen location (Strait of Messina) is estimated, with the addition of a model for a tidal current turbine system. Lastly, a generating machine with predetermined characteristics is analyzed. The goal is to describe and apply a procedure for assessing the energy potential of marine currents to obtain, based on actual marine-weather data available, a replicable methodology that could contribute to further studies.

Contents

List of Figures and Tables

Acronyms

1. Introduction	11
1.1. Energy demand and Ocean energy	11
1.2. Energy availability and Trend of search	12
1.3. Tides as renewable energy	15
1.4. Tidal range.....	16
1.5. Tidal stream.....	18
2. Tidal stream turbines	21
2.1. Classification of tidal stream devices and Existing turbines.....	21
2.1.1. Horizontal Axis Water Turbines (HAWTs).....	21
2.1.2. Vertical Axis Water Turbines (VAWTs).....	22
2.1.3. Oscillating devices	22
2.1.4. Venturi Effect Tidal stream devices	23
2.1.5. Other concepts	23
2.1.6. Floating Tidal turbines	26
2.2. Operations on tidal stream turbines.....	28
2.2.1. Control and Regulation	30
2.2.2. Installation – Foundation	33
2.2.3. Installation – Support structure.....	34
2.2.4. Maintenance.....	39
2.3. Economic aspects	44
2.3.1. Levelized cost of energy	44
2.3.2. Policy support	48
3. Current energy in the Mediterranean Sea	51
3.1. Preliminary considerations	51
3.2. Connection with environmental problems	53
3.3. Coast characterization from the current metric point of view.....	55
4. Energy potential assessment procedure	63
4.1. Reference mapping of energy producibility.....	63
4.2. Fluid dynamic modeling and Energy producibility estimation for the Strait of Messina	69

4.2.1 Modelling and Simulation of Tidal Current Turbine System.....	80
4.3. Numerical analysis procedure for a generating machine	86
5. Conclusions.....	95
6. Matlab scripts	97
7. References.....	103
8. Acknowledgments.....	107

List of Figures and Tables

Figure 1. Market maturity for ocean technologies	12
Figure 2. Patents for tidal devices.....	13
Figure 3. Patents for tidal stream turbines.....	13
Figure 4. Cooperative Patent Classification code evolution for tidal stream turbines.....	13
Figure 5. Patents for country.....	14
Figure 6. Tidal stream resource map based on velocity of currents in Europe [AQUARET]	14
Figure 7. Example time series of diurnal (a) semidiurnal (b) and mixed (c) tides [NOS]	15
Figure 8. World distribution map of tidal range	16
Figure 9. Tidal range technologies.....	17
Figure 10. Diameter comparison between tidal turbine and offshore wind turbine	19
Figure 11. C_p and TSR for different wind turbines a tidal turbine	19
... Figure 12. C_p as a function of TSR for	
Figure 13. Horizontal axis water turbines [AQUARET].....	21
Figure 14. Vertical axis water turbines [AQUARET]	22
Figure 15. Reciprocating device (oscillating hydrofoil) [AQUARET].....	22
Figure 16. Venturi effect tidal stream device [AQUARET].....	23
Figure 17. THAWT [AQUARET].....	23
Figure 18. Tidal kite [AQUARET].....	24
Figure 19. Archimedes helical screw [AQUARET].....	24
Figure 20. Comparison between floating turbine support vessel (Multicat) and seabed-mounted turbine support vessel (the red one)	26
Figure 21. Current velocity profile.....	27
Figure 22. Basic components of tidal stream device [AQUARET]	28
Figure 23. Example of tidal stream energy device power curve, highlighting conditions where no power is generated.....	29
Figure 24. C_p and TSR of horizontal axis turbine.....	29
Figure 25. Profile of a turbine blade.....	30
Figure 26. Pitch regulation of the blade: towards stall (a) and towards feather (b)	31
Figure 27. VSVP control strategy (top) and VSFP control strategies with passive “AEDG” and speed assisted “ABCDGI” (bottom) stall regulation	32

Figure 28. C_p curves for pitch and stall regulated rotors design	32
Figure 29. Power curve for VSFP control strategies with passive “AEDG” and speed assisted “ABCDG1” stall regulation.....	32
Figure 30. Support structure systems (below)	34
Figure 31. Annual O&M cost per kWh in British Columbia (left) and in Northeast of USA (right)...	39
Figure 32. Correlation between TSR and C_P or C_T (left) and between rated power and peak bending moment (right)	40
Figure 33. RPN (Risk Priority Number) related to the different turbine components	41
Figure 34. Direct drive wind turbine (left) compared to geared wind turbine (right)	42
Figure 35. Magnetic gear structure (left) and section (right)	42
Figure 36. Clean current turbine before deploying in 2006 (left) and after removal in 2011 (right).	43
Figure 37. CAPEX and OPEX variation with deployment stage.....	45
Figure 38. LCOE trend related to learning rate.....	45
Figure 39. Expected LCOE reduction	46
Figure 40. Device cost breakdown	46
Figure 41. Summary of market push and pull mechanisms for ocean energy in the EU, based on Carbon Trust deployment scenarios.....	50
Figure 42. FRI-EL SEAPOWER turbine system.....	52
Figure 43. Surface Mediterranean Sea water potential temperature in summer (top) and winter (bottom) [CMEMS].....	56
Figure 44. Mediterranean Sea water potential temperature at sea floor in summer (top) and winter (bottom) [CMEMS].....	57
Figure 45. Mediterranean Sea water salinity in summer (top) and winter (bottom) [CMEMS].....	58
Figure 46. Surface Mediterranean Sea water velocity in summer (top) and winter (bottom) [CMEMS]	60
Figure 47. Italian Seas surface water velocity [CMEMS]	62
Figure 48. Sea surface height above geoid of Italian Seas [CMEMS].....	62
Figure 49. Average specific Power flow [W/m^2] at $Z=3m$ (below)	64
Figure 50. Average annual (03/2019-03/2020) specific Power flow [W/m^2] in Mediterranean Sea ($Z=3m$).....	66
Figure 51. Average annual (03/2019-03/2020) specific Power flow [W/m^2] in Italian Seas ($Z=3m$)	66
Figure 52. Average annual (03/2019-03/2020) specific Power flow [W/m^2] near the coast of Mediterranean Sea ($Z=3m$).....	67

Figure 53. Average annual (03/2019-03/2020) specific Power flow [W/m^2] near the coast of Italian Seas ($Z=3m$)	67
Figure 54. Max value of average annual specific Power flow in Mediterranean Sea for different depth levels	68
Figure 55. Mean total value of average annual specific Power flow in Italian Seas at different depth levels	68
Figure 56. Strait of Messina from satellite [Wikipedia]	69
Figure 57. SIC (blue) and ZPS (light blue) on the coastal area of Reggio Calabria province [RSE]	70
Figure 58. Average annual (03/2019-03/2020) specific Power flow [W/m^2] near the coast of Sicily ($Z=10m$)	71
Figure 59. Bathymetry of SoM [TRITONE]	72
Figure 60. Example of surface flow field and surface elevation in the SoM (winter case) [TRITONE]	73
Figure 61. Example of horizontal (top) and vertical (bottom) sections of the velocity field in the SoM (winter case) [TRITONE]	74
Figure 62. Bathymetry of the study area and position of monitor points [TRITONE]	76
Figure 63. Average annual (2018) specific Power flow [W/m^2] near the coast of Sicily ($Z=10m$)	76
Figure 64. Tidal current energy system	80
Figure 65. Tidal current speed profile for 40 days in Punta Pezzo (top) and Ganzirri (bottom)	81
Figure 66. Simulink model of tidal current turbine	82
Figure 67. Simulink drive train and shaft model	83
Figure 68. Simulink model for PMSG	84
Figure 69. Power and rotor angular speed at tidal current speed $v=1$ m/s	85
Figure 70. Reconstruction of the turbine geometry [Design Modeler, ANSYS from [30]]	88
Figure 71. Representation of the computation domain surface grid [ICEM-CDF, ANSYS from [30]]	89
Figure 72. Example of Pressure field (top) and Velocity field (bottom) for an assigned operating point [CFX, ANSYS from [30]]	92
Figure 73. Example of Pressure field (top) and Velocity field (bottom) for an estimated (optimal) operating point [CFX, ANSYS from [30]]	93

➤ Tables

<i>Table 1: Features and factors comparison between tidal current turbine and offshore wind turbine</i>	<i>20</i>
<i>Table 2: Comparison between existing turbines.....</i>	<i>25</i>
<i>Table 3: LCOE of traditional energy technologies.....</i>	<i>47</i>
<i>Table 4: List of Projects.....</i>	<i>48</i>
<i>Table 5: Existing "pull" mechanisms (first) and existing "push" mechanisms (second)</i>	<i>49</i>
<i>Table 6: Physical parameters for scenario simulation.....</i>	<i>73</i>
<i>Table 7: Results for the hypothetical floating system (first) and for the anchored system (second) from Web-GIS TRITONE.....</i>	<i>77</i>
<i>Table 8. Tidal harmonic components of the main sequence in the Strait of Messina according to ENEL monitoring.....</i>	<i>81</i>

Acronyms

OES – Ocean Energy Systems

RES – Renewable Energy Sources

NOS – National Ocean Service

OTEC – Ocean Thermal Energy Conversion

TST – Tidal Stream Turbine

TSR – Tip Speed Ratio

HAWT – Horizontal Axis Water Turbine

VAWT – Vertical Axis Water Turbine

FSFP – Fixed Speed Fixed Pitch

FSVP – Fixed Speed Variable Pitch

VSFP – Variable Speed Fixed Pitch

VSVP – Variable Speed Variable Pitch

O&M – Operation and Maintenance

LCOE – Levelized Cost of Energy

CAPEX – Capital Expenditure

OPEX – Operating Expense

AEP – Annual Energy Production

RSE – Ricerca Sistema Energetico

CMEMS – Copernicus Marine Environment Monitoring Service

ECMWF – European Centre Medium Weather Forecast

ISPRA – Istituto Superiore Protezione Ricerca Ambientale

GIS – Geographic Information System

SIC – Sito Importanza Comunitaria

ZPS – Zona Protezione Speciale

ORP – Ocean Renewable Power

PMSG – Permanent Magnet Synchronous Generator

1. INTRODUCTION

1.1. ENERGY DEMAND AND OCEAN ENERGY

“Global population is forecast to increase nearly 34% by 2050 to 9.47 billion.

This massive population growth will engender growing energy demand, so efforts to reduce greenhouse gas emissions, particularly CO₂, will continue to move towards a low-carbon global economy.

By the end of 2014, total renewable energy power generation capacity had increased to 1,712 GW, an increase of 8.5% over 2013. This increase came largely from non-hydro renewables – nearly 660 GW in total (an increase of 18% from 2013) – whilst hydro increased by only 3.6% to nearly 1,055 GW. Not surprisingly, increases in wind (51 GW, including 1.5 GW of offshore wind in Europe) and solar PV (40 GW) exceeded new hydro installations (22%) for the year 2014.

The renewable energy market has seen 30 - 40% growth rates in recent years, due to market-creating policies and cost reductions. For the last 6 years, more money has been invested in renewable energy than conventional generation.

Whilst the rate of growth of ocean energy has been slower than forecast over the last 15 years, modelling undertaken for this report indicates that ocean energy may experience similar rates of rapid growth between 2030 and 2050 as offshore wind experienced in the last 20 years.” [1]

“The ocean energy sector provides significant opportunities to contribute to the production of low carbon renewable energy around the world. Utilization of ocean energy resources will contribute to the world’s future sustainable energy supply. Ocean energy will supply electricity, drinking water and other products at competitive prices creating jobs and reducing dependence on fossil fuels. It will reduce the world energy sector’s carbon emissions, whilst minimizing impacts on marine environments.” [2]

The OES Vision for International Deployment of Ocean Energy estimated a global potential to develop 748 GW of ocean energy by 2050 (188 GW in Europe [3]). Deployment of ocean energy can provide significant benefits in terms of jobs and investments. The global carbon savings achieved through the deployment of ocean energy could also be substantial. By 2050 this level of ocean energy deployment could save up to 5.2 billion tons of CO₂.

1.2. ENERGY AVAILABILITY AND TREND OF SEARCH

There are different potential energy resources, which derive from seawater:

- Ocean currents (relatively shallow (< 1 m), slow-moving ($\cong 1$ m/s) and unidirectional)
- Tidal currents and tidal range
- Waves
- Ocean thermal energy
- Salinity gradient

Overall ocean energy resources are vast, far exceeding human demand, although converting them to useful products can be difficult. Technologies to convert these resources into reserves are still in development. Indeed, establishing commercial opportunities to develop these resources involves a complex, competitive balance between the sum of device and installation costs, operational and electricity export costs, and the costs of other forms of energy generation or product supply.

Despite recent progress, no ocean energy technology developed has so far achieved level of technological readiness required to be competitive with other RES.

Among the sources of renewable energy, tidal power has traditionally suffered from relatively high cost and limited availability of sites with sufficiently high tidal ranges or flow velocities, thus constricting its total availability.

However, tidal energy with its features like predictability and the low effect of climate changing on it, has in this contest a great potential, having demonstrated reliability and survivability through extensive testing (during storms or extreme conditions) and operational hours, and having also shown higher design consensus and a more engaged supply chain with respect to the other technologies. Therefore, its market results the most advanced: [4]

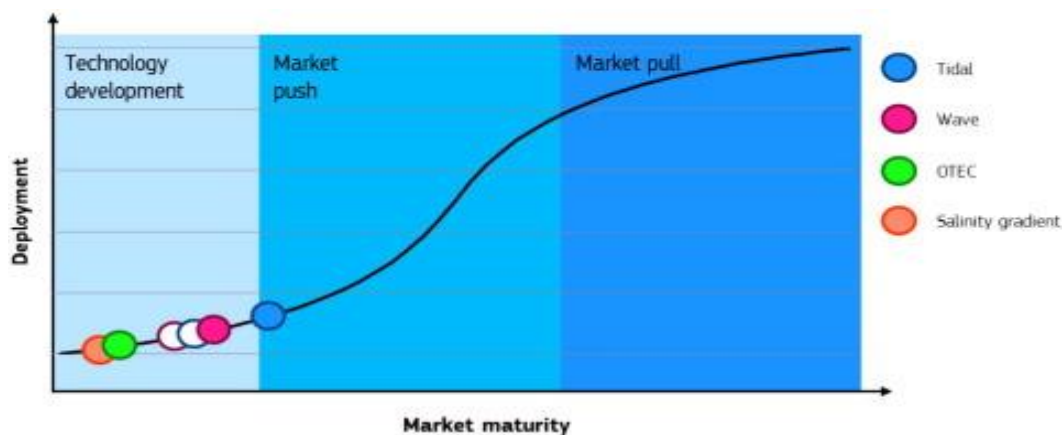


Figure 1. Market maturity for ocean technologies

A patent research through *patentinspiration.com*, in fact, confirms that the more studied technology is the tidal stream, intended as components for tidal devices, even if in the last two years there was a decreased of granted patents.

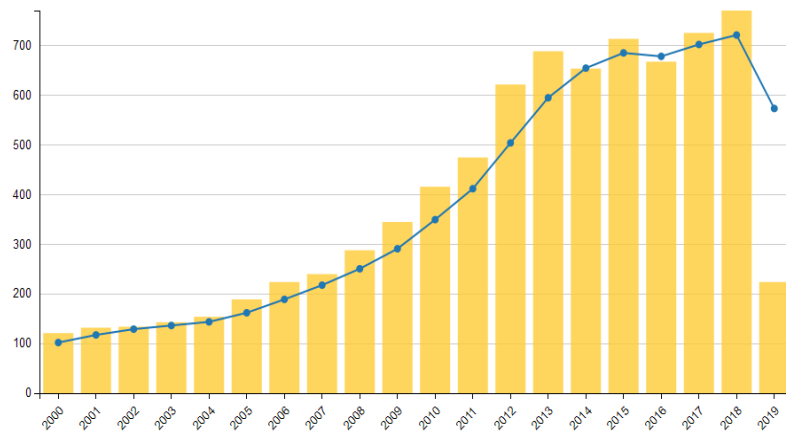


Figure 2. Patents for tidal devices

Focusing on tidal stream turbines, the trend is as follows:

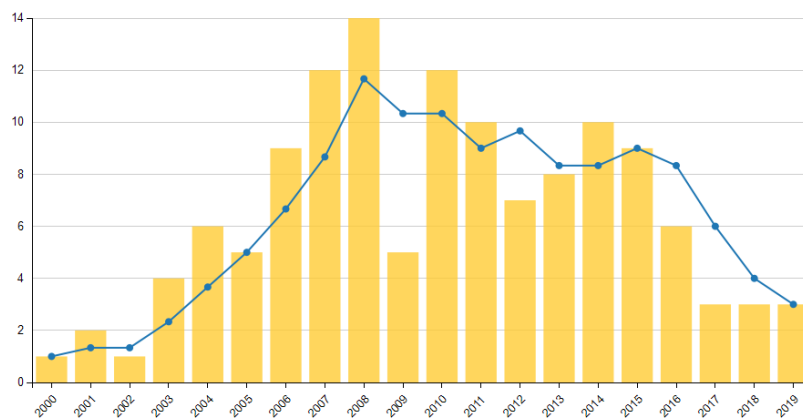


Figure 3. Patents for tidal stream turbines

Moreover, about tidal stream turbines, the most topic of research is the energy conversion.

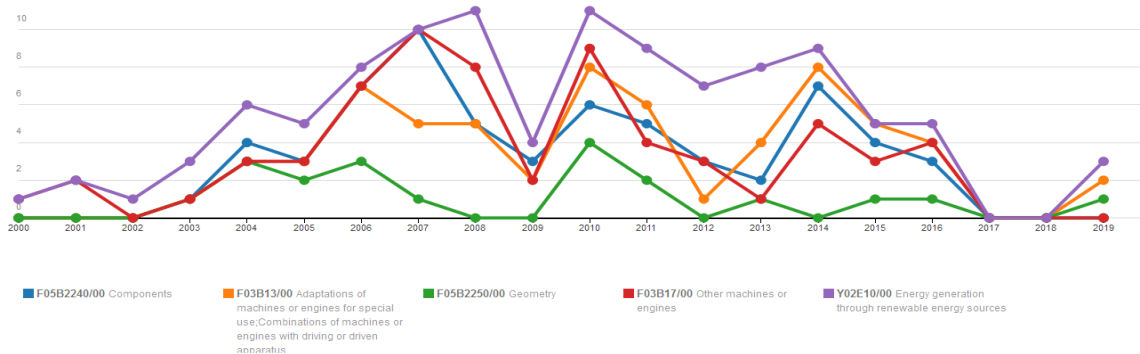


Figure 4. Cooperative Patent Classification code evolution for tidal stream turbines

The major country that granted patents has been the United Kingdom, being one of the countries with the highest level of tide.

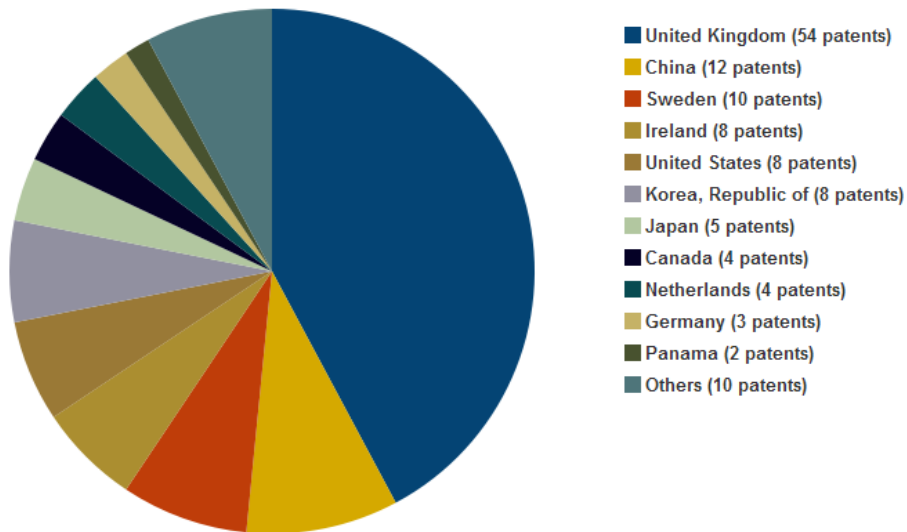


Figure 5. Patents for country

In United Kingdom in fact the assessment of the exploitable energy (both kinetic and potential) is about 50 TWh/year out of the European total of 105 TWh/year, followed by France with a slightly lower quantity. [5] In order to have an idea, the worldwide theoretical power of tidal energy, including both tidal currents and tidal range, has been estimated at around 1200 TWh/year. [1]

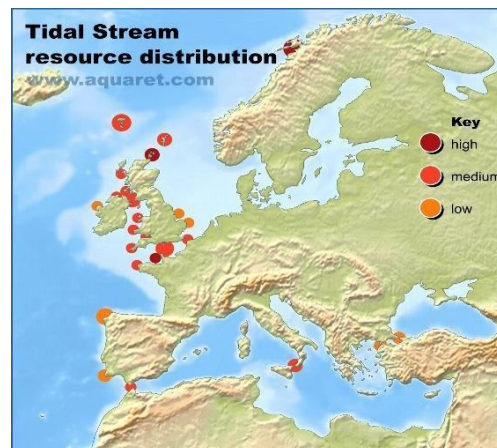


Figure 6. Tidal stream resource map based on velocity of currents in Europe [AQUARET]

1.3. TIDES AS RENEWABLE ENERGY

[6] [7] [8]

Tidal power is the only type of energy which comes directly from the relative motions of the Earth-Moon and Earth-Sun systems. The gravitational interaction forces produced by the Moon and Sun, in combination with Earth's rotation, are responsible for the generation of tides, periodic changes of water levels, and the associated tidal currents. The magnitude of the tide at a given location also depends on the local shape of the sea floor and coastlines. The stronger the tide, either in water level height or tidal current velocities, the greater the potential for tidal energy generation. Because of its nature, tidal power is fundamentally inexhaustible and can be classified as a renewable energy source. Furthermore, thanks to this strong attraction force, tides are independent from weather condition such as clouds, rain or wind and it makes it more predictable and reliable compared to other renewable sources which are threatened by these factors.

Tides have been known since Antiquity, but only with Newton and his theory of gravity that the primary cause of the tide was understood. However, the differences in the tide between regions could not be explained until much later, when Laplace introduced the concept of the tide as a wave propagating over a sea with certain water depths and boundaries (coastlines). As a periodic oscillation, the tide is described as a long wave that propagates over oceans, seas, and estuaries with the usual properties of waves (wavelength and amplitude). The crest or the trough of the wave reaches a particular point, high or low water respectively, so it is possible to classify tides in *diurnal*, if time interval between two consecutive high waters (period of the tide) is approximately 24 h, *semi-diurnal*, if it is 12 h, or *mixed*. The difference in elevation between consecutive high and low water is called tidal range, which varies in space and time. It is never very large in the open ocean, but it can become near shore, particularly in semi-enclosed seas and estuaries, due to resonance and convergence of the land boundaries. The forcing of the Sun and the Moon on the tides is not a constant phenomenon. When these forces work together, or come into phase, the tidal range maximizes and is called a “spring” tide. When the Sun and the Moon forces are out of phase, the tidal range minimizes and is called a “neap” tide. Spring and neap tides also vary depending on the alignment of the Sun, the Moon, and the Earth, with maximum spring tides occurring when the Sun and the Moon are on the same side of the Earth. The spring/neap cycle has a period of near 15 days, creating a fortnightly modification to the principal tides over that period.

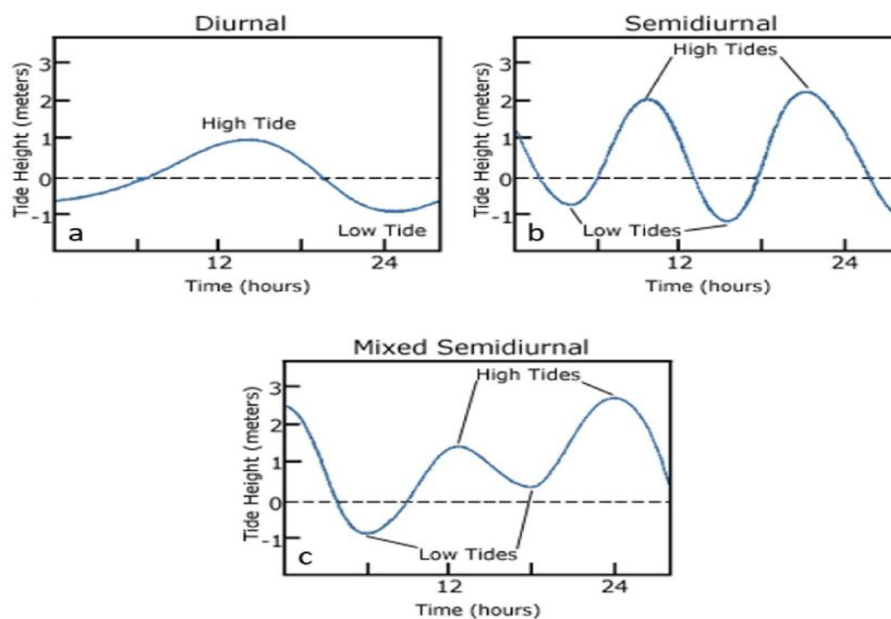


Figure 7. Example time series of diurnal (a) semidiurnal (b) and mixed (c) tides [NOS]

Exploitation of this tidal power can be done essentially in two ways: by constructing a dam-similar facility in high tide areas, employing potential energy with the same principles of hydroelectric power generation, except that tides flow alternatively in both directions, or by extracting power directly from flowing water (kinetic energy), with the same principles of wind turbines.

1.4. TIDAL RANGE

[1] [7]

The effects of tides are complex and most major oceans have internal tidal systems. Whilst the tidal range is not noticeable at sea, it becomes amplified close to shore. The rise and fall of the tide offer the opportunity to trap a high tide, delay its fall behind a barrage or impoundment, and then exhaust the potential energy before the next tidal cycle.

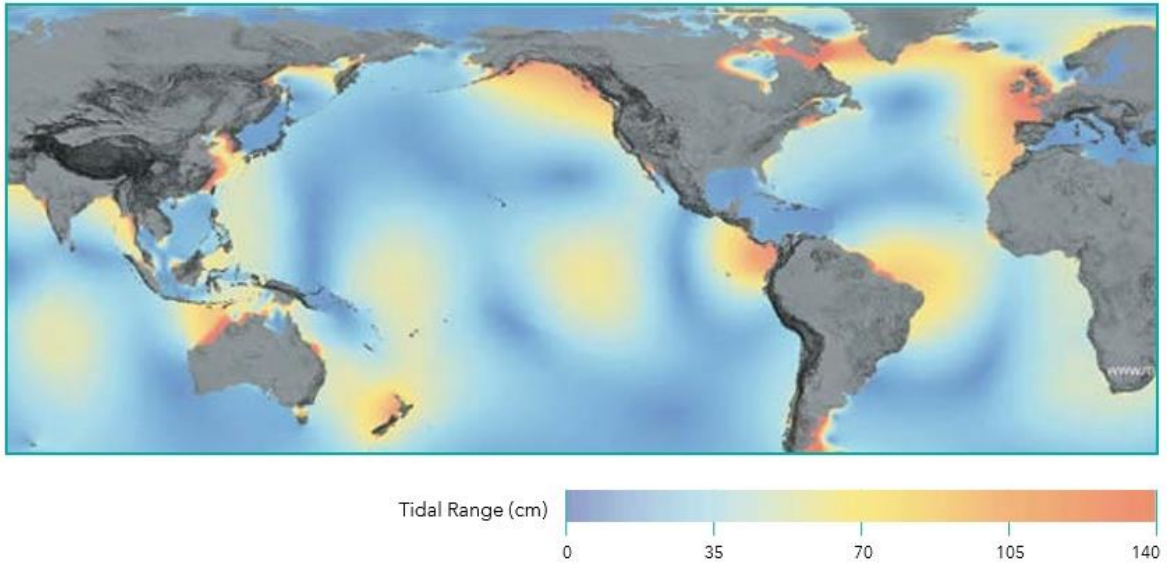


Figure 8. World distribution map of tidal range

Tidal range technologies have been thought for storing a large volume in an area where different level of water is created. Then water is let to flow in or out of this area through a low-head hydroelectric turbine. Tidal range generation uses the potential energy available due to the difference in water depth, defined as:

$$E_p = \frac{1}{2} \rho A g h^2$$

where ρ is the density (kg/m^3), A is the area of the basin (m^2), g is the gravity acceleration (m/s^2), and h is the head (m).

There are two types of civil tidal range systems: barrages and lagoons. These differ in that a barrage creates an impoundment across an estuary, while a lagoon is a standalone impoundment and so can be sited completely offshore. Tidal barrages are effectively conventional hydro dams, deployed in estuarine settings. Tidal impoundments are essentially offshore self-contained dams. Both tidal barrages and tidal impoundments require large capital investments and have been developed with multiple purposes to improve project economics. Presently, tidal range plants are mature technologies, which are being increasingly deployed in Korea and China.

- Estuaries and Enclosed Bays

Tidal barrages across estuaries or enclosed bays utilize mature run-of-river hydro turbines to convert this energy to electricity. In La Rance in northern France a 240 MW tidal barrage has been operational since 1967; in Sihwa Lake in the Republic of Korea has been operating a 254 MW tidal barrage since 2011; other tidal barrage plants of large and small scale have been proposed in Korea, China, Russia, and Ireland, since 2008.

- Lagoons and Impoundments

More recently, artificial tidal lagoons have been proposed, which use multi-chamber impoundments to extend electricity production beyond the diurnal tidal cycle. The impoundments are made from simple rock bunds to enclose a shallow offshore area. These tidal lagoons will utilize existing run-of-river hydro turbines for electricity generation on both flood and ebb tides. A proof-of-concept for a tidal lagoon is under development in Swansea Bay, Wales.



Figure 9. Tidal range technologies

1.5. TIDAL STREAM

[1] [7] [5] [9]

Tidal stream energy results from local regular diurnal or semi-diurnal flows caused by the tidal cycle. Tides cause kinetic movements, current flows, which can be accelerated near coasts, where there is constraining topography, such as straits between islands. The velocity of the flow over the effect of the Sun and the Moon is influenced by the bathymetry and the shape of coastline.

Tidal stream technology began to develop in 1990 and by the beginning of 21st century a huge range of devices are proposed, designed, and tested. In contrast to barrages and tidal lagoons, tidal stream turbines (TSTs) use the kinetic energy of the tide directly, allowing the water to pass through and around them and do not require the storage of water, unlike the impoundment schemes. Much of the fundamental technology associated with TSTs is derived from the wind industry, taking advantage of the medium in which TSTs operate, although it produces higher structural loading, when compared with air driven turbines, with the addition of biological fouling from marine life, possible impact from marine creatures and flotsam, increased material corrosion from salts and the possibility of blade cavitation at shallower water depths.

Tidal turbines are preferably located in shallow areas, where the morphology of seabed and the coastline can increase the velocity of the flow. In some locations the speed of the current is too slow (< 1 m/s), and the energy is too diffuse to be exploited. To allow a sustainable economic project the current must be 2-2,5 m/s otherwise the density of energy will be inadequate. A flow that advances with 2,5 m/s, represents a power flux of 8 kW/m², and it is a speed quite usual in a lot of location.

As said, the tidal energy content is mainly in the form of kinetic energy and it follows the same principles of wind turbines energy extraction. So, according to Betz's Law, it is ruled by the following equation:

$$P = C_p \frac{1}{2} \rho U^3 \pi R^2$$

where C_p , the power coefficient, is estimated to be in the range 0.35-0.45 for marine turbines, instead of the estimated 0.25-0.50 of wind turbines; ρ (kg/m³) is the fluid density, U (m/s) its velocity and R (m) is the blade length.

Just for the sake of comparison, assuming the same power obtained and the same power coefficient, a wind speed of 10 m/s and a water speed of 2.5 m/s (in a good site water speed is around 3 m/s, according to [9]), the blades radius ratio become:

$$\frac{R_{water}}{R_{wind}} = \sqrt{\frac{\rho_{wind} * v_{wind}^3}{\rho_{water} * v_{water}^3}} = 0.277$$

which means a significant reduction of the blade size.

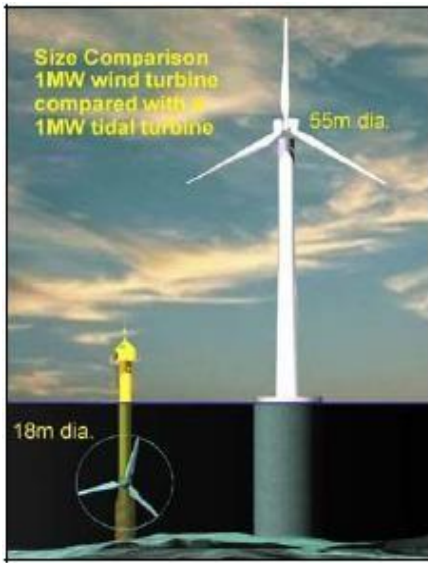


Figure 10. Diameter comparison between tidal turbine and offshore wind turbine

Another analogy with wind turbines is the dependence of C_p with another characteristic parameter, the TSR (Tip Speed Ratio), a function of turbine geometry:

$$TSR = \frac{U_{tip}}{U_0} = \frac{\omega R}{U_0}$$

Where R (m) is the turbine radius, ω (rad/s) is the angular speed of the rotor and U_0 (m/s) is the upstream fluid speed at the entrance of the rotor. The TSR must not be too large to avoid excessive noise or to avoid damage for the excessive speed, but at the same time it must not be too low to avoid lower thrust. Experimentally it is possible to obtain the perfect range for both wind (Figure 11) and tidal (Figure 12) turbines:

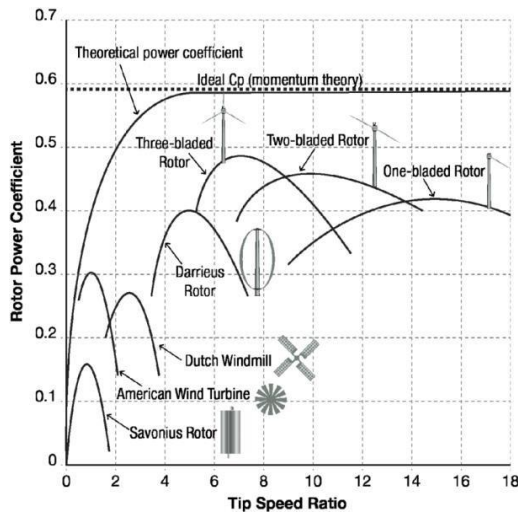


Figure 11. C_p and TSR for different wind turbines

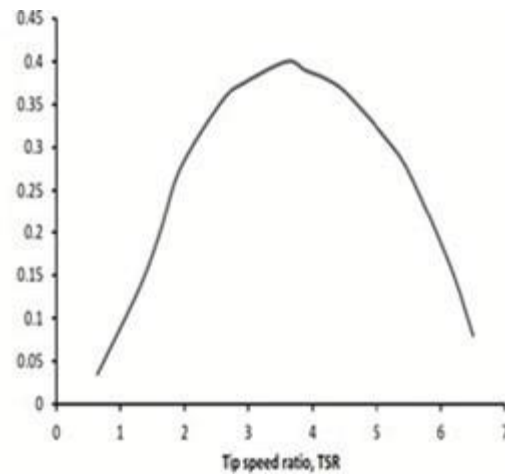


Figure 12. C_p as a function of TSR for a tidal turbine

Figure 12 shows the plot for a tidal turbine with $R = 10$ m and an average water speed of 3.08 m/s. For a three-bladed wind turbine, the better TSR is around 7, meanwhile for the selected tidal turbine, the better TSR is around 3.5. [9]

The main features and factors affecting wind and tidal stream turbines are provided in the table below: [14]

Table 1: Features and factors comparison between tidal current turbine and offshore wind turbine

Feature	Offshore Wind Turbine	Tidal Current Turbine
Fluid density	$\sim 1.25 \text{ kg/m}^3$	$\sim 1025 \text{ kg/m}^3$
Max velocity during normal operation	$\sim 25 \text{ m/s}$	2-5 m/s
Velocity for rated output	$\sim 12 \text{ m/s}$	2-5 m/s
Max velocity during life	50 m/s +	As for normal operation
Variation of velocity with time	Stochastic, variable in magnitude and direction over timescales of the order of seconds to years	Variation in magnitude and direction predictable for given location over period of years
Rotor diameter (typical)	90-120 m	15-30 m based on current design
Limitations on rotor diameter	Mechanical integrity, primarily fatigue life due to self-weight stressed	Mechanical integrity, cavitation at tip, water depth. Speed reduced as diameter increased. Limitation is on blade stress, primarily due to thrust forces being much greater resulting from higher density of fluid
Variation of flow pattern	Complex (turbulence)	Complex (turbulence + waves if top of rotor near surface)
Corrosion	Salt spray conditions	Immersion in salt water will require careful consideration of material combinations
Erosion	Unlikely to be a serious problem	Potential for serious problem; may exacerbate corrosion
Maintenance access	Weather dependent	Depends on deployment method but probably more difficult than offshore wind
Marine growth	Not an issue	Could be important for performance and maintenance
Rotor rotational speed	$< 15 \text{ rpm}$ for large machines	7-20 rpm based on current design

2. TIDAL STREAM TURBINES

2.1. CLASSIFICATION OF TIDAL STREAM DEVICES AND EXISTING TURBINES

[1] [7] [10] [14]

Tidal current devices convert the kinetic energy of a moving water current, into the motion of a mechanical system, which can then drive a generator.

Although there are several devices under development, most designs can be categorized based on whether they produce a rotational or linear motion, the direction of the rotational axis or linear motion and the inclusion of any flow acceleration mechanism.

Devices are generally small (<1 MW), modular and intended for deployment in multi-unit arrays for utility-scale generation and may be seabed mounted or floating. The main categories into which most devices fall are therefore horizontal-axis tidal turbines (HAWTs), vertical-axis tidal turbines (VAWTs), venturi effect devices and oscillating hydrofoils, though other novel concepts can be found.

2.1.1. Horizontal Axis Water Turbines (HAWTs)

These kinds of turbines have the axis parallel to the current flow; they work with the same principles and they are designed in the same way as conventional wind turbines. There could be a different number of blades, usually 2 or 3, noticing that the higher are the number of blades, higher is the thrust, but also higher are the hydrodynamical losses (there is a correlation between the number of blades, the TSR, and consequently the C_p as seen in *Figure 11* and *Figure 12*). Blades could have a fixed or variable pitch angle. The kinetic motion of the water current creates lift on the blades, causing the rotor to rotate and produce power.

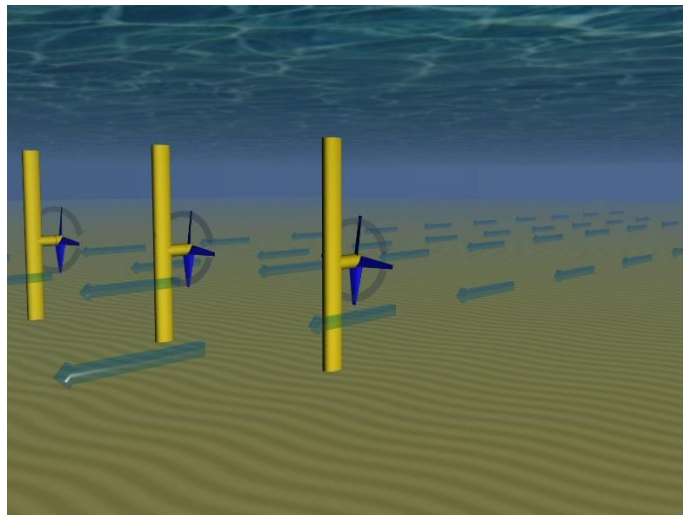


Figure 13. Horizontal axis water turbines [AQUARET]

2.1.2. Vertical Axis Water Turbines (VAWTs)

Vertical axis turbines that operate in marine currents are based on the same principles as the land Darrieus turbine, where the axis and fluid stream are at right angles. They work like horizontal axis turbines only with a different direction of rotation. The blades, which can be helical or straight, run along a cylindrical surface and due to the axial symmetry, develop a unidirectional rotation, regardless of the current direction. The use of a vertically oriented rotor allows to place electric components out of the water, making VAWTs particularly suitable for floating use, and the torque can be transmitted without the use of complex transmission systems.

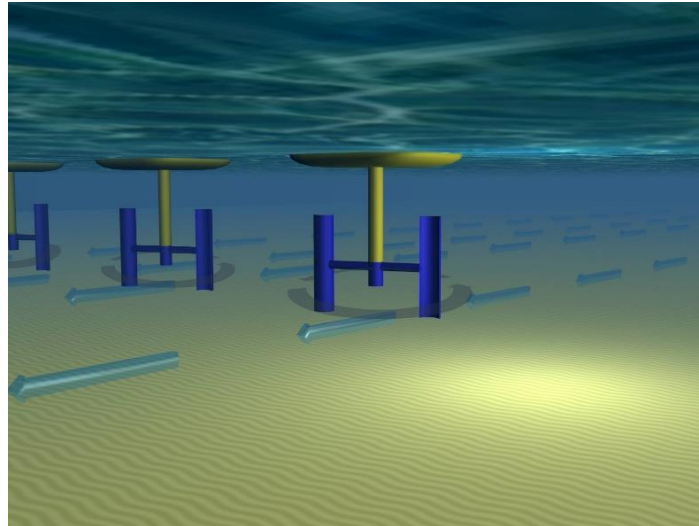


Figure 14. Vertical axis water turbines [AQUARET]

2.1.3. Oscillating devices

These devices have a hydrofoil that can move up and down in the plane orthogonal at the flow, instead of rotating blades. The oscillation motion is due to the lift force generated by current that passes through the hydrofoil on either side. It is used to produce energy by a hydraulic motor and a generator connected with the wing through a hydraulic circuit.

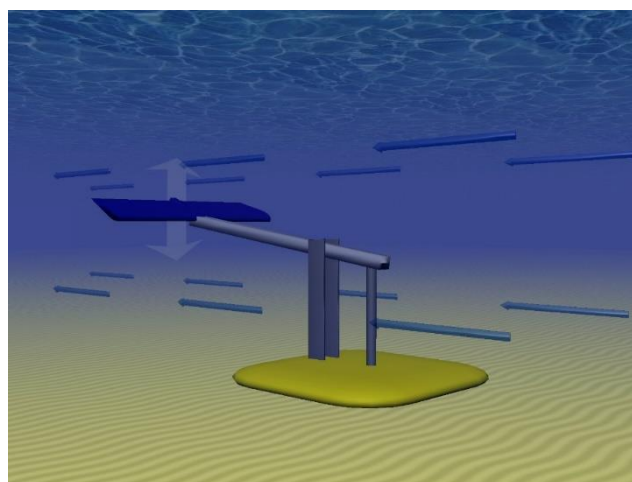


Figure 15. Reciprocating device (oscillating hydrofoil) [AQUARET]

2.1.4. Venturi Effect Tidal stream devices

The tidal stream is directed through a duct; it concentrates the flow and produces a pressure difference which causes a secondary fluid flow. The resultant flow can drive a turbine directly, otherwise the induced differential pressure in the system can drive an air-turbine.

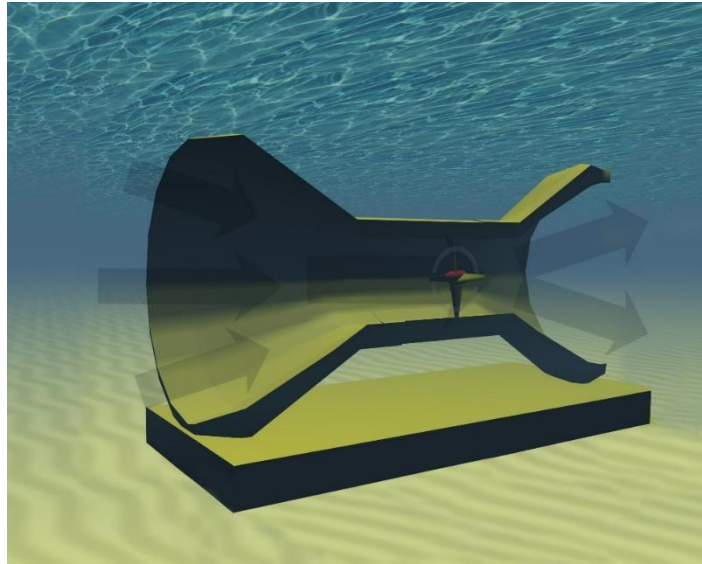


Figure 16. Venturi effect tidal stream device [AQUARET]

2.1.5. Other concepts

Some tidal stream devices, which are currently being developed and tested, use a unique technology or design, so cannot be placed into any of the previous categories. Between them, the crossflow turbines characterized by a cylindrical rotor, usually horizontal with a central axis transverse to the current direction (Transverse horizontal axis water turbine, THAWT), supported by two concrete posts at either ends. They can operate in both directions and even at very low current speeds (0,8 m/s).

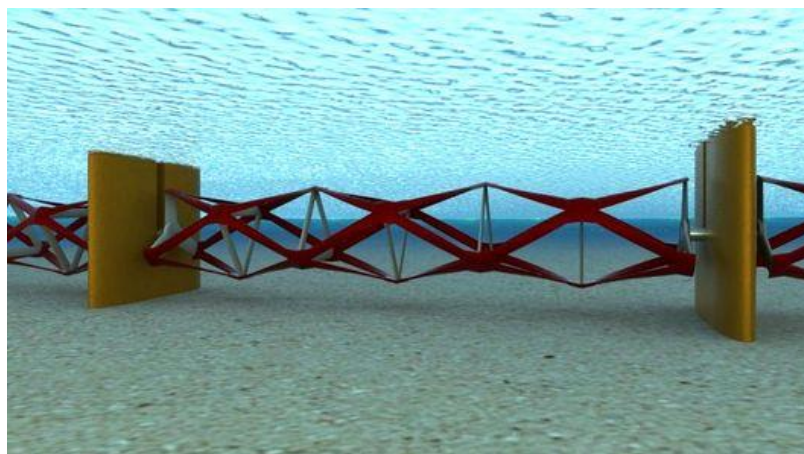


Figure 17. THAWT [AQUARET]

Another one is the Tidal Kite, which is tethered to the seabed and carries a turbine below the wing. The kite “flies” in the tidal stream, swooping in figure-of-eight shape to increase the speed of the water flowing through the turbine. In Italy, a prototype with a production capacity of 200 kW (*GEM*) was tested at sea in the Venetian lagoon as part of a regional project.

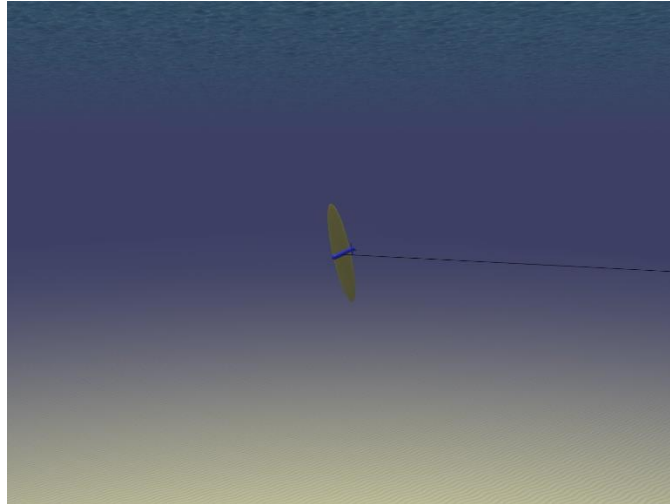


Figure 18. Tidal kite [AQUARET]

In the end, the Archimedes Screw, a helical corkscrew-shaped device (a helical surface surrounding a central cylindrical shaft) that draws power from the tidal stream as the water moves up/through the spiral turning the turbines.

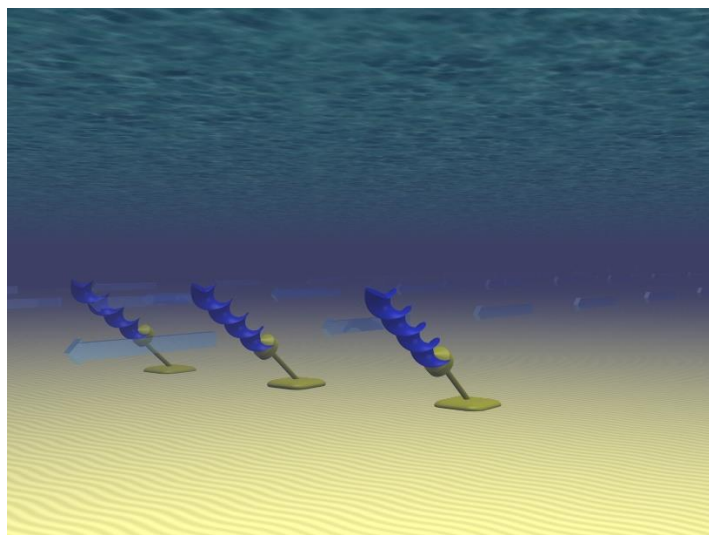

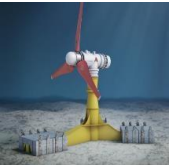
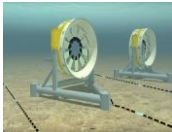




Figure 19. Archimedes helical screw [AQUARET]

Table 2: Comparison between existing turbines

Device <i>Company</i> Site of deployment	Illustration	Rated Power [11]	Axis (rotor)	Main features	Operational years [12]
SeaGen <i>MCT Ltd</i> Strangford Lough (Northern Ireland)		2 x 600 kW at 2.4 m/s	Horizontal (D = 20m)	<ul style="list-style-type: none"> - Raiseable rotors - Pinned to seabed - Full span pitch control 	2008 – 2016
AR1500 <i>SIMEC Atlantis Resources</i> Pentland Firth (UK - Scotland)		1.5 MW at 3 m/s	Horizontal (D = 18m)	<ul style="list-style-type: none"> - Removable rotor - Gravity based - Full span pitch control - Triple redundancy of key systems 	2016 – still operating
Open Hydro <i>OpenHydro Ltd</i> FORCE (Canada)		2 MW	Horizontal (D = 15m)	<ul style="list-style-type: none"> - Gravity based - Ducted and open center - Includes direct-drive generator in the shell 	2016 – 2018

Kobold <i>Ponte di Archimede S.p.A.</i> Strait of Messina (Italy)		30 kW at 2 m/s	Vertical (D = 6m, H = 5m)	<ul style="list-style-type: none"> - Buoyant - Moored to seabed - Electric components above sea level 	2001 – 2005
SR2000 <i>Scotrenewables Ltd</i> EMEC (UK - Scotland)		2 x 1 MW	Horizontal (D = 16m, L = 64m)	<ul style="list-style-type: none"> - Buoyant - Moored to seabed - Electric components above sea level - 360° self-adjustable - Blades with fixed pitch 	2016 – 2018

2.1.6. Floating Tidal turbines

[13]

SR2000 is a floating tidal turbine. These kinds of turbines, despite they could be both HAWT and VAWT, deserve to be treated on their own, not because of the rotor characteristics, but for their support structure. Their main feature consists in the simplified maintenance operations due to the simple accessibility to the electric components which are above the sea surface and workers can be easily carried there by a support vessel. Furthermore, construction and posing require less effort, also in terms of costs, because there is no need of heavy and special lift vessel to bring and install turbines offshore.

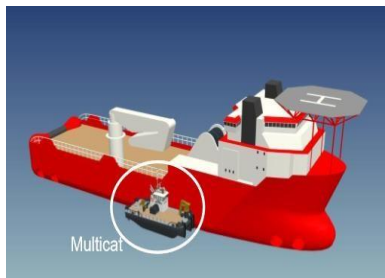


Figure 20. Comparison between floating turbine support vessel (*Multicat*) and seabed-mounted turbine support vessel (the red one)

Another advantageous point comes from the analysis of the underwater tides, because as can be seen in *Figure 21*, the underwater current profile shows the presence of a boundary layer that reduces water speed close to the seabed, where other turbines work. The use of a shallow turbine allows to harness the most powerful part of the current, allowing floating systems to capture almost twice as much energy as seabed-mounted devices with the same rotor size.

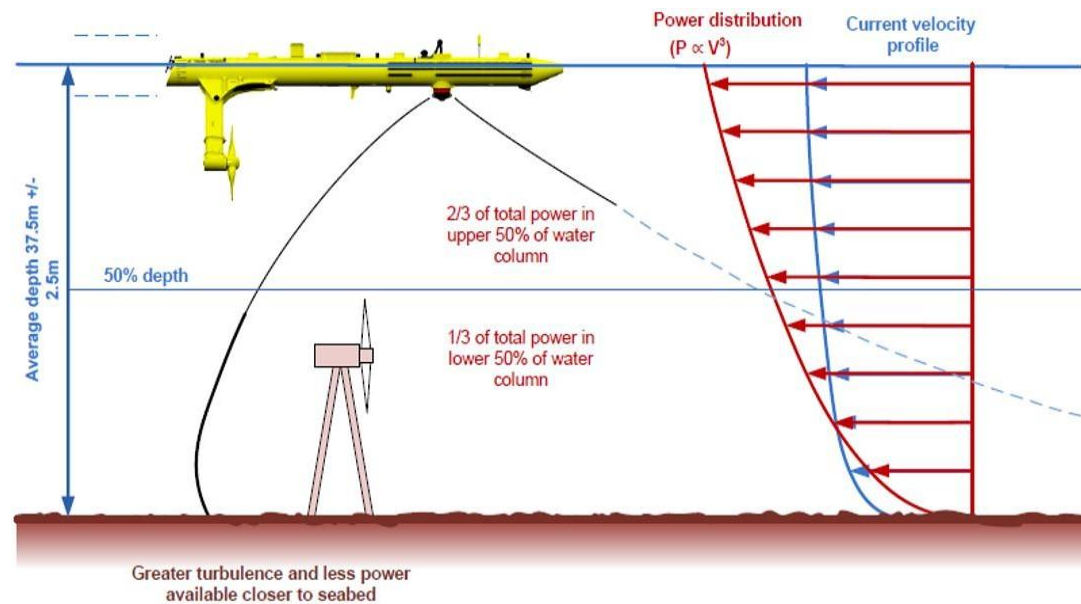


Figure 21. Current velocity profile

2.2. OPERATIONS ON TIDAL STREAM TURBINES

[14]

The main components of a tidal stream energy converter are four:

1. The prime mover which extracts the energy from the flow (rotor)
2. The foundation which holds the prime mover to the seabed
3. The power train (gearbox and generator)
4. The power take-off system (power electrical and control system, and submarine cable to onshore grid connection point)

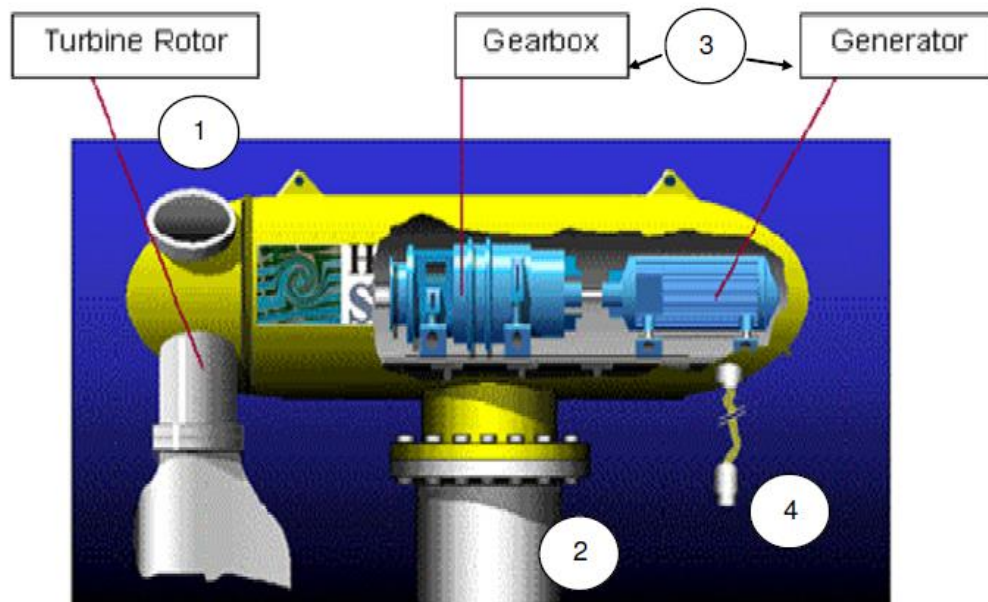


Figure 22. Basic components of tidal stream device [AQUARET]

The turbine rotor, driven by the current, converts the energy of the stream into rotational energy of the shaft with the optimization of the power by adjusting the angle between the rotor blades and the current.

The gearbox converts the low rotational speed of the turbine shaft to the higher speed of the generator shaft, while the generator converts its shaft energy to electric energy which is transmitted to the shore by a cable on the seabed.

Like in wind power, there are practical limits to the amount of power that can be extracted from tidal streams. Some of these limits relate to the design of tidal stream devices and other characteristics of the resource. A real tidal stream device cannot capture all the power in the stream cross-section that it intersects because there are certain conditions under which they cannot operate and, consequently, no power is generated, as can be seen in *Figure 23*.

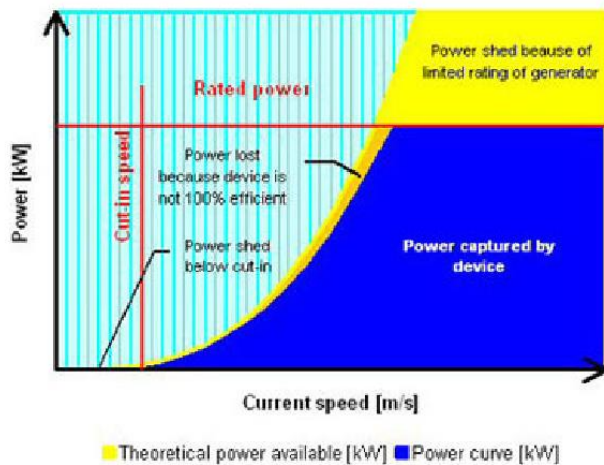


Figure 23. Example of tidal stream energy device power curve, highlighting conditions where no power is generated

The physical limit is represented by the Betz limit that is independent of the device's ability to convert the tidal stream energy into electricity. Its value is estimated at 0,593, so only 59% of tidal power can be educe from an unconstrained free-stream flow. In the real machine the rate of power is lower because of viscous effect on the blade, mechanical losses in the gearbox and electric dissipation.

In operation, performance is influenced by rotational speed of the rotor due to either the blades rotate too slow and the majority of flow pass without interfering with them or too quickly so that the turbulence generated by one bleed moves the following blade. Therefore C_p , the power or performance coefficient already introduced, is a function of rotational speed and its maximum occurs for a certain value of λ (TSR). If a turbine could operate at a fixed tip speed ratio, then the power produced would be constant; the choice would be a λ that gave a constant maximum C_p , but in practice this is not possible because it requires the tip speed and angular velocity to change proportionally over the entire range with free stream velocity.

Furthermore, it is not suitable to let the rotor turn very fast since this would mean that the blades are subjected to large forces, and the likelihood of structural failure (or the costs of avoiding it) would increase. Speed of rotation also affects the blades' energy capture performance because each blade experiences drag due to the pressure difference across it. In addition, at moderately fast speed, it is possible that cavitation occurs, so the bleads surface is damaged, and their efficiency decreases.

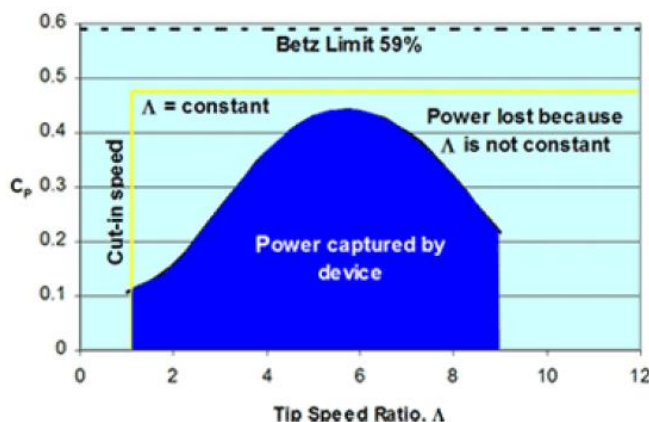


Figure 24. C_p and TSR of horizontal axis turbine

2.2.1. Control and Regulation

[15] [16]

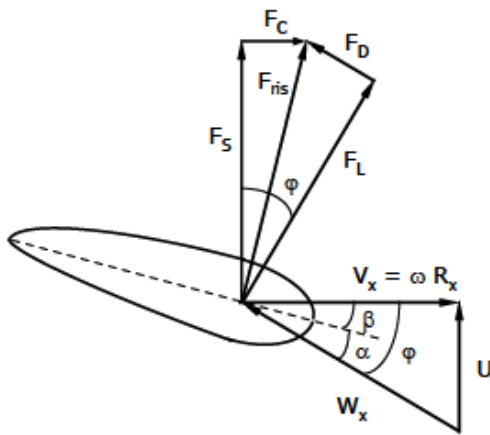
Despite the constraints mentioned above, there is scope for generating power close to the maximum C_p over a range of stream velocity by varying the blades' pitches (*feathering*). In this way the control of the blades' aerodynamic efficiency is possible.

Below the rated speed, the objective is to generate as much power as possible and allows the aerodynamic efficiency to be maintained as the free-stream velocity changes; above the rated speed, pitch control can be used to shed power and control the forces experienced by the rotor.

An alternative power control strategy is passive stall, whereby fixed-pitch blades are designed so that when a certain free stream speed is achieved, a region of turbulence created behind the blades overcomes the lift force and causes the rotor to slow. Although rotor efficiency is best maintained by varying the rotational speed, the opposite may be true for generation efficiency, since constant rotational speed is most straightforward to generate at constant voltage and frequency.

There are four basic methods that use these kinds of regulation:

- Fixed Speed Fixed Pitch



$$F_L = \frac{1}{2} C_L \rho A W^2; \quad F_D = \frac{1}{2} C_D \rho A W^2;$$

$$F_C = F_L \sin \phi - F_D \cos \phi; \quad F_S = F_L \cos \phi + F_D \sin \phi;$$

Here the forces applied on the blades; F_c is responsible for rotation, the torque component, while F_s is the thrust force. The equations show that forces are linked with the current speed and a coefficient; in the FSFP the angle of attack, ϕ , is very important to calibrate because it affects the stall condition: in fact, with a right angle, when the speed of the stream increase the torque component decreases.

Figure 25. Profile of a turbine blade

The FSFP is the easiest strategy for the control of a tidal stream turbine and allows not to overcome the maximum speed that the blades can endure (cavitation could occur, or the generator could go in over-spinning). The exceeding of the nominal value of the velocity U , produces, with the same pitch of the blades, a corresponding increase in both the angle β and the angle α which brings the blade towards the stall, with a consequent decrease in lift and power coefficient. This type of adjustment is inexpensive from the point of view of the turbine equipment but causes considerable stress to the structure due to the high thrust on the blades and on the tower.

- Fixed Speed Variable Pitch

Using the same principle, but reducing the thrust on the blades, the power regulation implemented with the active stall works (*Figure 26 (a)*): it is necessary to equip the blades with a rotation system around their axis. This system allows you to have optimal angles, below the nominal speed, and to bring the blade promptly and heavily into stall reducing the angle β , above the nominal speed. Without prejudice to the rotation system of the blade, but by acting in the direction of increasing the angle β , the control towards setting the flag behaves: this last method involves a variation of the angle greater than the previous one and therefore it is slower, but it allows to reduce to a minimum both the thrust on the blades, making the lift decrease (a decreases), and the stresses on the tower, as shown in *Figure 26 (b)*.

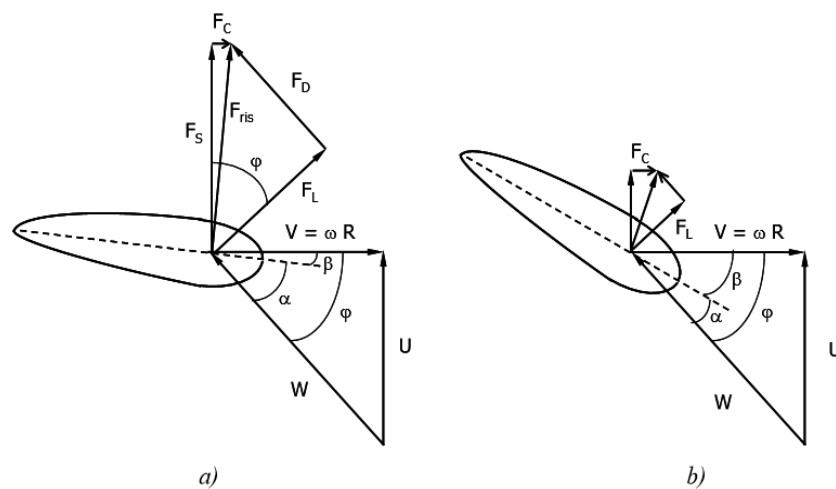


Figure 26. Pitch regulation of the blade: towards stall (a) and towards feather (b)

- Variable Speed Fixed Pitch

This type of control is possible only if the generator is not directly linked with the grid. Since the grid imposes the frequency of generation, consequently also the torque characteristic is imposed, and the speed of rotors would be constant. Often it is utilized a full power converter to allow the regulation of the generator. It is possible to shift the torque characteristic to control the speed of rotor, for instance tracking the optimum speed for increasing the energy capture. If variable speed occurs only below the rated speed, it is regulated with passive stall and it works like a FSFP turbine above rated speed. On the other hand, there is speed assisted stall and the regulation is made throughout operational zone.

- Variable Speed Variable Pitch

This method joins the variable speed and variable pitch, *pitch to feather* and *pitch to stall* are both possible. It is designed to work like variable speed and fixed pitch at rated power and like variable pitch above it.

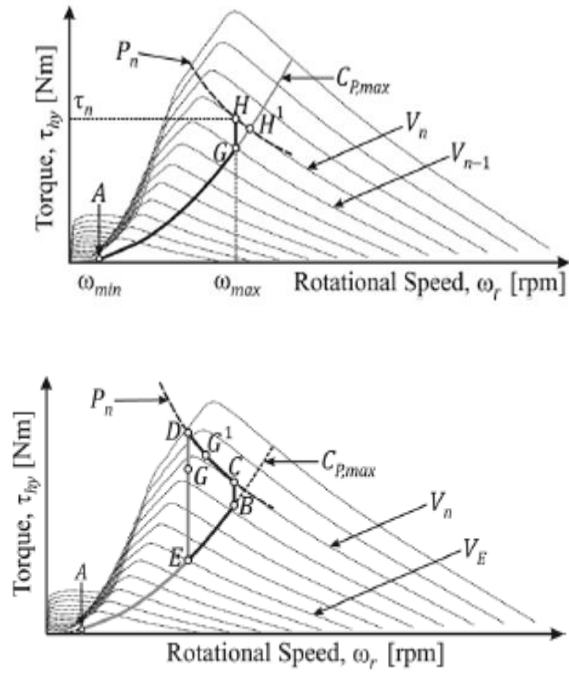


Figure 27. VSP control strategy (top) and VSFP control strategies with passive “AEDG” and speed assisted “ABCDG1” (bottom) stall regulation

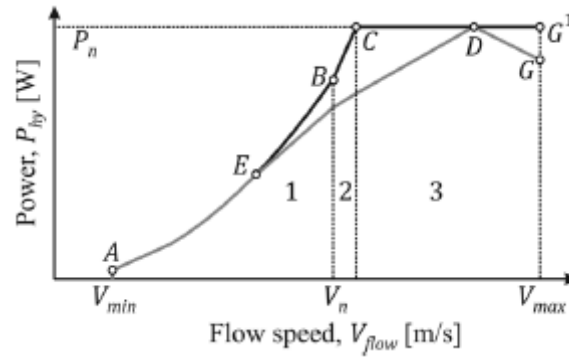


Figure 28. C_p curves for pitch and stall regulated rotors design

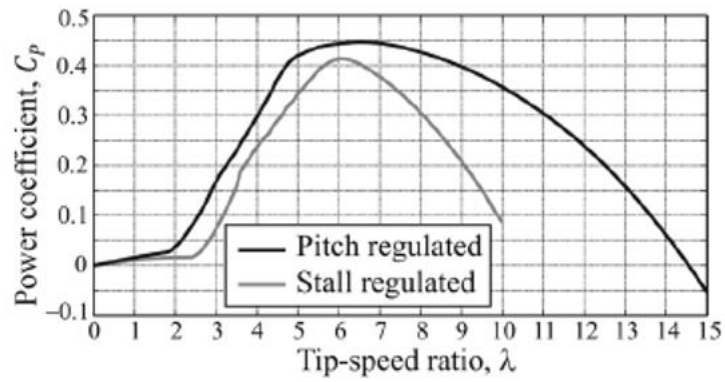


Figure 29. Power curve for VSFP control strategies with passive “AEDG” and speed assisted “ABCDG1” stall regulation

Beyond the analysis of the turbine's structure, its kind or its efficiency, there are other questions that require relevant studies and models because they largely affect the feasibility of the project. Due to their location, marine current turbines are threatened by sea conditions because they are more subject to damages, and even the maintenance and fix operations are complex.

2.2.2. Installation – Foundation

[17]

After the evaluation of a selected site, it must be considered the cost and feasibility of the turbine's installation since this is one of the most expensive parts of the project because it requires to work in both deep and fast flowing water. The best period to install the turbine is the one with lack of tidal current, during its inversion from ebbing to flowing or vice versa.

Anchoring the structure to seabed is made essentially in three ways, each with its own pros and cons, and it depends on the location and turbine characteristics.

- a) *Gravity-based structure*: a large mass of steel and concrete is leaning on the seabed and holds the turbine thanks to the force of gravity. Usually, the nacelle is connected to the base mass with a hollow steel tube filled with concrete. This solution has a small environmental impact because the whole structure can be fully removed during decommissioning, but on the other side, it involves the displacement of large vessels and cranes both in installation and removal operations. The *Atlantis Resources' AR-1500* placed in Pentland Firth uses this kind of technology, being held in place by three concrete masses.
- b) *Piled structure* using poles: a large hole is drilled for every of them, a steel pole is positioned inside and then the outer annular section is filled with concrete. Albeit this is a more stable solution than the pins' one, it has a more significant environmental impact because during decommissioning the poles are cut about half a meter under seabed and left in site. An example of this anchorage system is the *MCT's SeaGen* [18], which involved a marine Jack-up to complete installation operations and drill the single 4m diameter and 23m deep hole that keeps the structure in place.
- c) *Floating structure*: it involves the use of chains or wires to moor the structure to the seabed. This one is the cheaper method because it requires less materials and allows the turbine to self-adjust its direction with the current flow. Having the perfect angle between the current and turbine direction makes it more efficient because it minimizes hydrodynamical losses, maximizing energy extraction, and decreases vibrations, which reduces the turbine's requirement of maintenance. Furthermore, floating turbines can be towed on place from support vessel instead of being lifted by large cranes. Main drawback of this technology is the requirement of maintenance of mooring wires since they are more prone to corrosion; moreover, floating turbines are threatened by waves, limiting their installation to sites with strong tidal currents but not so strong waves. *Kobold* turbine and *SR2000* are two examples of this anchoring system.

2.2.3. Installation – Support structure

[19]

The support structure of tidal turbines is the component that allows the nacelle to be connected to the foundation, securing it to the seabed; it is mainly used to transmit the loads that insist on the rotor to the base to offer enough stiffness. Costs of the structure come essentially from the materials needed for construction, from maintenance requests and from the preparation of the seabed.

In terms of capital expenditures, often the structures that require less materials for construction are the ones that have the most expensive maintenance operations hence an accurate evaluation must be done before choosing one option. By the way, the decision of the structure is influenced by many other factors, such as the depth, the strength of the currents and the visual impact on the surrounding environment.

Below a short comparison of existing technologies is proposed.

Figure 30. Support structure systems (below)

- Telescopic structure system

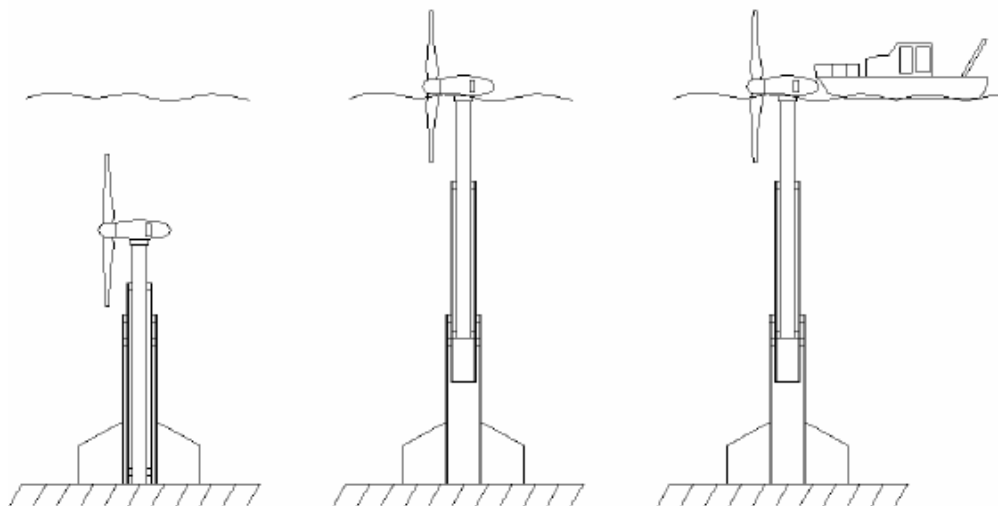


Figure 30(a). Telescopic structure system

Advantages & Disadvantages

<ul style="list-style-type: none"> - Section extended due nacelle's buoyancy - Fixed structure reduces bearings loads - Maintenance done out of the water reducing overall costs - No subject to wave impact and load - No visual impact - Divers should not be needed 	<ul style="list-style-type: none"> - High material requirement, hence, elevate costs, especially at high depth - Telescopic joints are complex and subject to failures - Raised structure must resist to wave loadings remaining stiff - Exposed to marine growth - Yawing and pitching mechanism required
--	---

- *Sheath system*

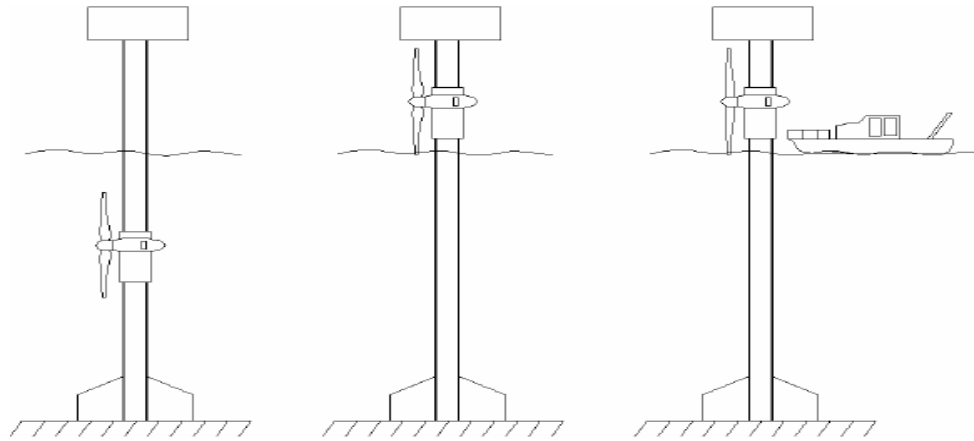


Figure 30(b). Sheath system

Advantages & Disadvantages

<ul style="list-style-type: none"> - Nacelle is mechanically moved out of the water for maintenance - Fixed structure reduces bearings loads - Electrical components are above sea level so low sealing requirements - Divers should not be needed 	<ul style="list-style-type: none"> - High material requirement, hence, elevate costs, especially at high depth - Risk of ship collisions - Exposed to marine growth - Yawing and pitching mechanism required - Subject to wave and wind loads and corrosion - Visual impact on surrounding environment
--	--

- *Top mounted nacelle system*

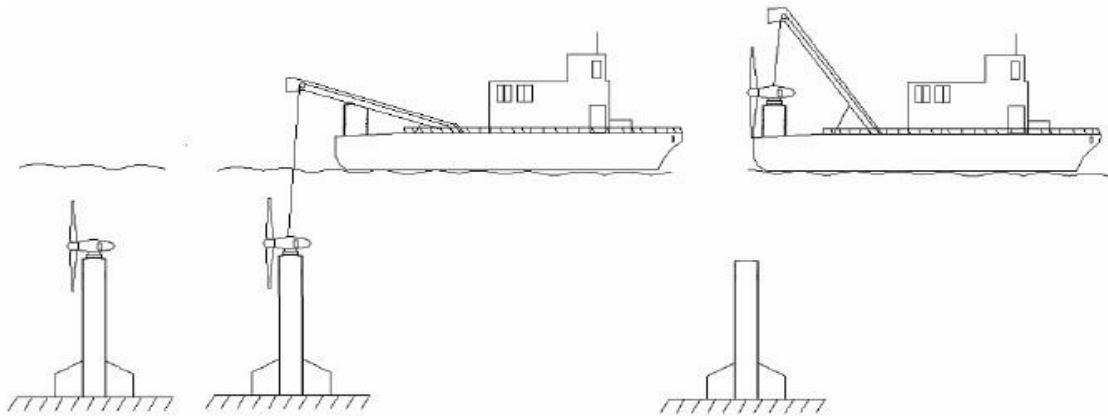


Figure 30(c). Top mounted nacelle system

Advantages & Disadvantages

- | | |
|---|--|
| <ul style="list-style-type: none"> - Fixed structure reduces bearings loads - No subject to wave and wind impact and corrosion - No visual impact - Tolerance for deeper waters | <ul style="list-style-type: none"> - High material requirement, but less than Sheath or Telescopic - Exposed to marine growth - Yawing and pitching mechanism required - Divers could be required - Nacelle must be removed even for smaller maintenance operations |
|---|--|

- *Anchored system*

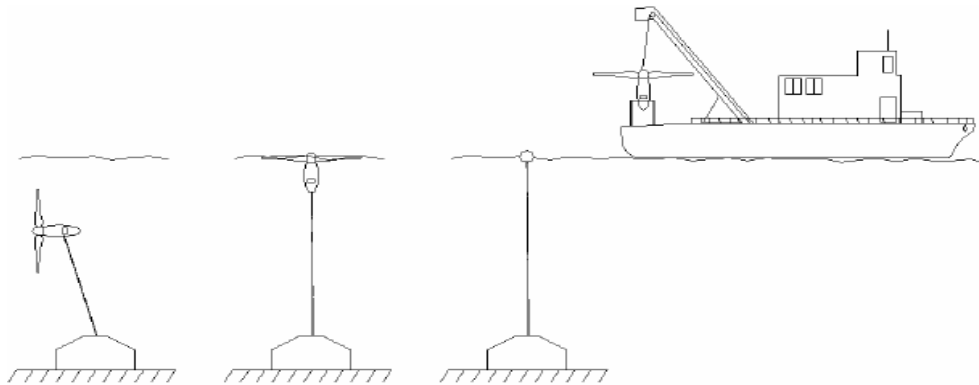


Figure 30(d). Anchored system

Advantages & Disadvantages

- | | |
|--|---|
| <ul style="list-style-type: none"> - No subject to wave and wind impact and corrosion - Low-cost structure due to little material requirement because uses chains instead of a pole - No visual impact - Tolerance for deeper waters - Self-aligning to the current, no need of pitching or yawing control system - Buoyancy of the nacelle used to raise it | <ul style="list-style-type: none"> - Exposed to marine growth - Nacelle must be removed even for smaller maintenance operations - Very flexible structure, hence subject to fatigue load and risk of failure - No surface components, need of accurate sealings |
|--|---|

- *Guyed tower system*

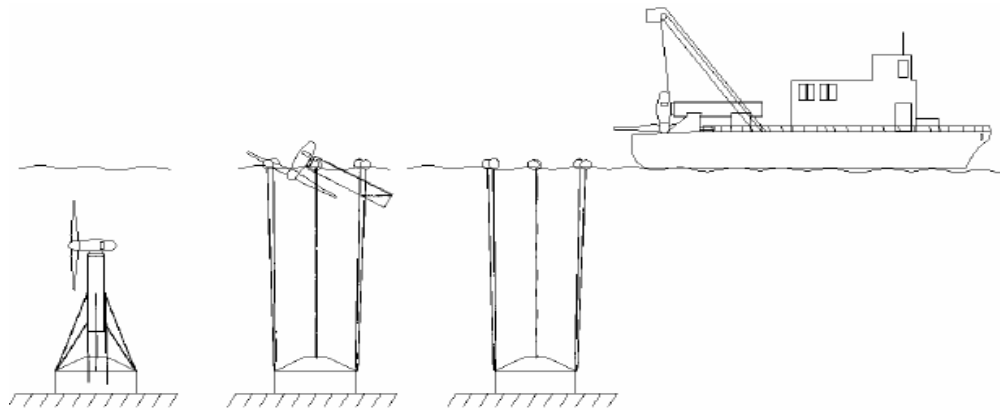


Figure 30(e). Guyed tower system

Advantages & Disadvantages

<ul style="list-style-type: none"> - Stiffer structure than anchored one - No subject to wave and wind impact and corrosion - Raised using buoyancy and fixed using chains - Less material requirement than fixed ones - Tolerance for deeper waters 	<ul style="list-style-type: none"> - Exposed to marine growth - Yawing and pitching mechanism required - Nacelle must be removed even for smaller maintenance operations - Flexible structure, hence subject to fatigue load and risk of failure - Significant underwater work to attach chains and probably divers deployment
---	---

2.2.4. Maintenance

[20]

A crucial aspect of this technology is the maintenance that needs to be evaluated to better support investments, due to its impact on the overall cost. Although O&M costs are smaller than the initial capital investment, a correct prediction of failures can improve the project reliability, optimizing the maintenance operations before the break of a component.

The expected lifetime of a project significantly affects the O&M costs because the older the equipment is, the more attention it requires. Because of the lack of studies on this technology, lifetime of a commercial-scale tidal turbine might be compared to the one of offshore wind platforms, estimated to be around 20-30 years. Furthermore, some tests on pre-commercial small-scale devices show a working period of over five years despite the absence of a systematic maintenance program.

Beyond the reliability of the single component, also the size of the farm affects the maintenance cost since the space between turbines is a very important factor. In this direction a compromise must be made because a smaller space reduces the efficiency due to the interference among closer turbines, but on the other hand, it reduces the number of additive components such as cables and their requirement of maintenance, and the movements of vessels.

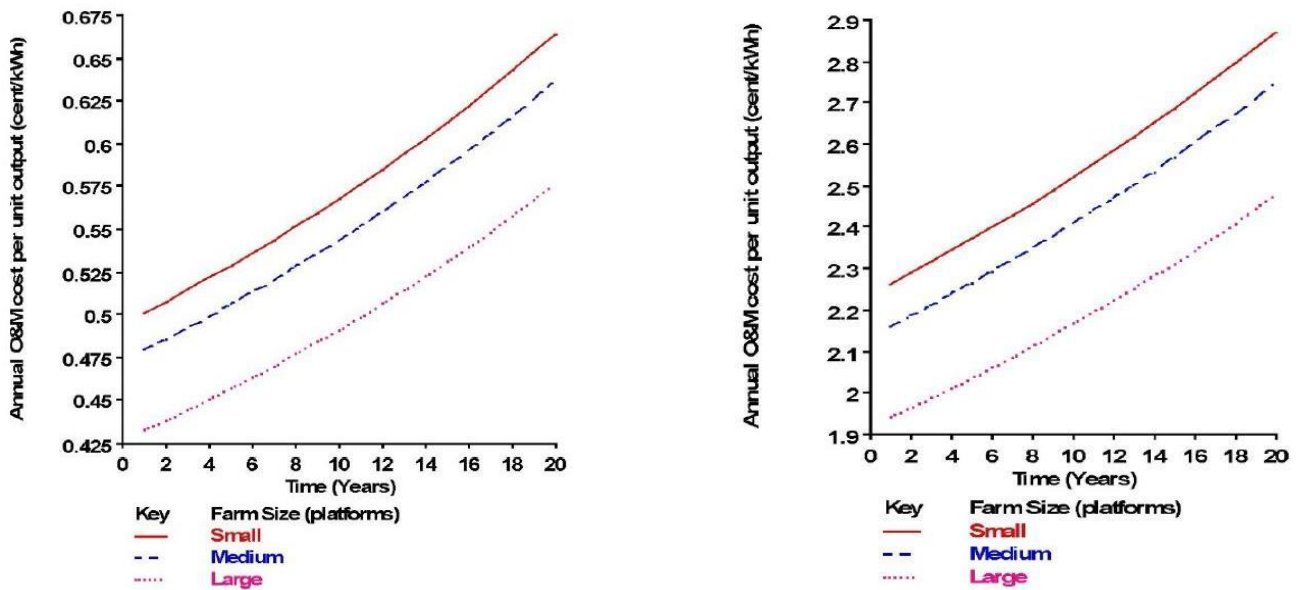


Figure 31. Annual O&M cost per kWh in British Columbia (left) and in Northeast of USA (right)

Usually the O&M costs are related to the energy produced during a year to get a rate of the worth of the installation. The comparison shown in Figure 31 is between two hypothetical turbine farms located in two different sites in North America; the one on the left, which shows the lower costs, is in British Columbia, Canada, a site with very strong currents that challenge the turbine's blades, but also generates much more energy. In the other installation the site is characterized by slow currents and strong winds, thus it leads to higher maintenance costs due to the more frequent issues. However, first site is significantly smaller than the second, thus a large-scale installation is not feasible. In both the figures the same trend is followed, with a raise of the costs as the time passes as previously stated.

- Blades' failure [21]

One of the gentler turbine components is the blade, due to the high bending moment that charge its structure, which can be fixed or with variable pitch. The latter is more widespread because has the advantage that the load can be optimized by the variation of the angle towards the current flow, even if this makes the blade more subject to failure than the fixed one. For example, in the *SeaGen* turbine the blades had been bended three times from 2008 to 2011; even the *Open Hydro* tidal turbine had suffered of blade failure in 2009 due to Bay of Fundy's hard conditions.

For pitched blades, an equation similar at the one seen in *paragraph 1.5* can be obtained to describe the thrust force that charge the blade, with the same structure and the same connection to the TSR:

$$T = C_T \frac{1}{2} \rho U^2 \pi R^2$$

For the same fluid velocity, a larger C_t leads to larger thrust force acting on the rotor, and so higher bending moment (*Figure 32 (left)*).

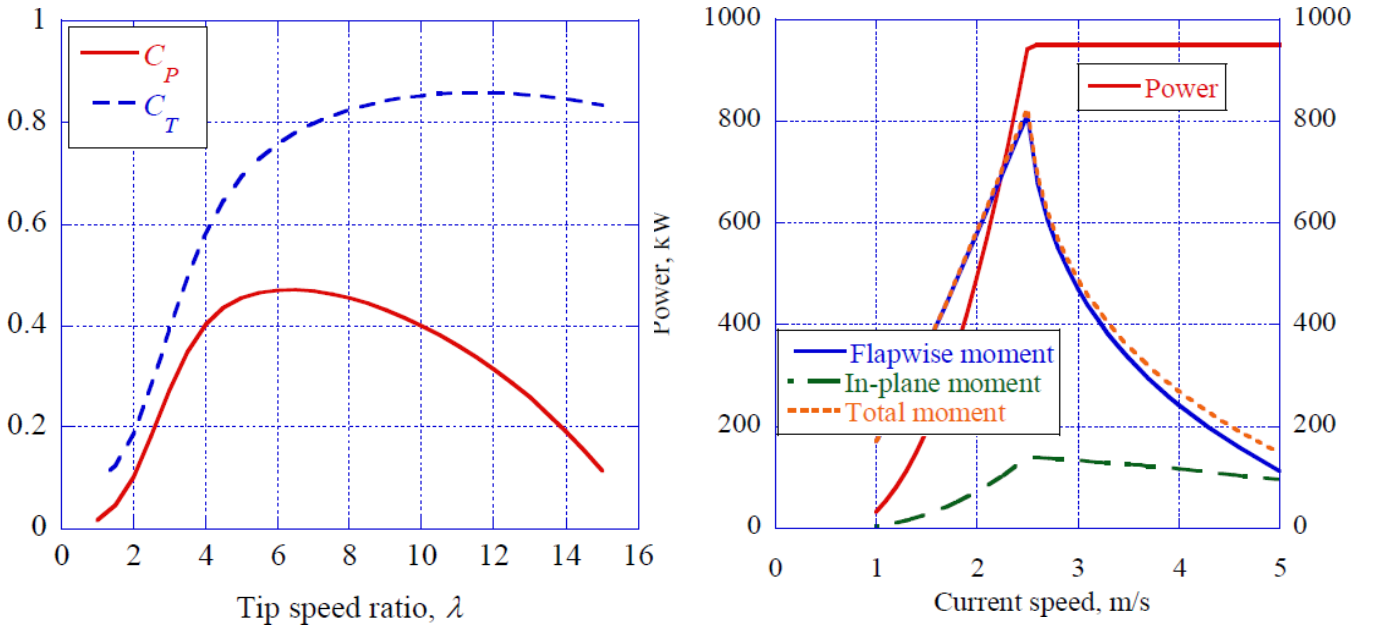


Figure 32. Correlation between TSR and C_P or C_T (left) and between rated power and peak bending moment (right)

In *Figure 32 (right)* it is shown that the peak of the moment occurs when the rated power is reached; it happens mainly because when there are slower currents the thrust on the blade is not at its maximum power, while at water flow speed above the rated speed, the pitch angle must be raised to increase hydrodynamical losses and dissipate the exceeding power, reducing the angle of connection. This makes little variation of water speed not concerning, because usually the turbine works at speed above the rated value. If a failure occurs on the pitch control system, the current forces the blade out of the minimum pitch angle, so the bending force decreases rapidly; together with the emergency shut down of the turbine, they prevent massive damages at the blades structure and limits issues to the pitch control system instead of the whole turbine structure.

- Gearbox [22]

Among the turbine components, the gearbox must be analyzed because as can be seen in *Figure 33*, several studies demonstrated that it is the one with the highest chance of failure; furthermore, it has been shown that gearbox downtime and fixing times are the longest among all because of its complexity, even though it is a mature technology.

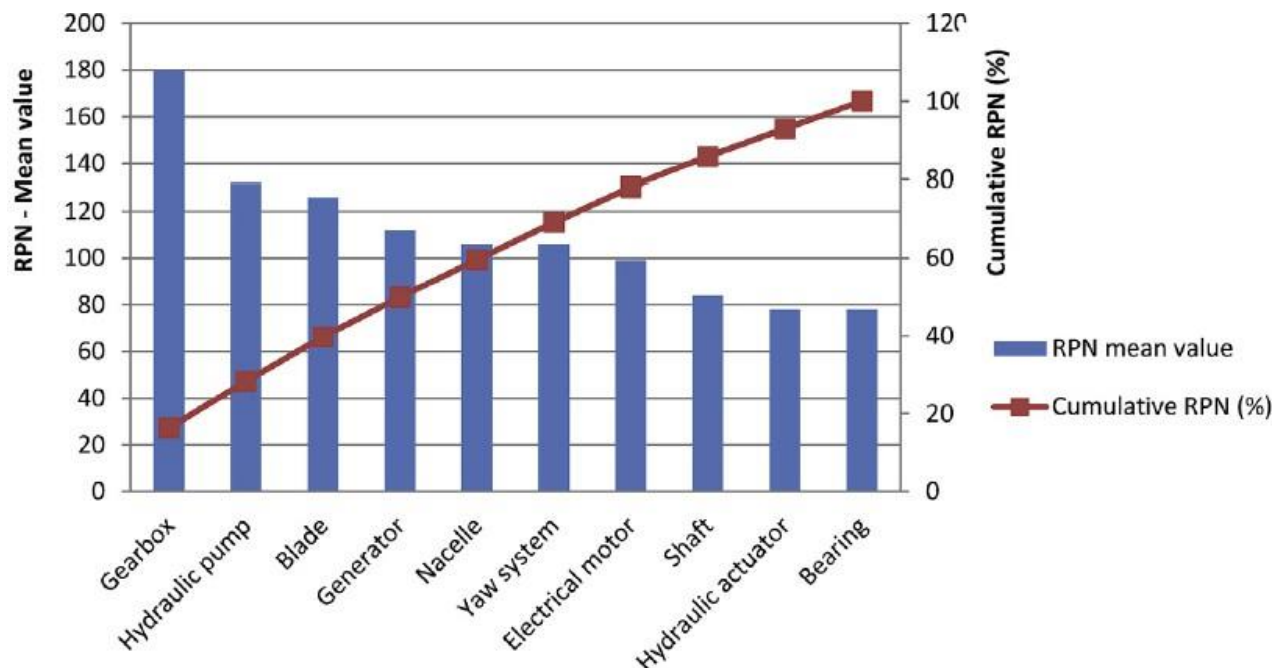


Figure 33. RPN (Risk Priority Number) related to the different turbine components

Because of the relatively high failure rate, several solutions had been proposed to increase the reliability, especially in offshore application, even though every of them has been previously tested on wind turbines, due to their major spread.

- The first solution proposed is the *direct-drive* technology, which consists in the removal of the gearbox connecting the shaft to the generator; this obviously increases the reliability but, on the other hand, the turbine will require lower speed, which leads to increased diameters and considerably increased mass. The main drawback of this solution is that decreasing the gearbox failure rate by removing it has brought, as surveys on gearless wind turbines assesses, to an increased failure rate of electrical parts and a build-up of copper losses due to the larger number of coils.

In the figure below it can be also noticed the large permanent magnet rotor instead of the wound one in the direct-drive solution; recently the reduction of permanent magnet costs has relaunched its development.



Figure 34. Direct drive wind turbine (left) compared to geared wind turbine (right)

- b) Another solution proposed consists in the so-called *magnetically geared* tidal stream turbines; it no longer needs a typical gearbox because the torque is transmitted via attraction and repulsion of rotating permanent magnets (*Figure 35*), which have a higher torque density than the mechanical ones. Furthermore, the deployment of magnetic gearboxes reduces mechanical problems such as need of lubrication, acoustic noise, maintenance requirement, and consequently the failure risk, due to reduction of component fatigue. In addition, it has also been demonstrated that magnetic gears are much more efficient than mechanical ones reaching values of above 99% and increasing the project lifetime.

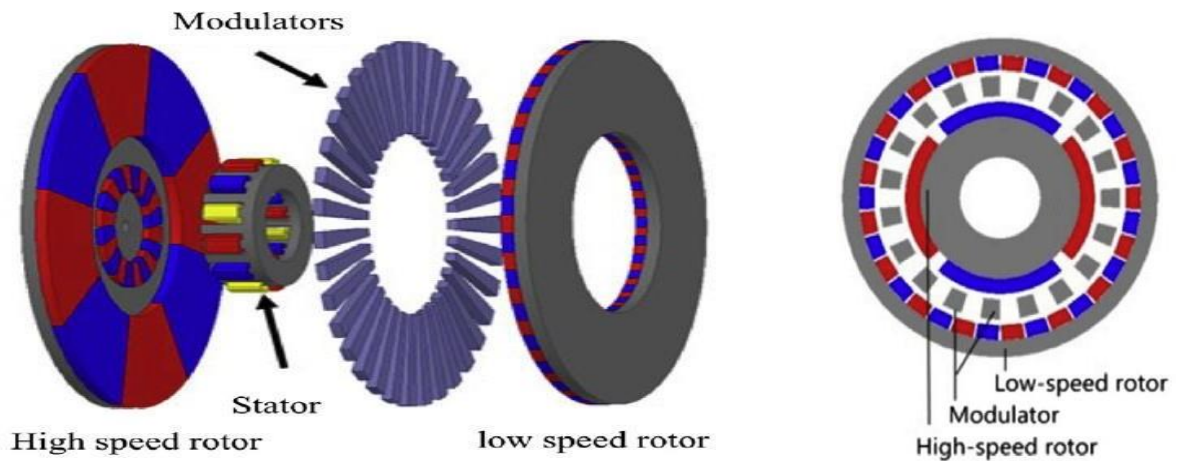


Figure 35. Magnetic gear structure (left) and section (right)

- Biofouling issues

Marine environment is challenging for technologies not only because of the difficult access and the high forces that must be countered during installation, but also for the organisms that inhabits its waters. Every device left under sea for a long period suffers the attachment of these organisms, which leads to several problems. This marine growth, in fact, can cause obstructions to the rotating parts, decreasing their efficiencies, and then an increase of the structure weight and its inertia to the currents, changing lift and drag coefficients of the turbine that comes to be stressed by stronger thrusts.

Even blades suffer from these attachments, that change the way the water flux affects them and consequently the roughness and blades' power coefficient (until 6-8% for TSR above 4 [22]), leading to a drastic reduction of generated power. In this context the kind of gearbox deployed hardly affects the biofouling impact because a direct-drive solution, characterized by larger diameters (thus surfaces), will be more subject to this problem.

However, not enough studies have been done to extract a general solution, except for reducing static parts size, even if this is in contrast with the trend of setting up more powerful turbines to reduces overall costs.

At today's state-of-the-art, it is still necessary to periodically clean up turbines, despite high costs of the operation and requirements of working men.



Figure 36. Clean current turbine before deploying in 2006 (left) and after removal in 2011 (right)

2.3. ECONOMIC ASPECTS

“OES believes that the first wave and tidal current device arrays and OTEC plants will be expensive by comparison with existing mature onshore electricity generation technologies (coal, gas, oil and nuclear) but the cost difference is typical for new energy technologies. Ocean energy technologies can be expected to follow the same cost reduction pathways of wind and solar energy. As the technologies become technically advanced and more efficient and their designs become mature and settled, they can be manufactured at scale”. [1]

Tidal devices are the most mature between the ocean technologies for power generation; some prototypes are working in many parts around the world, the technology is quite well-know and there is less uncertainty on the cost of investment than other ocean technologies. However, the cost for the kWh is still too much high for the commercial distribution.

2.3.1. Levelized cost of energy

[23]

This parameter is a crucial one to understand the development of an energy source. It can be estimated starting from capital investments and helps to assess the economic feasibility of the selected technology. Despite there is not an international standard to estimate the LCOE, the IEA (International Energy Agency) proposes a model to calculate this index:

$$LCOE = \frac{CAPEX + \sum_{t=1}^n \frac{OPEX_t}{(1+r)^t}}{\sum_{t=1}^n \frac{AEP_t}{(1+r)^t}}$$

Where *CAPEX* is the initial capital investment, *OPEX* is the operational expenditures at year *t*, *AEP* is the annual energy production at year *t* and *r* is the discount rate. The LCOE is difficult to exactly evaluate because it also depends on other factors, such as the sum of the installed projects, the expected project lifetime, the variable discount rate, and the capacity factor. Furthermore, the project cost is a function of the development stage, because the more a technology is developed, the more it can be learned from what has been already done, which leads to a reduction in costs.

From the OES' study, it can be observed (*Figure 37*) how the parameters in the LCOE expression vary with the project's scale. In both the figures it is shown the variation of the selected parameter as a function of the deployment stage and in both there is a reduction due to the “learning rate” (with time spent working on the development of a technology, its know-how increases, and this bring to a reduction of overall costs; it reflects the hypothetical state-of-the-art). As deployment level increases, CAPEX reduces because of the reduction of components cost and OPEX reduces because developers become more confident with expected failures; it can be also noticed that OPEX variation range remains high due to its uncertain nature.

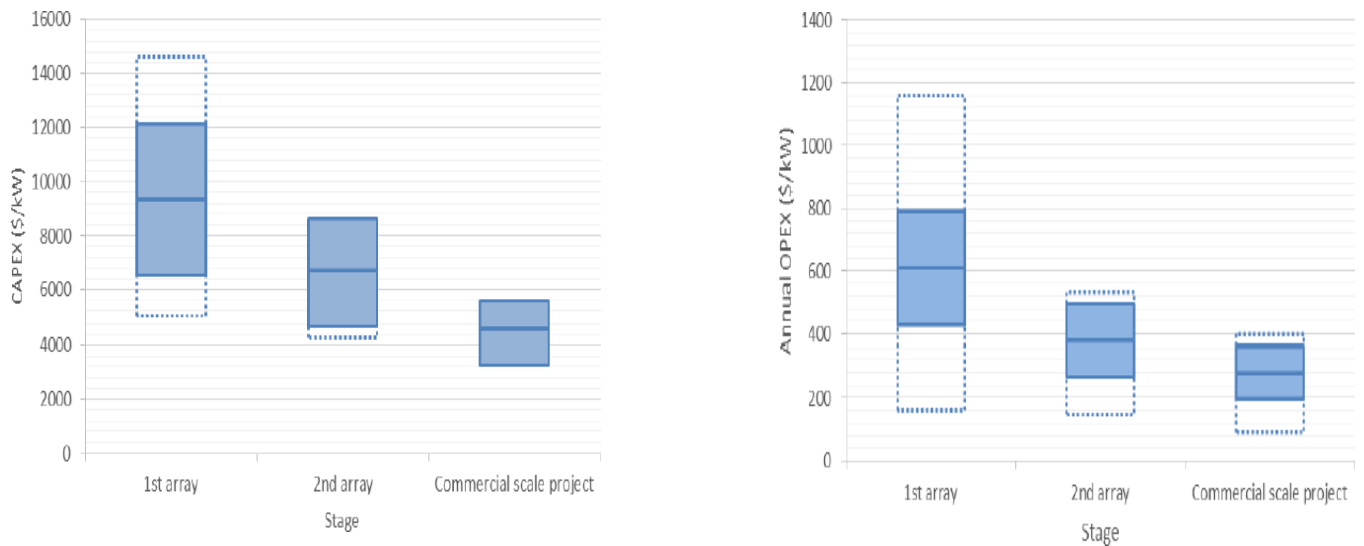


Figure 37. CAPEX and OPEX variation with deployment stage

In Figure 38 it has been assumed a learning rate of 10% in an industry-level project scale that is based on a scenario in which the tidal energy LCOE would reach the value of 240 \$/MWh within 1250 MW of cumulative deployment, a competitive value with the offshore wind; it is also expected a reduction of the LCOE with a larger scale roll-out even if it would require continuous support and investment. It must be specified that plotted LCOE comes from datasets provided by the stakeholder engagement and it is averaged across the sector to ensure anonymity.

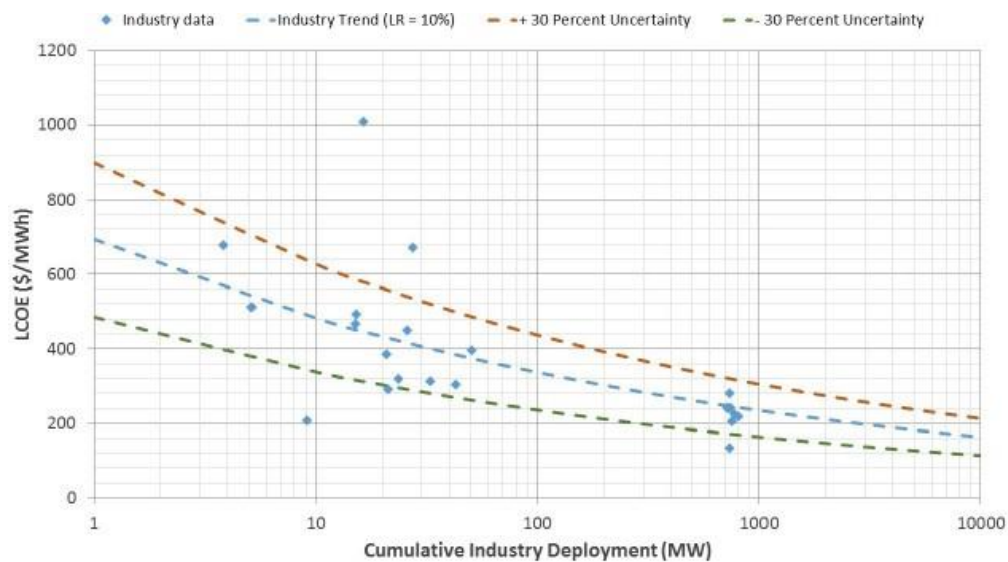


Figure 38. LCOE trend related to learning rate

Another crucial graphic is taken from [24] and shows the impact of the single costs on the resulting LCOE; this analysis is important because it helps understanding where to operate to reduce the costs and it makes this technology competitive with respect to existing ones.

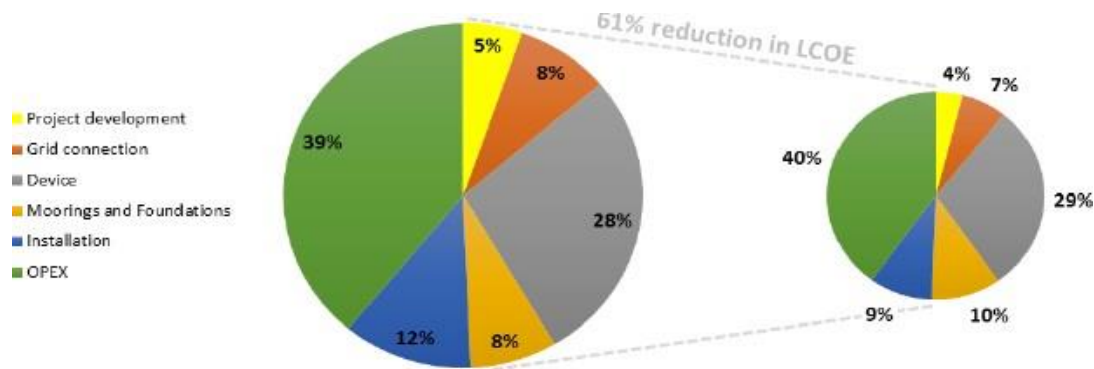


Figure 39. Expected LCOE reduction

The charts in *Figure 39* represent the current stage of development LCOE (*left*) and the commercial target (*right*), with the total LCOE equals to the pie chart area. As expected, the main cost breakdown comes from OPEX, whose percentage is almost stable although the overall cost decreases.

The device cost is also important in determining the price of energy, and it can be analyzed directly from [25], where can be found *Figure 40*.

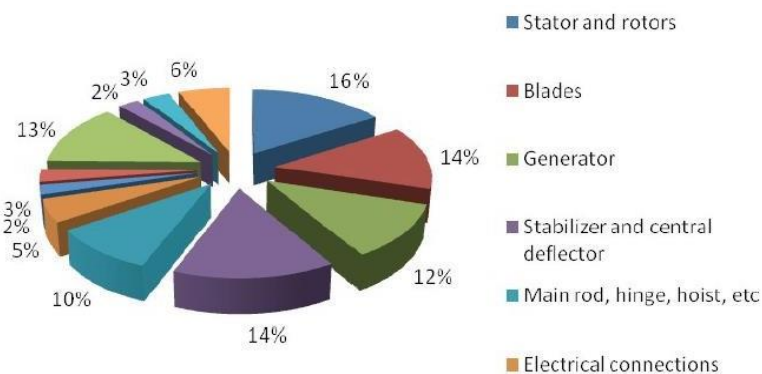


Figure 40. Device cost breakdown

Analysis of costs are proposed by many researchers and agencies, but they are hardly comparable due to the different approach and the difficult assumptions.

According to [26] the capital cost is expected to fall in the range of £1400/kW - £3000/kW, of which about 30%-50% is related to the turbine. Ongoing maintenance costs, which include insurance, O&M, decommissioning, and others, in literature are expected in the range of £191000/year and £302000/year, so an averaged value of £232250/year is taken in. The capacity factor which is the average power generated divided by the rated power and represents the effective exploitation of a selected device, is assumed at 30%. With these values the obtained LCOE is in the range of 140 – 250 €/MWh which with today's exchange rate means 160 – 290 €/MWh. For offshore wind plants the same study obtained an LCOE of 100 – 220 €/MWh; this difference because the offshore wind is further developed since various farm around the world, meanwhile tidal stream turbines are just prototypes-like.

Table 3: LCOE of traditional energy technologies

Technology	LCOE (€/MWh)
PWR nuclear (pressurized water reactor)	49.96
CCGT (combined cycle gas turbine)	43.17
IGCC coal (integrated gasification combined cycle)	36.59
IGCC coal with CCS (carbon capture and storage)	55.76
Retrofit coal	44.40
Pulverized fuel	32.57
Pulverized fuel with CCS	50.79
CCGT with CCS	59.78

Compared to traditional energy technologies, is clear that a cost reduction is needed to obtain a positive response from the market, and this can only be earned by increasing the power displacement around the world and consequently the knowledge around this technology. Even in the best scenario, hardly the LCOE of this renewable source could reach the ones proposed in *Table 3*, even if there are many factors not directly evaluable that should be included in the LCOE calculation.

These factors are called *externalities* and represent the consequences, environmental or social, of an energy source. One of these could be the carbon intensity, estimated to be around 6 gCO₂/kWh for tidal energy against the average of 250 gCO₂/kWh for traditional ones. Others could be the “labour intensiveness” (creation of new jobs: in fact, main costs come from the human sources employed in creation and development of devices) of renewable sources, or the reduction of supply risk due to fuels cut. External costs are hardly evaluable, but an example could be the oil's external cost that is around 60 €/MWh, against the 1.75 €/MWh for offshore wind energy. Including externalities would modify the point of view, reducing the differences among the LCOEs and making tidal energy, as other renewable sources, more interesting.

2.3.2. Policy support

[27]

The trend of last years changed in 2016, when many projects were proposed and commissioned. Europe leads this market, in fact more than 50% of companies involved are based in EU, with their energy sites located mostly in France and England. From that date, seeing the increasing request of manufacture, most important firms, such as Atlantis Resources, have opened clusters of smaller companies to contribute to the development of the final project. Seeing the excitement around this technology, several funding programs have been opened, dedicated to low-carbon energy technologies; in the table below a short list of ongoing projects is shown:

Table 4: List of Projects

Project name	Capacity	Funding	Status
MeyGen phase 1A	6 MW	10 m GBP from MEAD	Operational since November 2016
Sound of Islay	10 MW	20.65 m EUR from NER 300	Entry into operation expected in 2018
Stroma / MeyGen phase 1B	8 MW	16.77 m EUR from NER 300 / 10 m EUR upfront	Entry into operational expected in 2017
Nephtyd	5.6 MW	51 m EUR from PIA	Entry into operational expected in 2017
Normandie Hydro	14 MW	51 m EUR from PIA	Entry into operational expected in 2018
Skerries Array	10 MW	10 m GBP from MEAD	Project was halted by Siemens/MCT but Atlantis Resources considers to revive
Bay of Fundy	4.5 MW	5 m C\$ from SDTC	Turbine deployment expected in 2016
Bay of Fundy	4 MW	6.3 m C\$ from SDTC	Deployed in 2016

Cited funding schemes are:

- PIA: Programmes des Investissements d'Avenir, France
- NER 300: European Commission
- MEAD: Marine Energy Array Demonstrator, UK
- SDTC: Sustainable Development Technology Canada, Canada

Public support is fundamental in developing a tidal energy market, so many countries have their own programs beyond European common ones. Policy support instruments for ocean energy technology include both *push* (aimed to boost the research by providing funds) and *pull* (aimed to attract developers from a Country, buying the electricity produced) mechanisms to boost the development:

Table 5: Existing "pull" mechanisms (first) and existing "push" mechanisms (second)

Country	Rate and eligibility
Denmark	Maximum tariff of 0.08 EUR/kWh for all renewables including ocean energy.
France	Feed-in Tariff for renewable electricity. Currently 0.15 EUR/kWh for ocean energy.
Germany	Feed-in Tariff for ocean energy between EUR 0.035 and 0.125 depending on installed capacity.
Germany	Feed-in Tariff for electricity from hydro power, wave and tidal at least 7.67 cEUR/kWh.
Ireland	Market support tariff for ocean energy set at €260/MWh and strictly limited
Italy	0.34 EUR/kWh tariff (capacity installed until 2012).
Italy (from 2012)	For projects until 5 MW 0.3 EUR/kWh. For to 30 MW.projects >5 MW 0.194 EUR/kWh.
Netherlands	The SDE+ (feed-in premium) supports ocean energy with a base support of 0.15 EUR/kWh minus the average market price of electricity in the Netherlands (support is given for a 15-year period). Total budget for SDE+ capped (EUR 8 billion in 2016).
United Kingdom	Renewable Obligation (RO) Scheme. Renewable Obligation Certificates (ROCs) price set to 44.33 GBP in 2015/16. Will be replaced by a Contract for Difference (CfD) scheme in 2017. Wave and tidal energy technologies will be allowed to bid for CfDs; however, they are currently expected to compete with other technologies (e.g., Offshore Wind) to access CfDs.

Country	Rate and eligibility
France	Two projects awarded funding: Normandie Hydro (EUR 52 million funding) and Nephthd (EUR 51 million).
Ireland	SEAI Prototype Development Fund, dedicated to ocean energy. Total amount available not known.
Ireland	Ocean Energy Development Budget in-creased to EUR 26 million.
Portugal	Fundo de Apoio à Inovação (FAI) for renewable energies, 76 m EUR total.
United Kingdom	Renewable Energy Investment Fund (REIF) Scotland, 103 m GBP.
United Kingdom	Marine Energy Array Demonstrator (MEAD), 20 m GBP.
United Kingdom	Energy Technologies Institute (ETI), 32 m GBP for wave and tidal projects.
United Kingdom	Marine Renewables Commercialization Fund (MRCF) Scotland, 18 m GBP.
United Kingdom	Marine Renewables Proving Fund (MRPF), 22.5 m GBP.
United Kingdom	Saltire Prize, Scotland, 10 m GBP. For first device delivering > 100 GWh for two years.
United Kingdom	Wave Energy Scotland funding, GBP 14.3 million until end of 2016.

Even from [27] can be taken *Figure 41*, that shows in which stage of development funds are stationed:

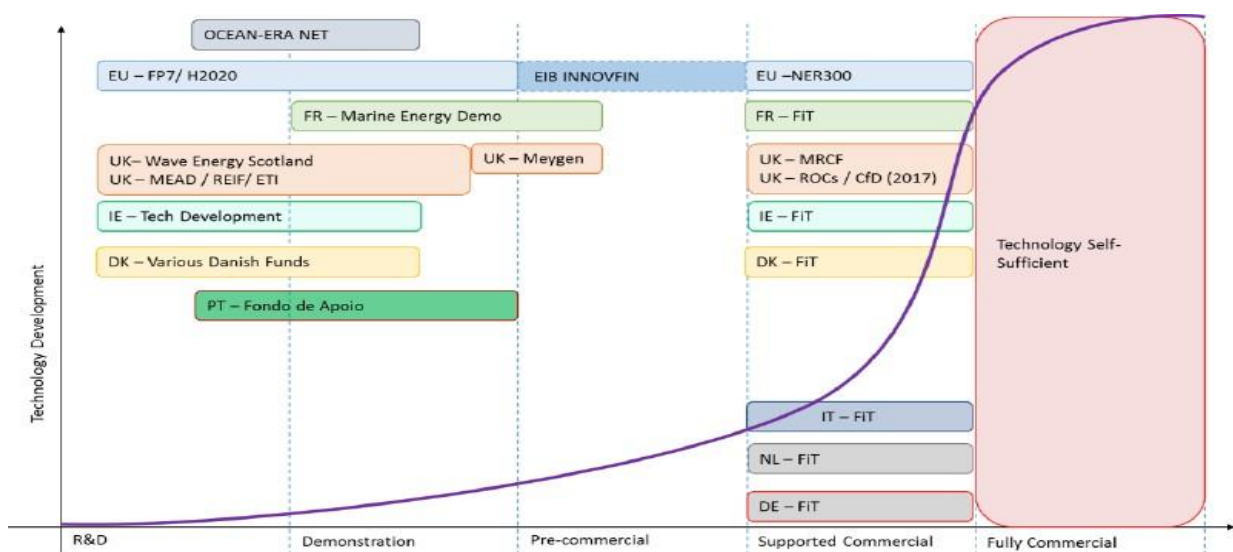


Figure 41. Summary of market push and pull mechanisms for ocean energy in the EU, based on Carbon Trust deployment scenarios

3. CURRENT ENERGY IN THE MEDITERRANEAN SEA

[28] [29]

3.1. PRELIMINARY CONSIDERATIONS

In the previous chapters, it was discussed how tidal currents are generated by water masses moving parallel to the bottom of the sea because of the influence of the Moon and the Sun. Different types of currents can be classified:

- a) Based on the effects that create them; in this case the following are identified:
 - *Gradient currents*, caused by a non-uniform distribution of pressure on water surface and by different density of surrounding water. These flows are generated when water surface is characterized by a specific inclination, which happens because of winds or due to the presence of nearby water with different temperature and salinity. Generally, to reestablish a horizontal sea water surface, gradient currents are moderately intense in open sea, while they can assume significant values close to the coast.
 - *Drift currents*, caused by the dragging due to the existing friction between water and air moving on its surface. Strong constant winds, such as trade winds, blowing on Atlantic Ocean, and the monsoon, blowing on Indian Ocean, generate majority of constant drift currents. The wind tends to drag the marine water surface in its direction and the drift movement spreads to the lower layers with decreasing intensity and progressively variable direction. The superficial drift current intensity, for what concerns speed, is about 1.5% of the velocity of the wind which generated it.
 - *Tidal currents*.
 - *Geostrophic currents*, caused by the Coriolis force due to the rotation of the Earth.
- b) Depending on water temperature, when big water masses move with a different temperature with respect to the surrounding ones.
- c) Concerning the depth at which they take place; in this case they can be distinguished in:
 - *Superficial currents*, involving the surface layer up to 50÷100 m depth.
 - *Internal currents*, involving the water layer below 100 m depth, but far from the seabed.
 - *Bottom currents*.

The above classification shows the complexity of the factors playing a role in the characterization of a field affected by marine currents, therefore, any modeling approach can not overlook the seabed structure, costal morphology, weather conditions and the physical structure of the water body.

The study of actual technologies employed to marine currents for power energy production underlines a necessary requirement of at least 1.2 m/s velocity generated in marine current field to run the turbines, and in any case their maximum efficiency is with currents of at least 2 m/s. In Mediterranean Sea, unlike in North Europe seas and oceans, the currents are averagely weak and of variable direction. However, the growing interest towards renewable energies opened to the design of projects involving the use and transformation of kinetic energy of currents even in presence of fields with low intensity, particularly with the research of new devices optimized to low intensity currents.

Despite Mediterranean Sea is an almost closed basin, therefore with scarce currents development, it provides a limited number of sites with a remarkable energetic potential. In Italy, the only interesting area for the development of a technology based on tidal currents is the Strait of Messina. A study conducted by ENEA in collaboration with the University of Naples “Federico II”, shows that the total real potential of the Strait of Messina is about 250 MW of installed power which would allow a year production of about 160 GWh. To be more precise, such energy production is supposed to use only the areas close to the coastline without considering the central part of the strait, which could be utilized in future with more mature technology. Other places present very modest energy resources, such as Bocche di Bonifacio between Sardinia and Corsica, and Venetian Lagoon.

The two technologies in advanced phase of prototypal development for the Italian background are *KOBOLD* e *GEM*. The first one is from the south-east Asian area, a project from Indonesia by Indonesian Walinusa Energy Corporation designing the implementation of 120-150 kW turbines to provide power to remote communities; the second one is being experimented in Venetian Lagoon: a project co-financed by the Region of Veneto and some French companies, interested in the Atlantic development plan.

Additionally, in Italy was developed an innovative system by FRI-EL GREEN POWER S.p.A. composed of a floating body attached to the seabed to which are connected four rows, each presenting five horizontal axial turbines; each row incorporates the power and motion drive shaft produced by all the turbines. Many trials were performed with this device in the naval tank available at the University of Naples “Federico II” and a real scale prototype is already in advanced state of production: it is a 500 kW model destined to the Strait of Messina.

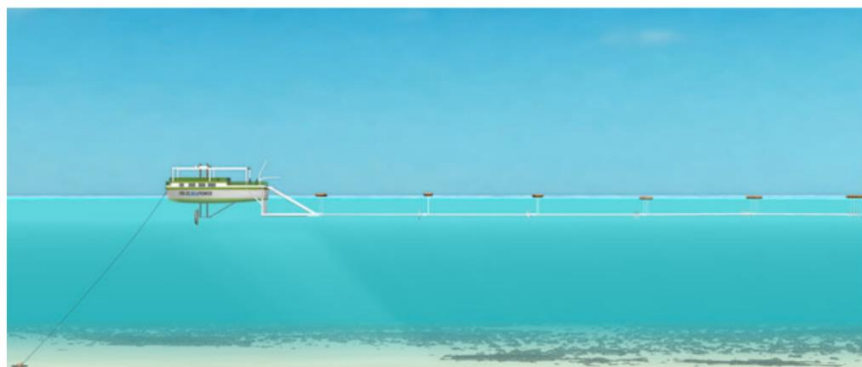


Figure 42. FRI-EL SEAPOWER turbine system

Although precise objectives were defined regarding the exploitation of marine motion as an energy resource and despite the above-mentioned projects, nationally and from a European perspective, a substantial delay in their application is evident. Such delay, suffering from a widespread prejudice regarding the energetic potential of the Mediterranean Sea, is not due to technological faults, but rather due to the need of accurately quantifying the available resources (to use such motions properly) and their environmental impact.

3.2. CONNECTION WITH ENVIRONMENTAL PROBLEMS

European Union is active from time in promoting renewable resources and this dedication is part of a wider strategy linked to the struggle against climate change, along with CO₂ emissions reduction and the promotion of energy efficiency. The EU promoted a binding objective in 2008 “Climate and energy package” to substitute 20% of energy consumption with renewable sources. The European directive *77 of 27 September 2001* states that for security and diversification of energy sourcing as well as environmental protection, the community must promote a higher contribute of renewable energy sources to the internal market energy needs.

Italy followed up to the EU directive with *D.Lgs. 387 of 29 December 2003* establishing the basis of a regulatory framework on the subject of promoting renewable sources and how pursuing such objective, i.e. instituting a unique procedure containing all necessary authorization to the realization and execution of renewable sources plants. Such requirements are:

- a) The evaluation of projects’ environmental impact, with the objective of protecting human health, contributing with a better environment to the quality of life, preventing animal species extinction and the integrity of the ecosystem reproducing capacity. For this purpose, the directive appropriately identifies, describes, and evaluates each case according to the legislative regulation, considering possible direct and indirect impacts on the following factors:
 - Mankind, flora, and fauna.
 - Soil, water, air, and climate.
 - Material goods and Cultural Heritage.
 - The interaction among the factors above.
- b) Impact evaluation. New construction projects, within SIC (Community Site of Importance) or ZPS (Special Protection Zone), require an impact evaluation in accordance with the protection objective preset.
- c) Authorization to proceed in areas where an environmental restriction is in place.
- d) “No impediment to proceed” certificate is required from the managing institution of a specific protected area.

It is evident that to define a procedure to draw an Italian map of the energetic potential exploiting marine currents, it is necessary to include the evaluation criteria resulting from a regulatory and environmental perspective, in addition to engineering-based reasoning.

Therefore, from an environmental point of view, it is required to consider some parameters beyond physical ones, since it is of fundamental importance the evaluation of the impact of a sea installation. For each site potentially appropriate to the exploitation of marine currents it is necessary to consider and evaluate:

- a) The presence of environmental restriction in place for a zone of 300 m depth from the seashore.
- b) Presence of Marine Protected Areas
- c) Presence of sensitive areas, according the regulatory specifics of *Attachment 6 of D.Lgs. 152 of 11 May 1999*.
- d) Presence of Military Areas.
- e) Presence of docklands. Docklands entail naval traffic with important limits to the installation of plants based on marine currents exploitation, particularly of superficial ones.
- f) Distance from the shore. The installation of a power plant of this type implies that the energy produced is a direct input to the electrical grid, through an underwater cable connecting the generators to the mainland; the placement and maintenance costs are directly proportional to the length of the cable, same to the losses distributed along the cable: it is necessary to define the best compromise between the best positioning in terms of productive efficiency and the minimum distance from the plant to the grid.

Renewable resources, such as marine currents, are potentially non-polluting energy sources and their use does not compromise natural resources for future generations; they also contribute to minimize the dependency on fossil fuels, to diversify the energy sources and to reduce the subordination from foreign resources. The installation of an energetic potential exploitation system through marine currents presents several advantages with respect to traditional energy sources, e.g. the absence of emissions of any kind when fully operating. However, despite many underwater devices using sea energy are already present in different parts of the world, for many of them it is not very clear the specific nature of the effects they have on the environment; however it is necessary to keep in mind that the energy produced by such devices represents in any case a reduction of global emissions, i.e. CO₂. Therefore, many projects are still at a prototype stage and only the latest studies are trying to determine their impact. From the first results, it is possible to practically subdivide the produced environmental effects in four categories:

- 1) Potential ecosystems alterations: influences on feeding, reproductive and movement habits of fish fauna; acoustic impacts; chemical-physical water quality.
- 2) Visual and landscape impact.
- 3) Seabed impact.
- 4) Electromagnetic effects (underwater cables).

It is also to be considered the socio-economic impact due to navigation and fishing alterations in the areas where these technologies are installed.

3.3. COAST CHARACTERIZATION FROM THE CURRENT METRIC POINT OF VIEW

Concerning the seabed topography, the Mediterranean Sea is divided in two main basins, which can be considered half-closed. The first is the West Mediterranean Basin, delimited by the Sicilian Channel and characterized by wide abyssal plains; the second is the East Mediterranean Basin, dominated by the Mediterranean ridge system and much rougher. Regarding the chemical-physical characteristics, Mediterranean waters differ significantly from ocean waters because of their salinity, temperature, and lack of nutrients. These characteristics originate from the scarce connection between the Mediterranean Sea and the Atlantic Ocean, as the sea water exchange occurs only through Strait of Gibraltar, while the freshwater flow is connected to precipitation and down flow of rivers. The relationship between evaporation and precipitation is a fundamental parameter for the basin equilibrium: an abundant evaporation, not sufficiently compensated by rain and fluvial contribution, leads to waters rich in salt, therefore very dense. This causes higher pressure on the seabed and consequently produces a current flowing through Gibraltar Strait. The Atlantic water, relatively fresher, flows near the surface towards the Mediterranean Sea to replace the evaporated water, while the deeper, saltier, and denser water flows towards the Atlantic near the seabed. Nearby the Strait, the superficial water not always enters the Mediterranean Sea as tidal current, where presents considerable values. Because of the complex circulation in the Mediterranean Sea, it is estimated that the complete renewal of Mediterranean water because of the presence of the Atlantic Ocean requires around 100 years.

The average temperature of deep waters in east basin is about 13.5°C, while it is 12.5°C in the west one. On average, these are the same temperatures recorded on surface water in winter, given the general homothermia developing in the cold season. However, local superficial temperatures in winter can shift consistently from these average values, recording, for example, only 7°C at the extreme north of Adriatic and Aegean Seas, while along the seashore of Palestine it is possible to find 17°C. In summer, the temperature records 21-23°C in Gulf of the Lion, at Gibraltar and in Strait of Dardanelles, 25 °C throughout the rest of the sea with a maximum of 28 °C in northern Adriatic Sea, in Sirtica and South Anatolia.

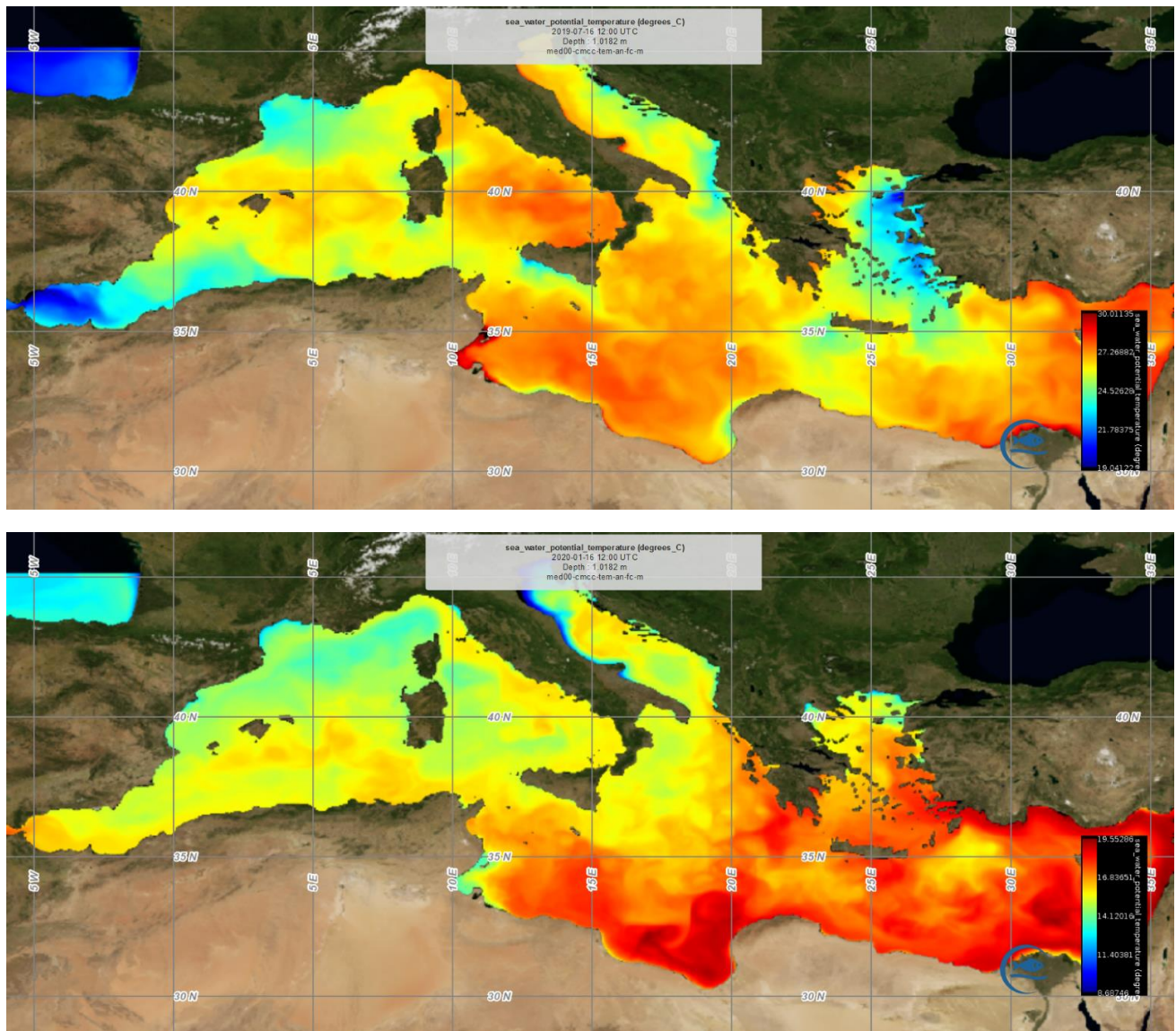


Figure 43. Surface Mediterranean Sea water potential temperature in summer (top) and winter (bottom) [CMEMS]

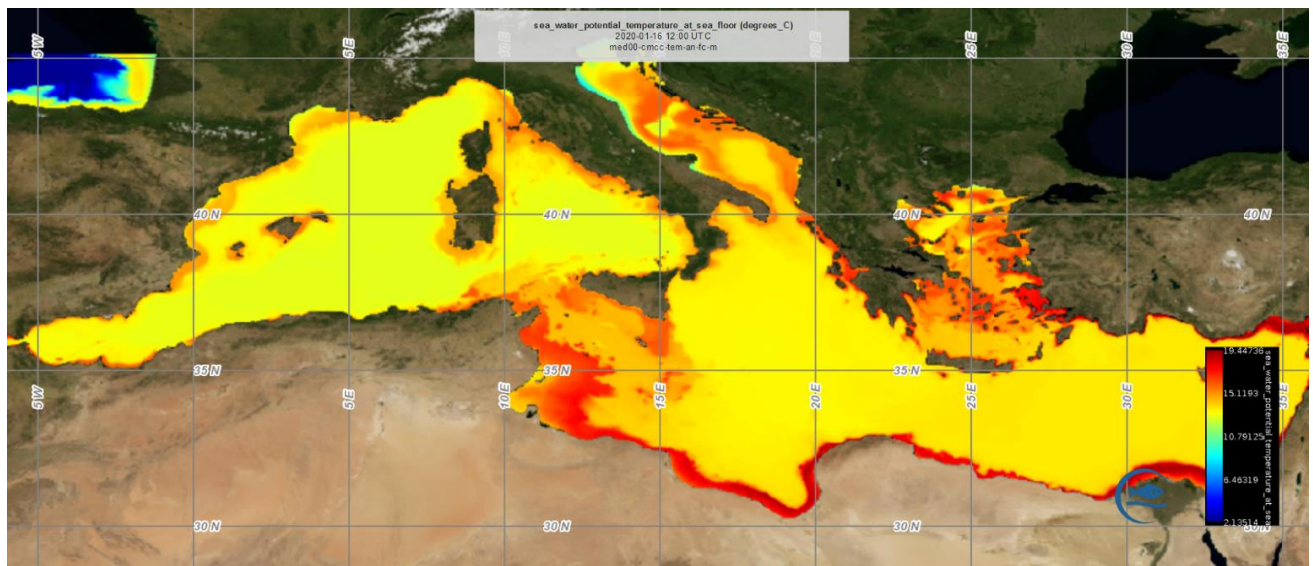
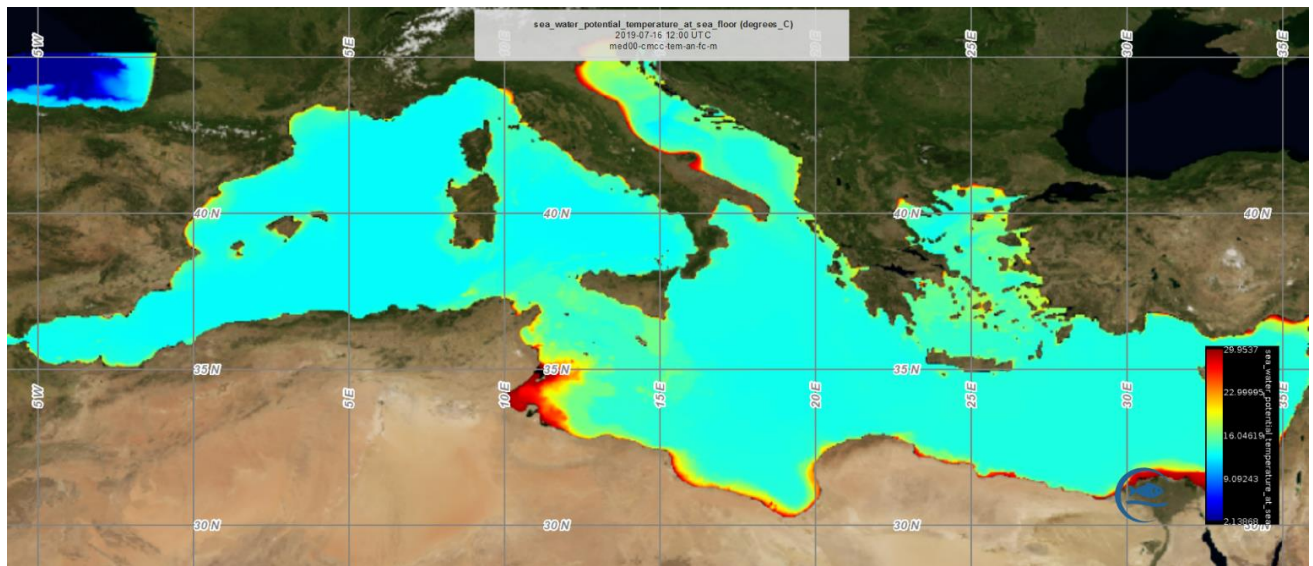


Figure 44. Mediterranean Sea water potential temperature at sea floor in summer (top) and winter (bottom) [CMEMS]

The average salinity is around 38.5 g/l but can reach higher than 39 g/l in east sea, while in superficial layer of the west basin the salinity progressively decreases towards Gibraltar, where it settles around 36 g/l. Low superficial salinity are recorded in North Adriatic (in average around 35 g/l) and North Egeo.

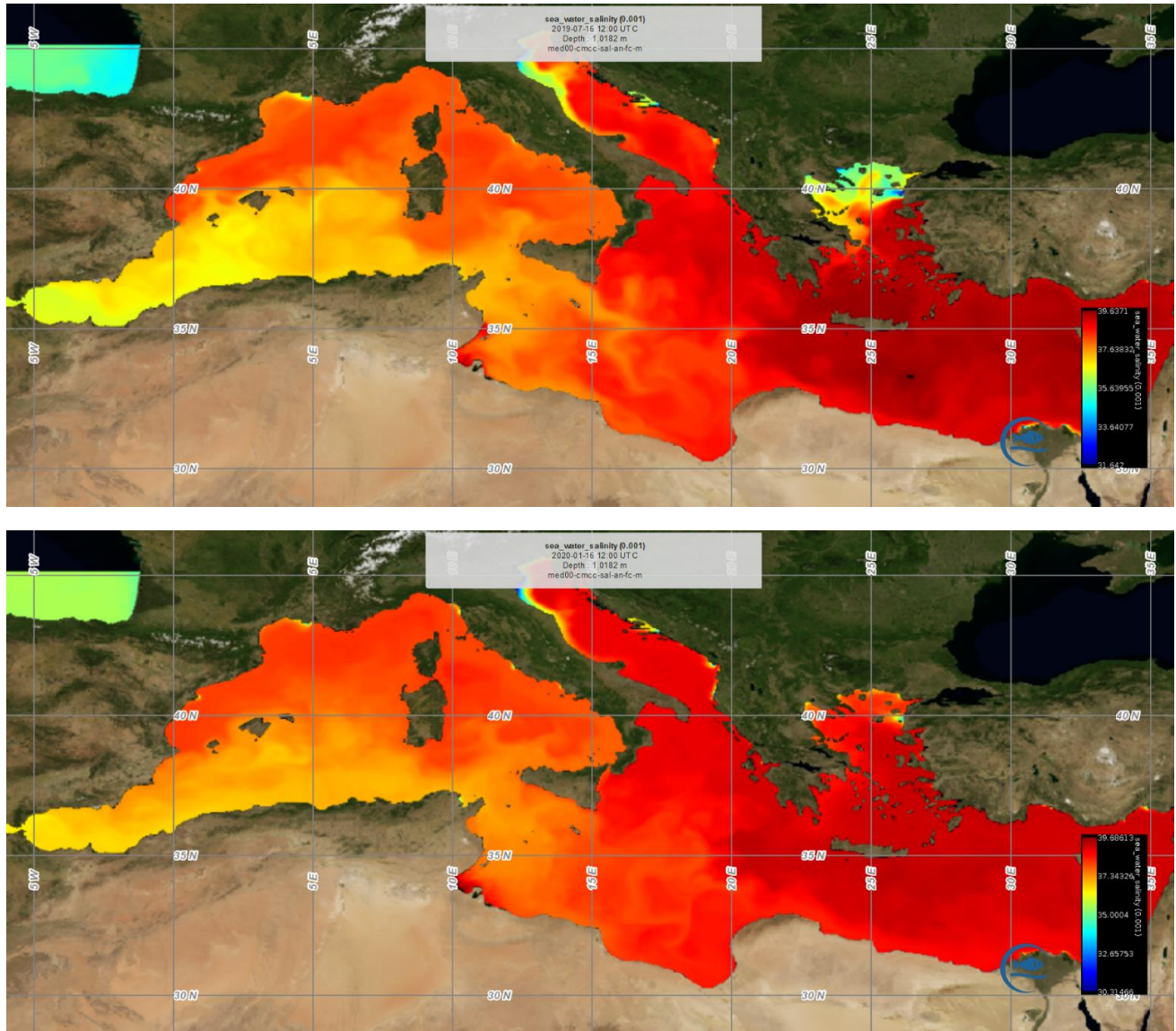


Figure 45. Mediterranean Sea water salinity in summer (top) and winter (bottom) [CMEMS]

The vertical structure of the Mediterranean Sea is characterized by the presence of three distinct water masses:

- 1) A superficial layer of about 100-200 meters of water of Atlantic origin, relatively fresh and whose temperature is subject to strong seasonal fluctuations.
- 2) An intermediate layer of relatively warm and salty water of eastern origin which settles between 300 and 600-800 meters.
- 3) A deep layer, relatively cold and less salty than the intermediate one, which originates from convection processes of secondary cells.

Considering that the installation of devices for the extraction of energy from marine currents cannot exceed 100-150 meters depth, it is beneficial to examine in depth the circulation zone of interest, that is the superficial layer. The Mediterranean Sea superficial currents originate from the flow of Atlantic water and they mainly follow a cyclonic-type trend: about 80% of Atlantic water, colder but less salty (reason for which it remains on the surface), enters the Mediterranean Sea after brushing the Moroccan seashore, while a smaller part mixes with the outward water. Once this water crosses the Strait of Gibraltar, it is pushed south by Coriolis force and mainly follows the north Africa shore originating the Algerian current: one section forks in the north, towards Balearic Islands, hit by the anticyclonic current of Alborán Sea. The Algerian current, along its flow, splits again: one fork proceeds towards the Channel of Sicily, the other flows northbound towards Corsica and joins the first fork to Balearic Islands creating the Ligurian Provençal Catalan current, which flows west brushing Catalan, French, and Ligurian shores through the Lion Gulf. The shallow sea of Channel of Sicily breaks the Algerian current in two again: one third of its waters flows towards the Channel of Sardinia and enters the Tyrrhenian Sea originating a cyclonic current that partially brushes the Ligurian shore and merges with the Ligurian Provençal Catalan current; the other part able to flow through the Channel of Sicily crosses firstly the area overlooking the Tunisian and Libyan coastline, with variable flow according to the specific season (in winter it is almost twice that in summer) and it is characterized by anticyclonic currents, then it forms the African current flowing along the eastern sea creating the Minor Asia current, which brushes the Turkish coast up to Rhodes Island.

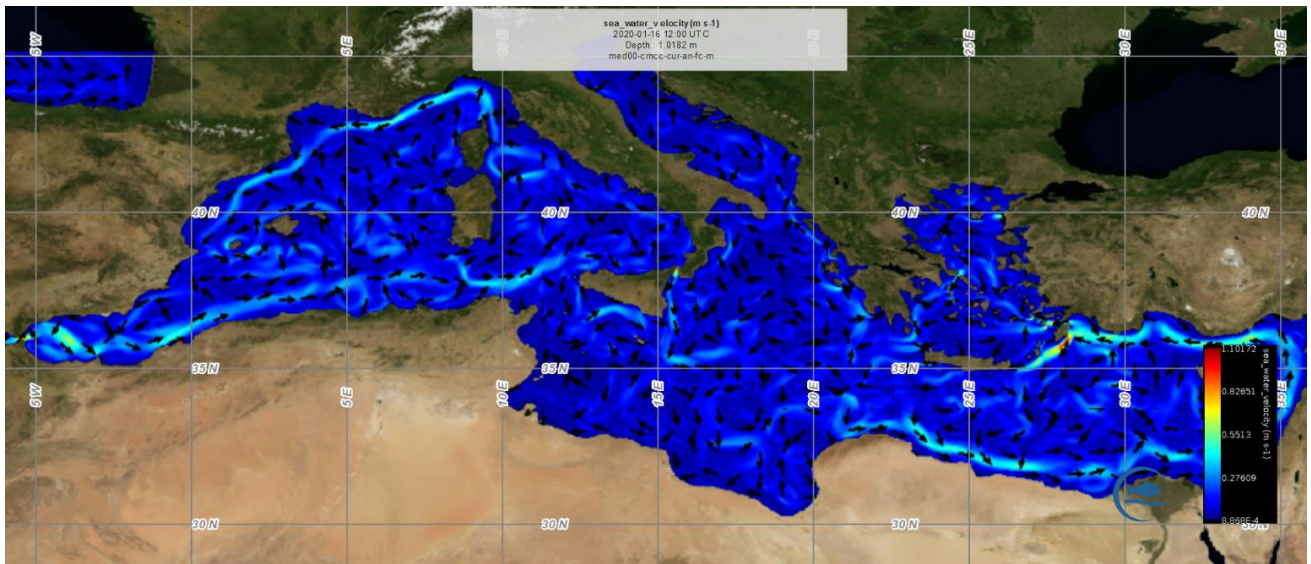
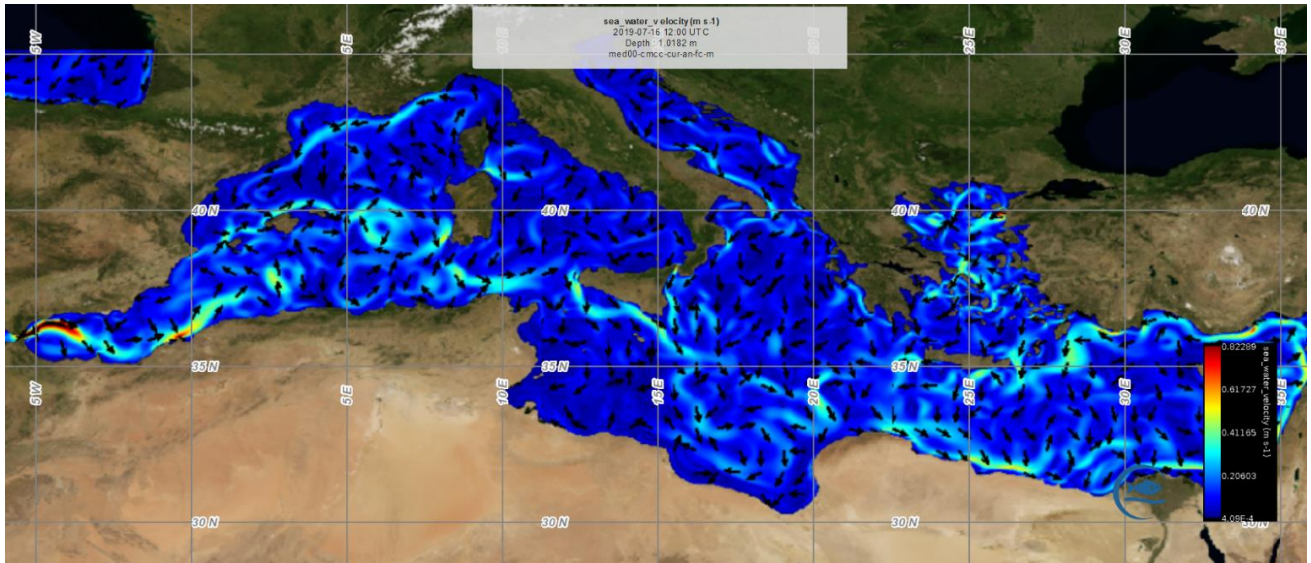


Figure 46. Surface Mediterranean Sea water velocity in summer (top) and winter (bottom) [CMEMS]

Therefore, the seas in the Mediterranean Sea are characterized by a complex circulation, determined both by remote forcing, linked to the general flow, and local forcing low scale, both bathymetric and atmospheric. Then, it is fundamental the collection and classification of marine weather data and bathymetry regarding the zone closest to the coastline to define a procedure of evaluation for potential production sites.

Once described the general superficial circulation of the Mediterranean Sea it is useful to deepen the characteristics of the seas that border with the Italian Peninsula, to study their currents and understand them from a bathymetric point of view. In particular:

- a) Adriatic Sea. It covers a surface of about 135,000 km² and a maximum depth of 1230 m. The northern part is completely dominated by the Po river delta and presents very weak slopes with a depth not above 75 m. The central area, between Ancona and Gargano area, is characterized by the presence of depression called “Middle Adriatic Pit” (266 m), while the southern area has a continental platform thinning in front of Puglia region up to 20 km. Between Puglia and Albania there is the Adriatic Plain with an average depth of about 1000 m (max 1200 m). From here it rises to about 800 m at Otranto Channel, which divides Adriatic to Ionian Sea.
- b) Ionian Sea. It expands on a surface of about 616,000 km² from Libyan and Tunisian costs to Greece and Southern Italy. It reaches its max depth at Hellenic Pit (5,093 m). Ionian Sea presents the vastest abyssal plain of the Eastern Mediterranean, which is subdivided in minor plains separated by underwater mountains and plateaus; for this reason, it is recognized a Sicilian Basin, closed in the north by the Rise of Messina and bordering in the south part of the Mediterranean ridge. The Adriatic and Ionian Seas are two adjacent basins that, through interchanges at the Strait of Otranto, interact and form the mechanism for the thermohaline circulation of the Eastern Mediterranean. The peculiarity is that the waters of these two seas mesh and cyclically invert the flow (every 7-10 years) of this part of the Mediterranean.
- c) Tyrrhenian Sea. It presents important depths between Ponza and Ustica reaching the deepest point of Western Mediterranean with 3620 m. The continental platform develops mainly from the Piombino plateau to Sorrento Peninsula, along the coast of Cilento, East Sicily, North Sardinia, and South Corsica. The sea is close to the fault dividing Africa and Europe, which caused the formation of active volcanos and underwater mountains ridges that, if not surfacing like Stromboli Island or other volcanic islands now inactive, reach only tens or hundreds meter of depth.
- d) Ligurian Sea. It is divided into two basins and only the western one reaches remarkable depths up to 3000 m. In the southern part of the basin, overlooking the Eastern Ligurian Coastline, the continental platform is wider while the seabed is deeper offshore.
- e) Sardinian Sea. It is affected by the current from the Strait of Gibraltar that, after entering the Tyrrhenian Sea, divides in two branches: the first flowing in the south of the island and the other one heads towards the Ligurian Sea. The east coast of Sardinia is then mainly characterized by a north-south current, the west coast from one in the opposite direction.

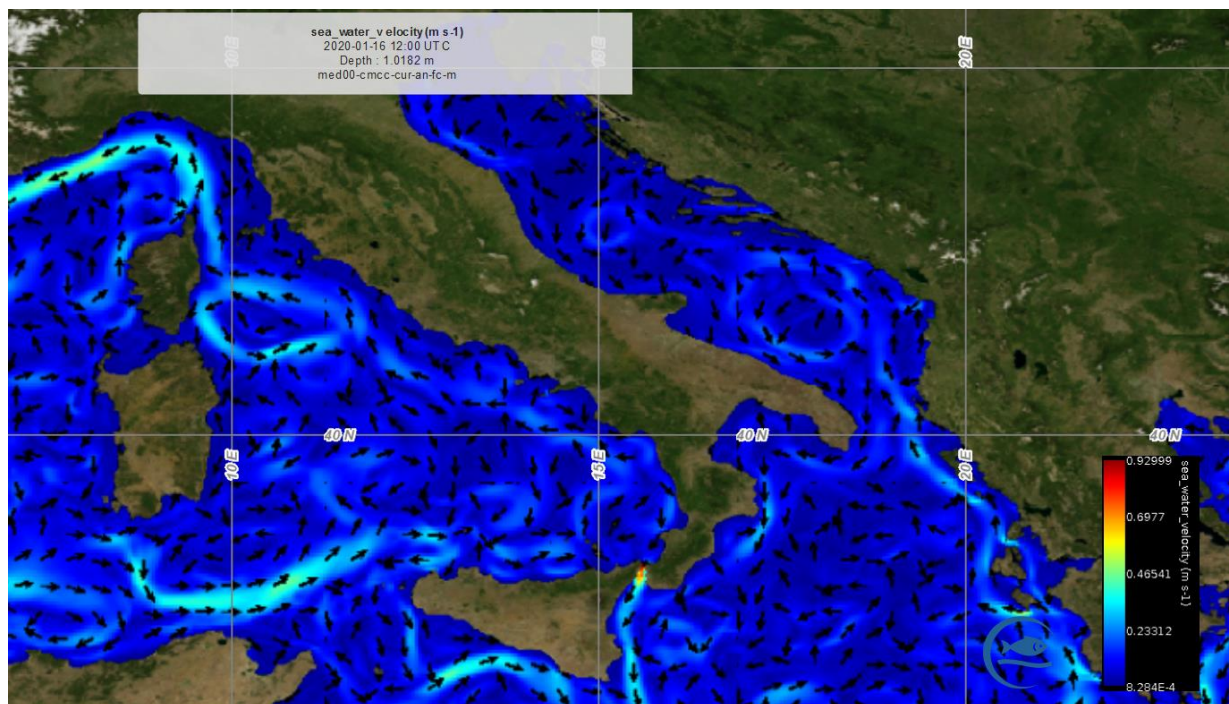


Figure 47. Italian Seas surface water velocity [CMEMS]

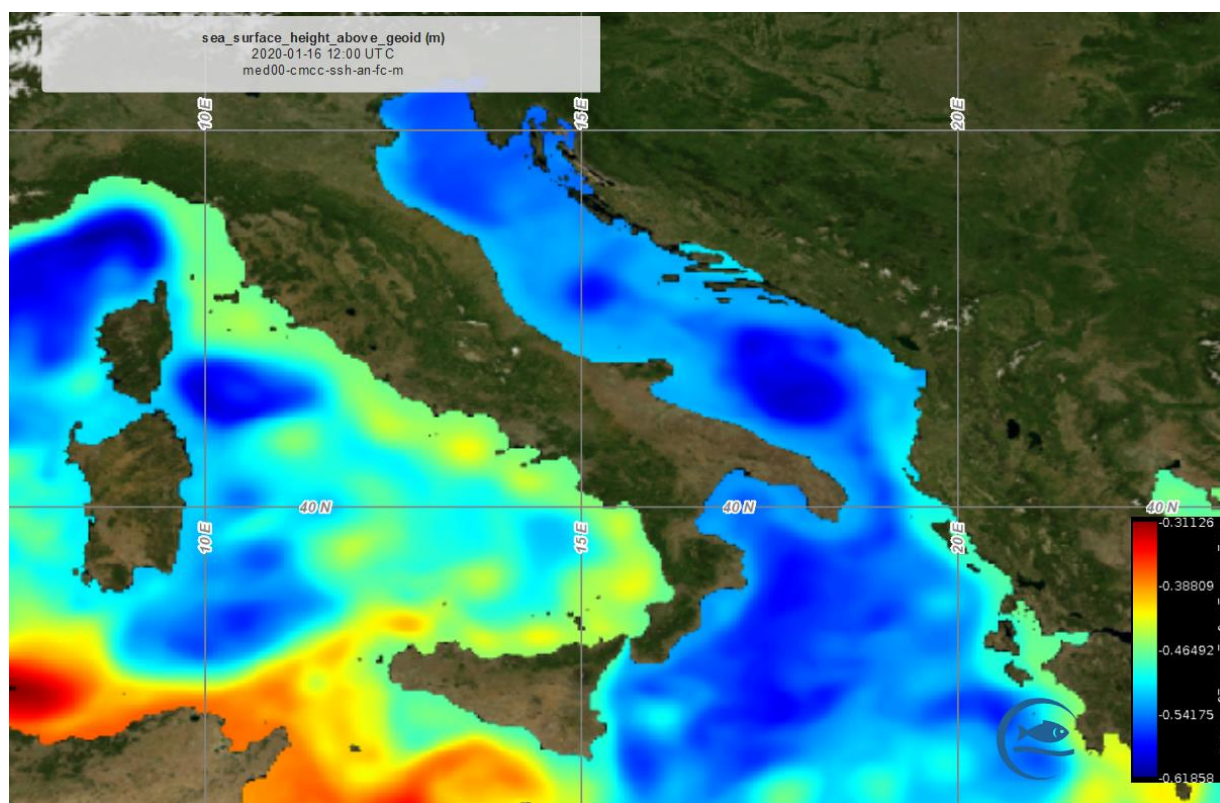


Figure 48. Sea surface height above geoid of Italian Seas [CMEMS]

4. ENERGY POTENTIAL ASSESSMENT PROCEDURE

[29] [30]

The classification of Italian seas, as a function of the power flux specific to the marine currents in synoptic scale, provides overall data to mesoscale and microscale studies aiming at exploiting energy from marine currents. A preliminary consideration, of general character, is the availability of Italian currents data. It is evident a significant lack of data and availability (in terms of free access or at least at modest costs) from Italian public organizations. Other than the Messina Strait, indeed, it was not possible to obtain adequate data of current analysis for micro-scale studies. Furthermore, the analysis in synoptic scale was introduced in this section only thank to its availability on the *MyOcean* project website.

4.1. REFERENCE MAPPING OF ENERGY PRODUCIBILITY

The downloaded data in NetCDF format was processed through Matlab software, based on which a Mediterranean map was achieved showing different specific Flux of power values (W/m^2) calculated with the following formula:

$$F_p = \frac{1}{2V} \int_V \rho v^3 dV$$

Where ρ represents water density (reference value: 1030 kg/m^3 in winter, 980 kg/m^3 in summer), v (m/s) the speed (calculated from eastward sea water velocity and northward sea water velocity provided by the website) and V (m^3) the volume of integration which the power value refers to. A uniform velocity was considered inside every calculation cell. The spatial volume of the database is about 4-7 km horizontally and with 71 levels vertically (up to the maximum depths of the Mediterranean Sea, over 5000 m). The output was produced as daily or monthly average of the velocity components. It was then calculated a year average with the most recent available data.

Maximum values were obtained around the Strait of Gibraltar (up to about 300 W/m^2). Elsewhere, specific power fluxes relatively high (between 30 e 100 W/m^2) where recorded along Moroccan and Algerian shore (influenced by the current of Gibraltar Strait) and between Tunisia and the big Italian islands. Eastward, the relative maximum can be found out at sea in front of Libya, Egypt, Turkey, shout-east of Aegean Sea, and at the Strait of Dardanelles. Finally, further north, similar levels of F_p can be reached nearby the south end of France.

Figure 49. Average specific Power flow [W/m^2] at $Z=3m$ (below)

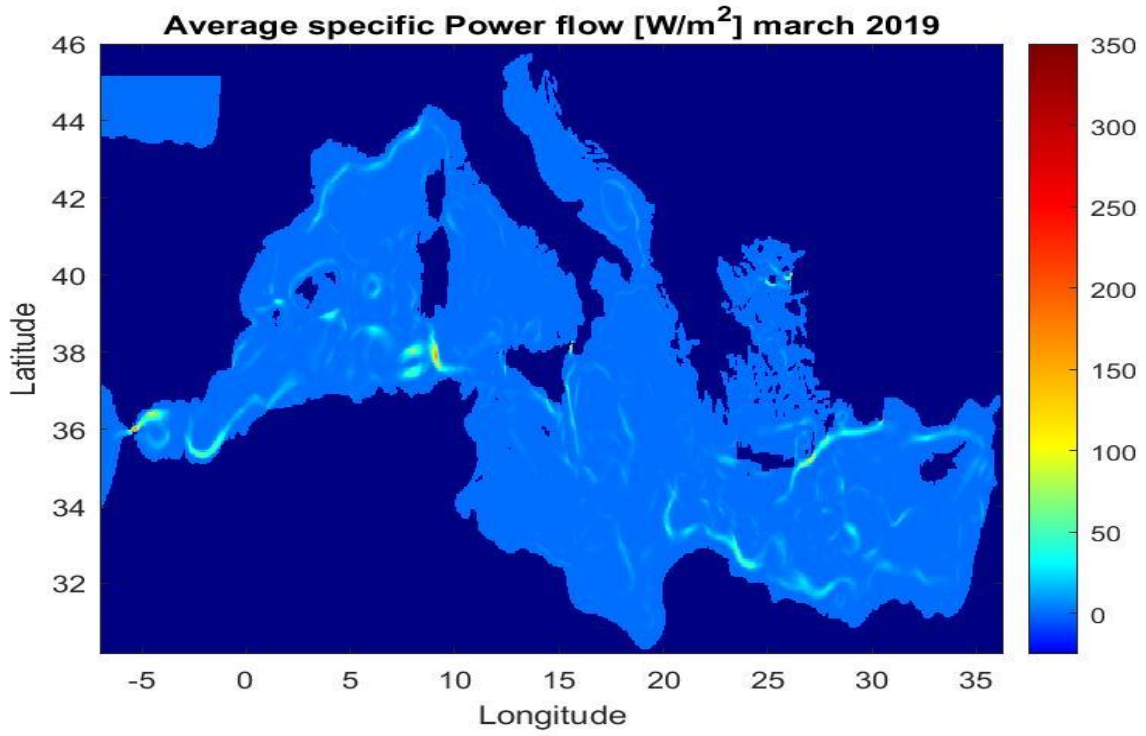


Figure 49(a). Average specific Power flow [W/m^2] in March 2019 ($Z=3m$)

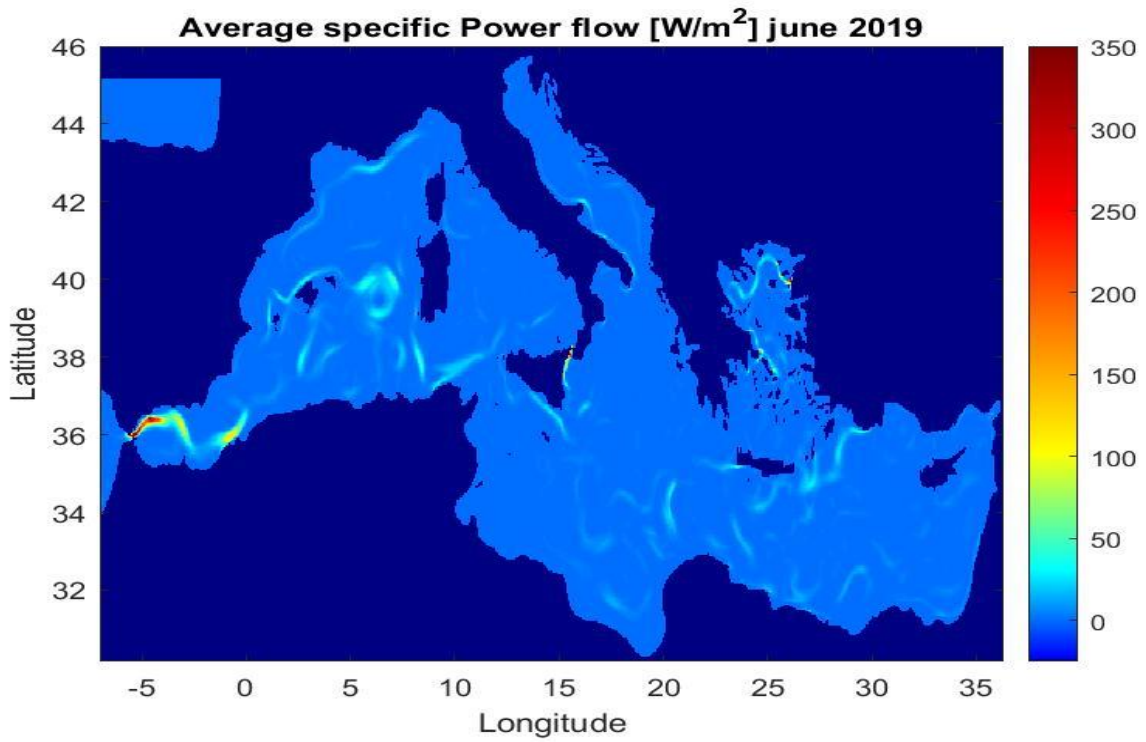


Figure 49(b). Average specific Power flow [W/m^2] in June 2019 ($Z=3m$)

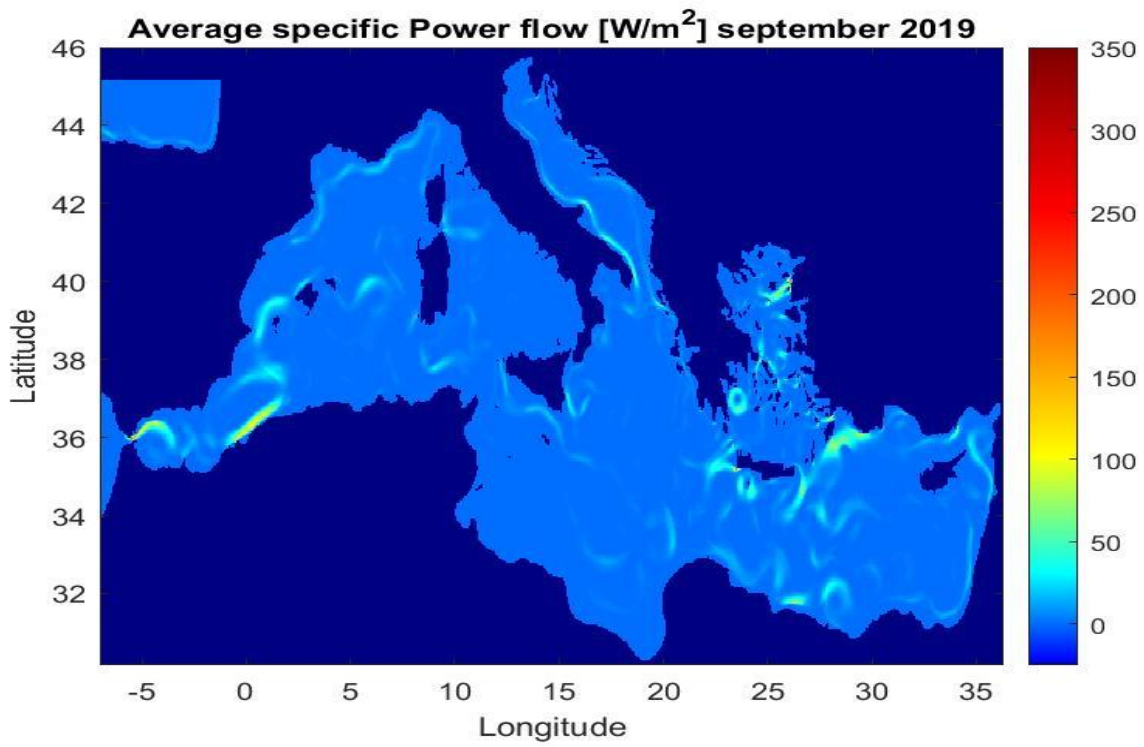


Figure 49(c). Average specific Power flow [W/m^2] in September 2019 ($Z=3m$)

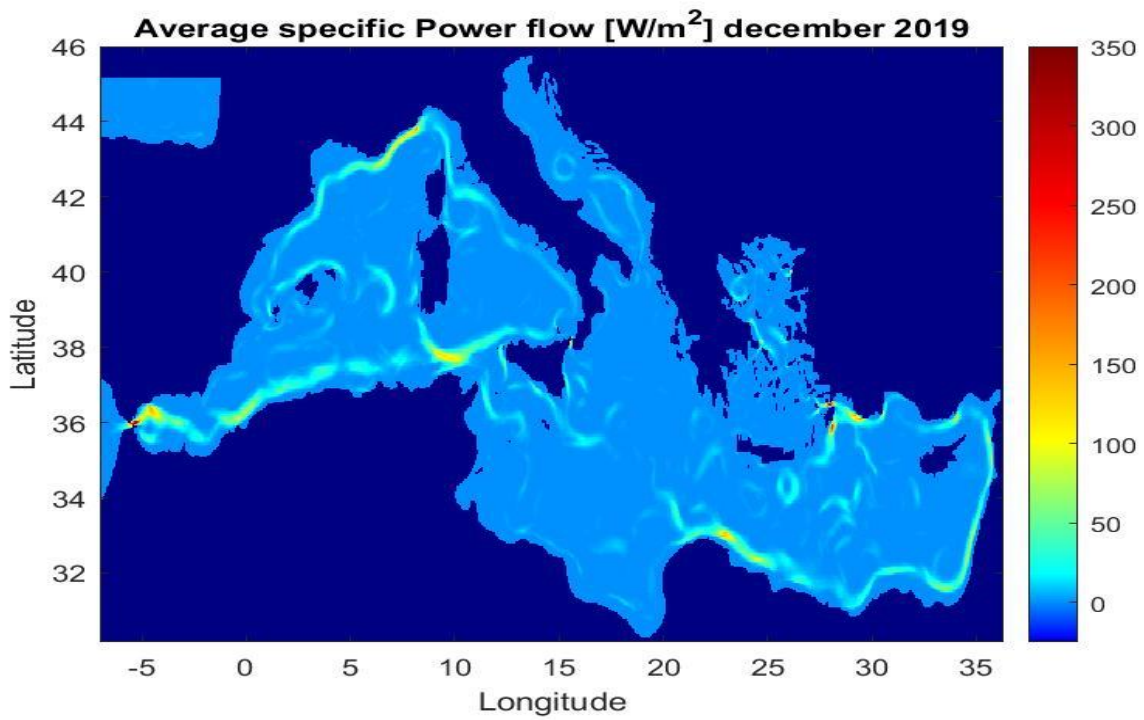


Figure 49(d). Average specific Power flow [W/m^2] in December 2019 ($Z=3m$)

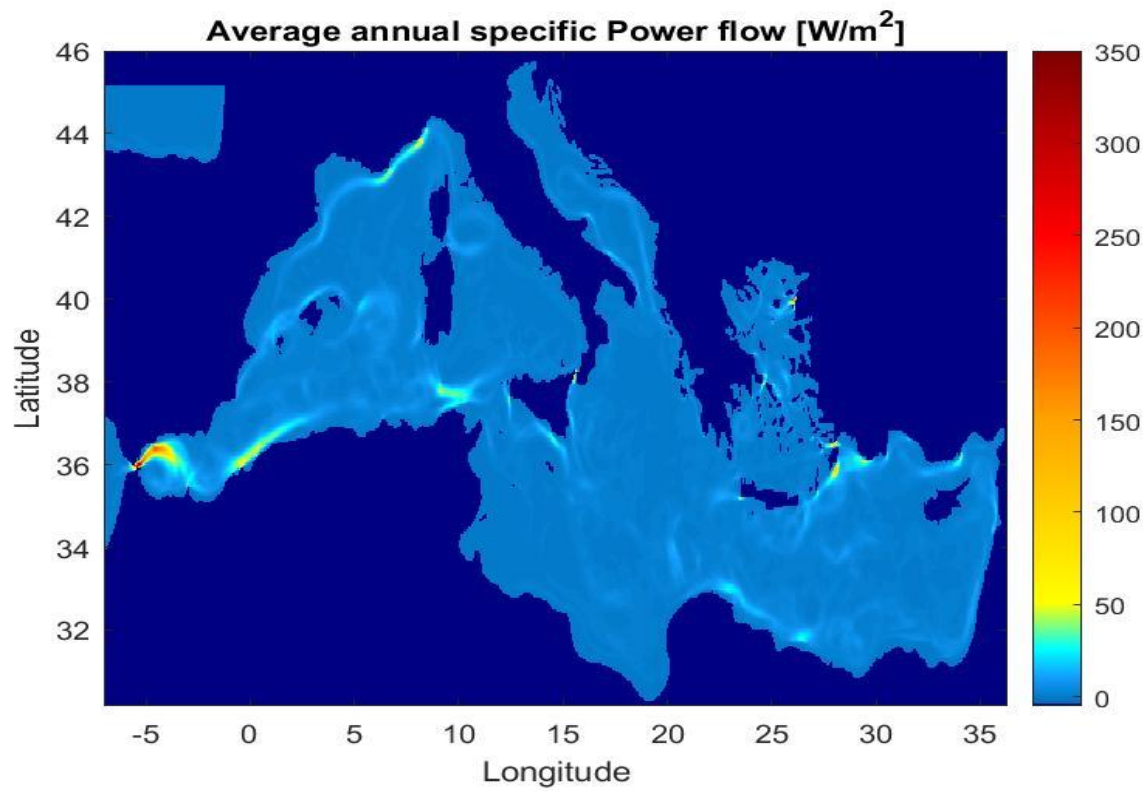


Figure 50. Average annual (03/2019-03/2020) specific Power flow [W/m^2] in Mediterranean Sea ($Z=3\text{m}$)

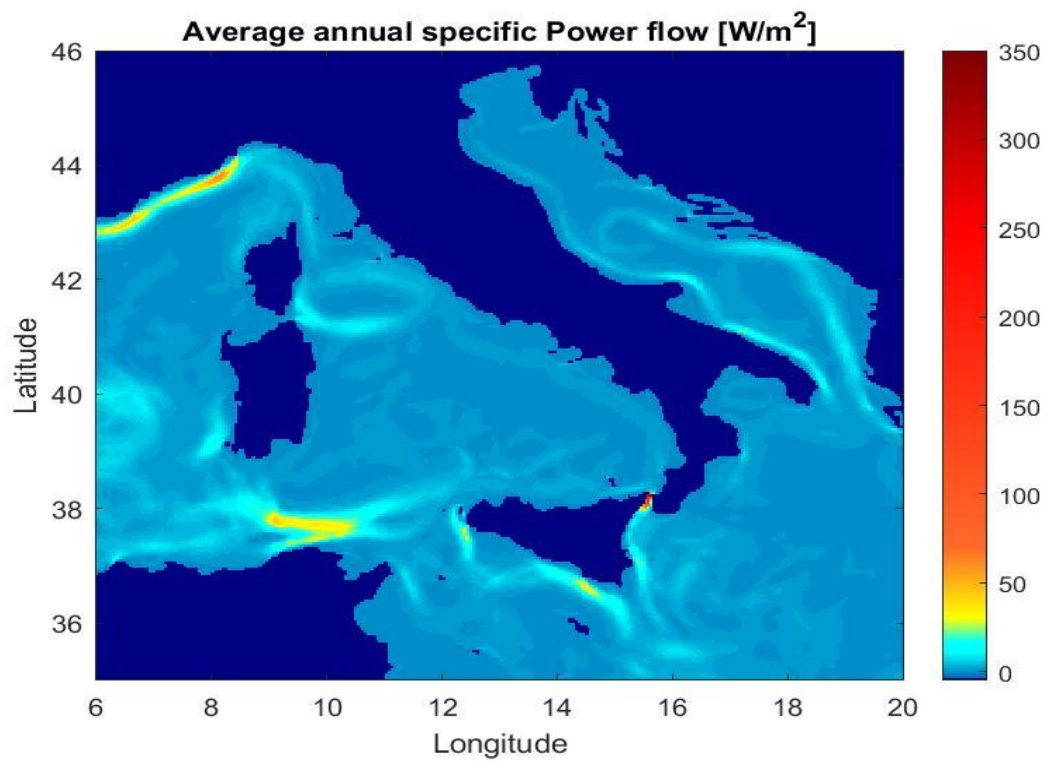


Figure 51. Average annual (03/2019-03/2020) specific Power flow [W/m^2] in Italian Seas ($Z=3\text{m}$)

As previously stated, a turbine system for energy exploitation of marine currents should be positioned as close as possible to the seashore (max distance 10 km) because of its connection requirements.

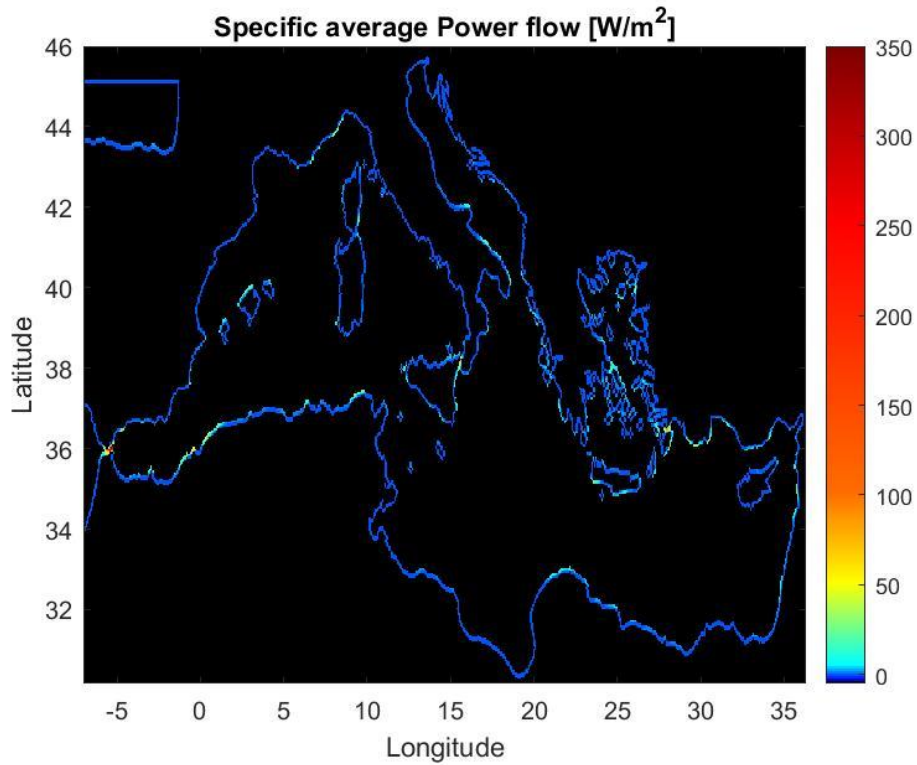


Figure 52. Average annual (03/2019-03/2020) specific Power flow [W/m²] near the coast of Mediterranean Sea (Z=3m)

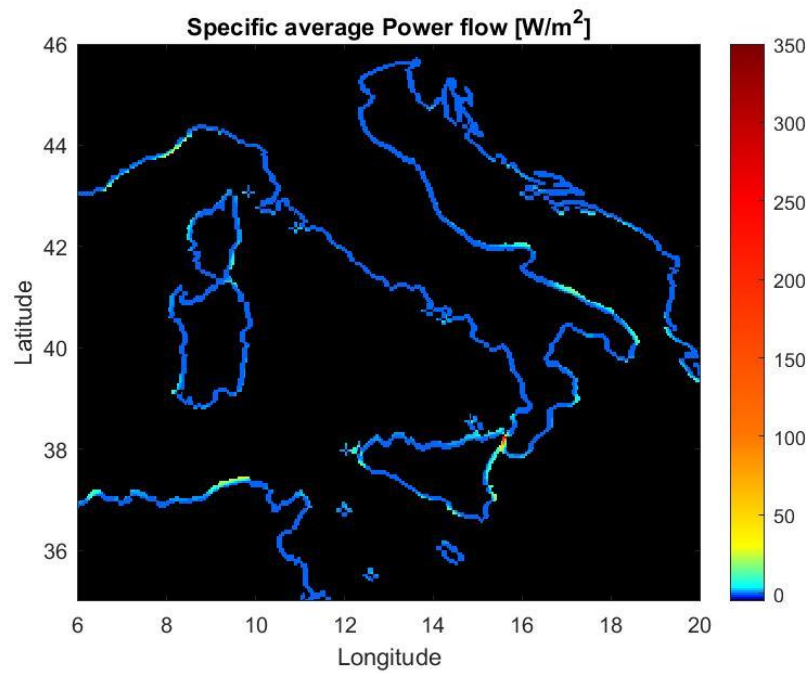


Figure 53. Average annual (03/2019-03/2020) specific Power flow [W/m²] near the coast of Italian Seas (Z=3m)

3 m depths were considered in previous maps, because higher velocity values were recorded on the superficial layer (surface currents), as shown in the diagrams below.

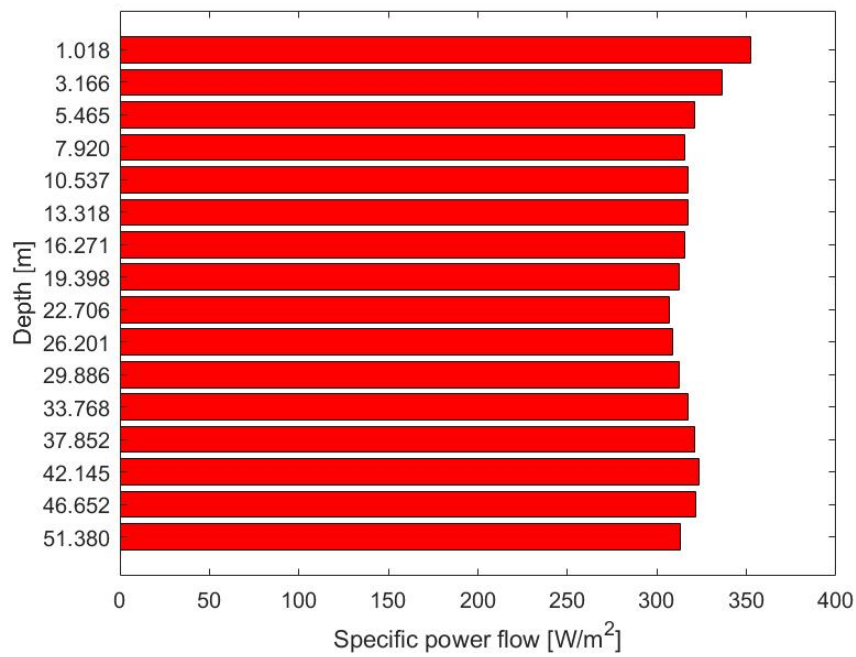


Figure 54. Max value of average annual specific Power flow in Mediterranean Sea for different depth levels

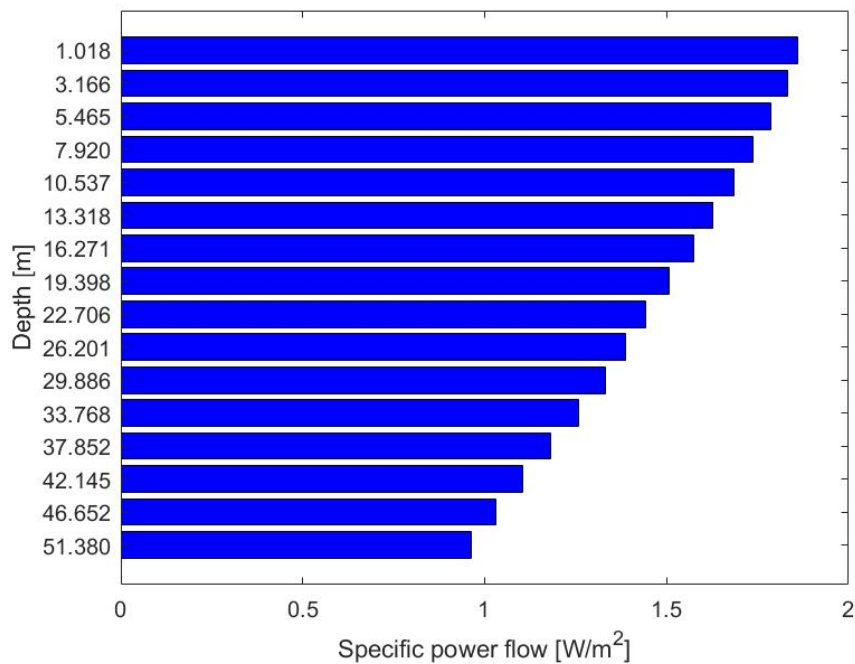


Figure 55. Mean total value of average annual specific Power flow in Italian Seas at different depth levels

It was confirmed, through the results obtained, that the Strait of Messina is the place with the highest energy potential. It was then decided to examine in depth this site to estimate the producibility of a possible plant situated in this area.

4.2. FLUID DYNAMIC MODELING AND ENERGY PRODUCIBILITY ESTIMATION FOR THE STRAIT OF MESSINA

A typical approach to properly evaluate the energy potential of a site involves the following operative steps:

- a) **Characterization of the site from an environmental point of view** through the analysis of previous current data, marine weather data and morphology data, to define the extension of the sea area being studied.



Figure 56. Strait of Messina from satellite [Wikipedia]

The Strait of Messina, border between eastern and western Mediterranean Sea basins, joins Ionian Sea to Tyrrhenian Sea, with an amplitude of 3 km between Punta Peloro (ME) and Punta Torre Cavallo (RC) and 16 km between Capo All (ME) and Punta Pillar (RC). Depths varies from about 200 m in Tyrrhenian side to over 2000 m in Ionian side. The two areas are divided by a saddle along the joining line Ganzirri-Punta Pezzo, an area of remarkable hydrodynamic importance because of the smaller depths present: a significant area fraction, in fact, results having a depth around 100 meters, presenting also numerous underwater canyons.

The Strait of Messina is of particular importance since it is possible to observe high velocity currents and a tidal range relatively low, causing intense semi-tidal currents. The total current, thanks to these characteristics combined with other factors of weather, climatic and oceanographic nature, reaches quite high values (up to 2 m/s), even though only in delimited areas. To better understand this phenomenon, when the north side of the Strait Tyrrhenian Sea is at low tide, the bordering Ionian Sea in the south is at high tide, and vice versa in the following cycle. Because of this difference in height, which tops 27 cm, the waters of one or the other basin flow alternately into the adjacent one to level out, producing, with a 6hr semi-period, a northbound current towards Tyrrhenian Sea or a southbound current to Ionian Sea. The “slope” produced is, on average, 1.7 cm per km of distance, with highest value corresponding to the ideal conjunction line between Ganzirri in Sicily and Punta Pezzo in Calabria. The stationary currents, present in correspondence of the underwater saddle, flow southbound from the surface to 30 m depth and then in the opposite direction to the seabed, topping a velocity of 0.5 m/s in particular marine-weather conditions. The simultaneous oscillation of the water masses in the strait, caused by the tides of the bordering seas, originate tide currents that, with almost the same amplitude and opposite phase, add to the stationary currents previously described. Relative speeds, along the area corresponding to the saddle Ganzirri-Punta Pezzo, reach maximum values of more than 2 m/s in both flow directions (northbound and southbound - rising and descending currents) with approximately the same intensity for the whole water mass.

Since the evaluation procedure considers the understanding of typical scenarios of currents behavior to consequently determine the location of the plant installation, a preliminary study was performed on possible restrictions from protected areas, influencing the location selection. Furthermore, Messina Strait is one of main migratory roads of Mediterranean Sea for numerous ichthyic species; between these, of particular relevance from an environmental and economic point of view are: large pelagic, such us tuna, swordfish, bonito and cetaceans such as dolphins, fin whales, and sperm whales.

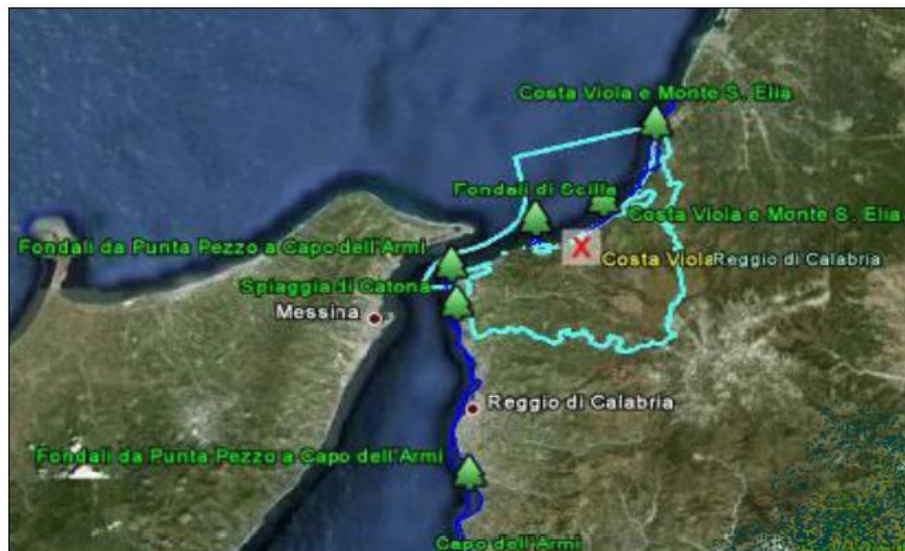


Figure 57. SIC (blue) and ZPS (light blue) on the coastal area of Reggio Calabria province [RSE]

b) *Definition of background restrictions*

This is an important aspect since local simulations, after they have been performed, are placed in large scale and general contexts. More precisely, in this phase the info regarding the general marine circulation behavior and tide levels are imposed as background conditions. In the absence of data, it is possible to utilized results from oceanographic modeling in large scale, such as those previously obtained during the mapping step.

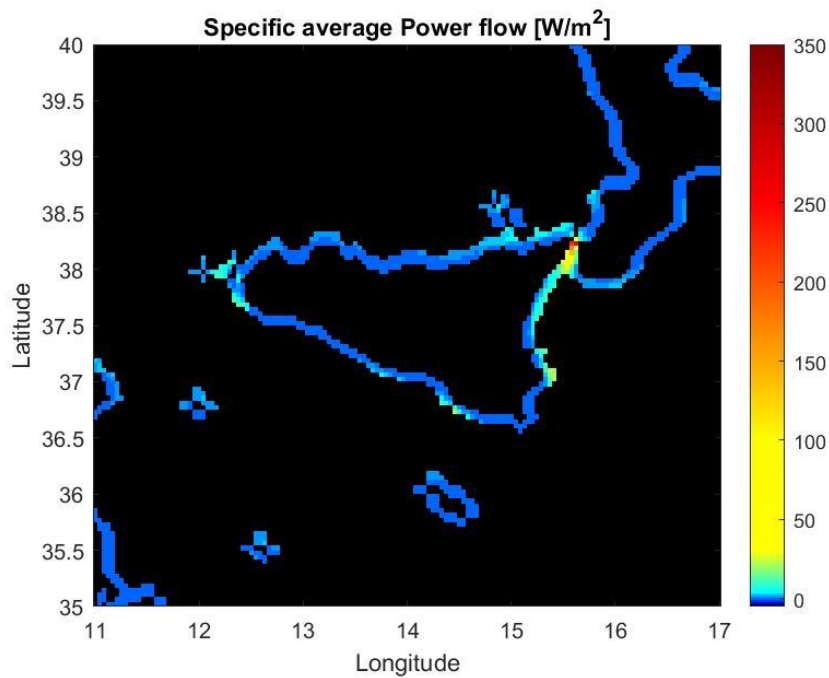


Figure 58. Average annual (03/2019-03/2020) specific Power flow [W/m^2] near the coast of Sicily ($Z=10m$)

c) *Production of a numeric model of fluidics simulation*

Numerical modelling has the objective of simulating in time the trend of the velocity field as a function of the background and marine weather conditions, to define, with the best possible accuracy, the most effective locations for energy production and the actual quantity of energy that it is possible to produce. Obviously, the more the time-space description of currents is accurate, the more accurate will this information be. The nature of the phenomena involved determines the trend of such field, whose characteristics are essentially dynamic, therefore it is necessary to use a tridimensional approach based on Navier-Stokes equations. [29 (cap.7.2)]

In this phase it is necessary to define a calculation model, to create a tridimensional bathymetry, and produce a computing spatial lattice.

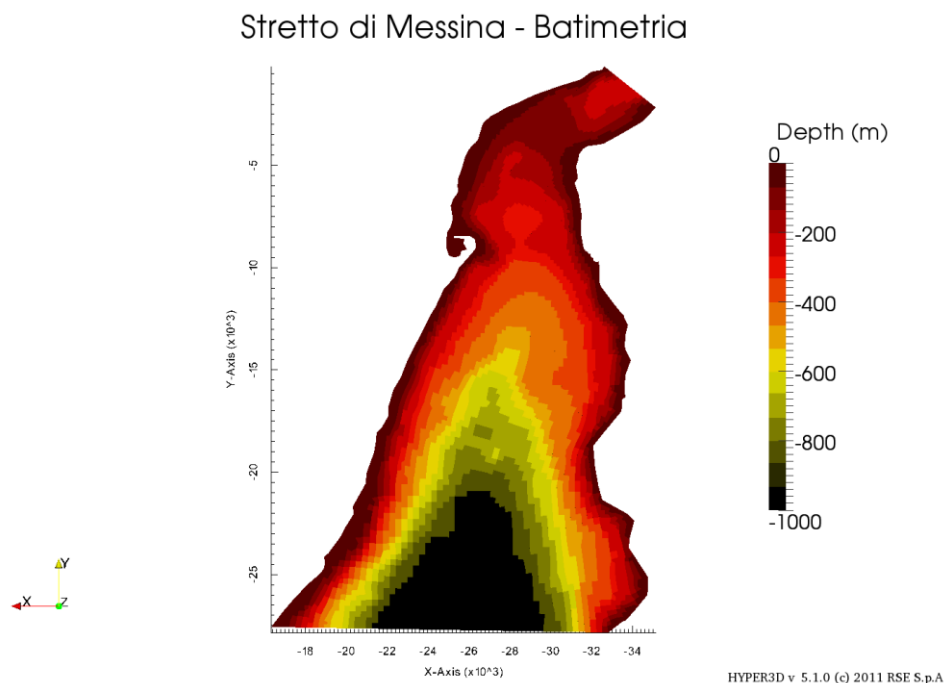


Figure 59. Bathymetry of SoM [TRITONE]

d) Definition and simulation of scenarios

In this step the scenarios characterizing the site from a current-metric point of view are selected. A typical series is represented by seasonal scenarios, for which are considered, for example, typical average data of wind, tide, temperature, and water salinity. For each scenario a simulation is performed for a period of time sufficiently long to represent seasonal trends; then the simulations are linked in series to include the whole year. Certainly, it is possible to enhance the accuracy of the simulations considering more scenarios, for example every month, but it is important to notice that phenomena connected to marine currents do not always present variability in such small temporal scales.

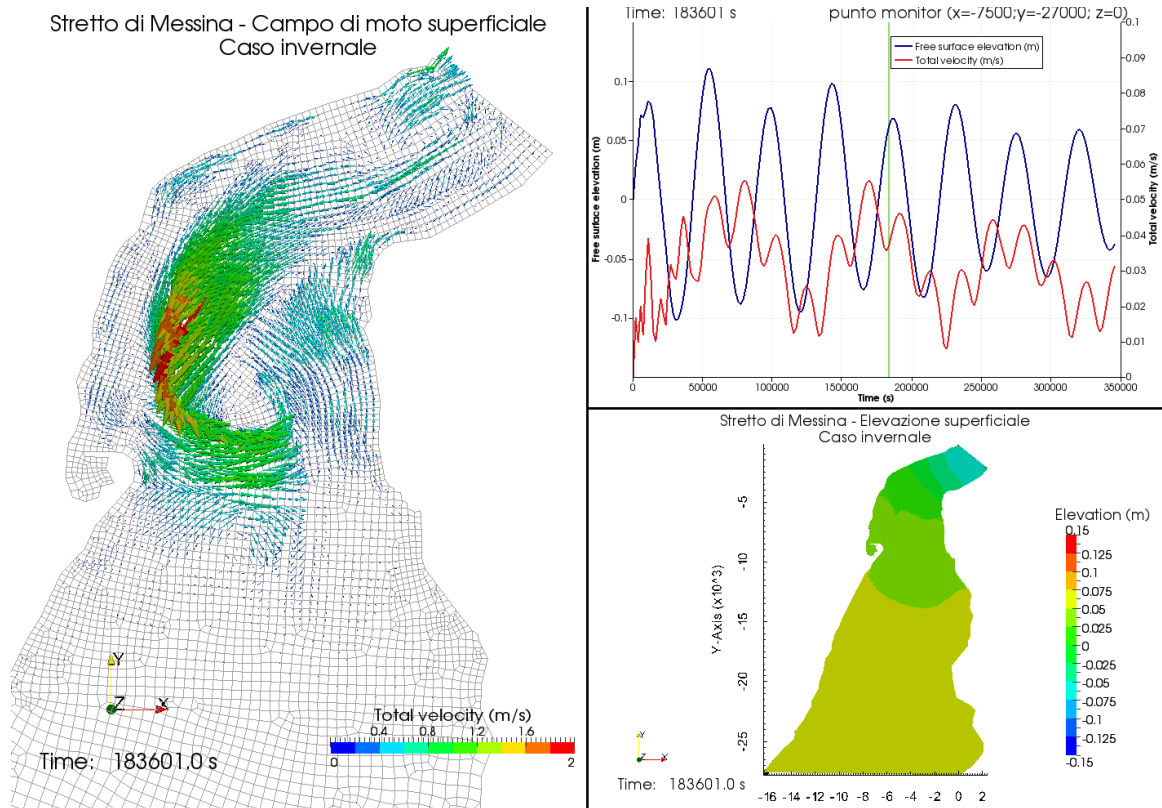
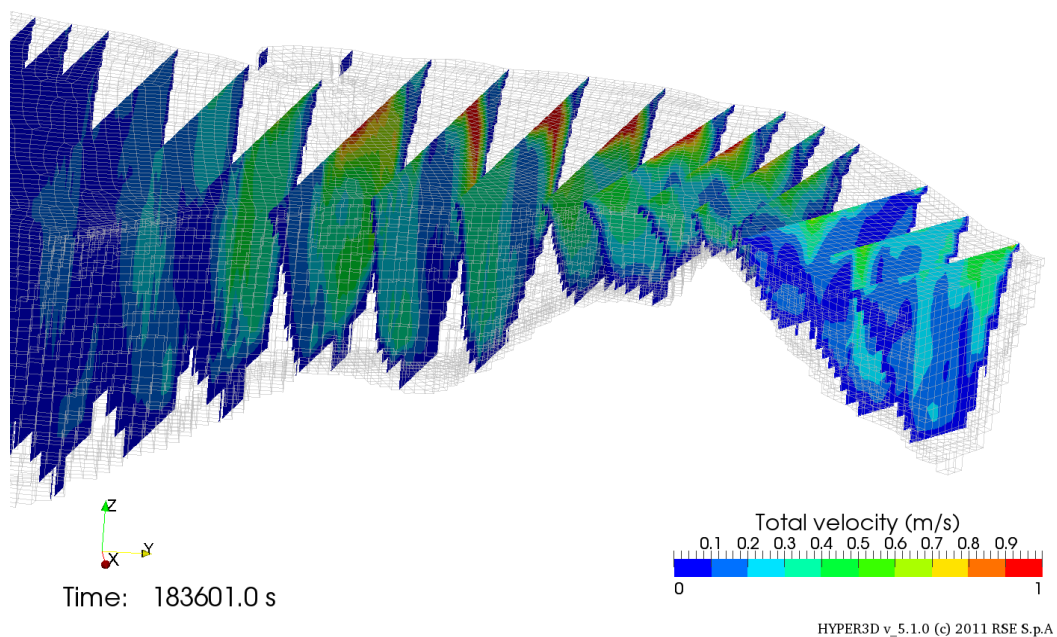


Figure 60. Example of surface flow field and surface elevation in the SoM (winter case) [TRITONE]

Table 6: Physical parameters for scenario simulation

Physical Parameters	Winter	Summer
Temperature (°C)	10	20
Salinity (‰)	38	38
Water Density (kg/m ³)	1030	998
Specific heat at constant pressure (J/kgK)	4180	4180
Water Viscosity (m ² /s)	0.002	0.002

Stretto di Messina - Campo di velocità sezioni verticali.
Situazione Invernale



Stretto di Messina - Campo di velocità sezioni orizzontali.
Situazione Invernale

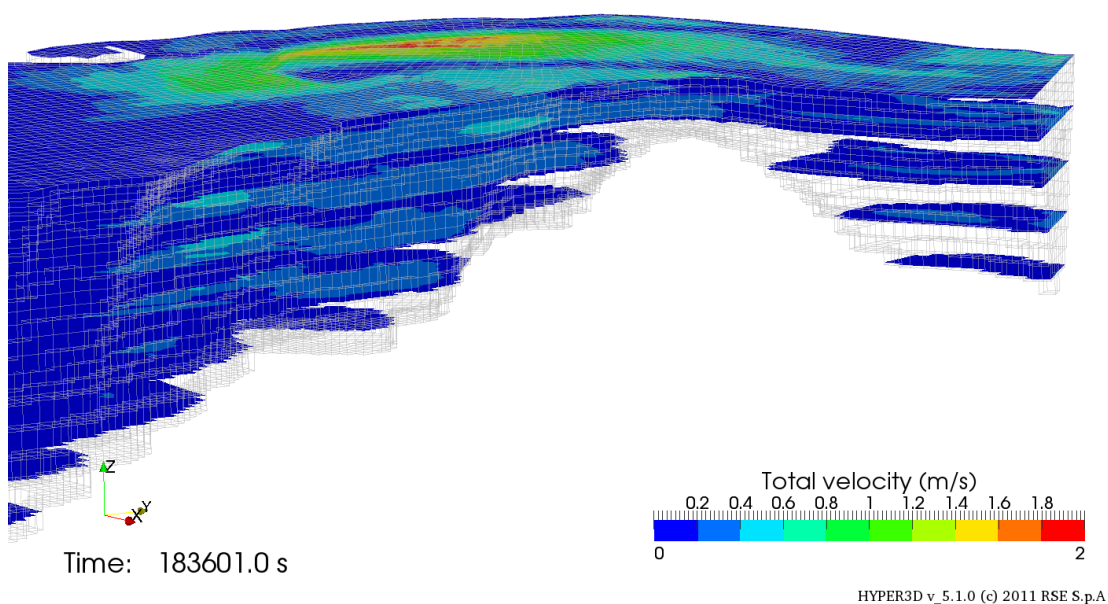


Figure 61. Example of horizontal (top) and vertical (bottom) sections of the velocity field in the SoM (winter case) [TRITONE]

e) *Analysis of energy production*

Knowing the intensity and direction of the motion field, allows to pinpoint the best position for the machine installation and, through its characteristics and performance, enables to express a prediction of the energy production over a certain amount of time.

Following this procedure, a *calculation model* was developed in RSE, through which it is possible to evaluate the average Power Flux (W/m^2), the annual average Power (kW) and the annual total Energy produced (MWh), defining the monitor reading points (6 positions, at 10, 20, and 30 m depth and 10, 20, and 30 m from the seabed), the cut-in value (m/s), the angle of inclination of current with respect to the x-axis ($^\circ$), the efficiency (%), and the active Surface (m^2) of the machine/plant.

If we consider the expression of theoretical power relative to a water flux with density ρ impinging orthogonally to a surface S with a velocity of intensity $|v|$, it is easy to demonstrate that the power per unit surface (power density) is equal to $1/2 \rho |v|^3$, from which it is obtainable the theoretical total power P_{th} , integrating on N elementary surfaces constituting the active section.

$$P_{th} = \frac{1}{2} \sum_{i=1}^N \rho_i |v_i|^3 S_i$$

If the theoretical power value in time is integrated on the entire period considered, it is possible to obtain the total quantity of theoretical energy E_{th} . However, the velocity trend can assume locally too low values to permit a proper functioning of the turbine, either because variable in time or in space. Close attention must be paid to the values below that of cut-in, for which it is necessary to calculate the total theoretical effective energy E_f considering only data to the space-time integration on elementary surfaces whose normal velocity is above the prefix cut-in value, through the Heaviside function (step) H, equal to 1, if its argument is bigger or equal to zero, or null otherwise. T1 and T2 are the extremes of the entire period of simulation, while t1 and t2 are the extremes of each elementary temporal step of simulation:

$$E_f = \int_{T1}^{T2} \sum_{i=1}^N \left(\frac{\rho_i |v_i|^3 S_i}{2} \right) H(|v_i| - |v_{i, cut-in}|) dt$$

Known the global efficiency η of the generating machine, it is possible to calculate the quantity of total energy possibly produced (E_p) in the considered period.

$$E_p = \eta E_f$$

The data of the currents are from “Istituto Idrografico della Marina – Tavole di marea 2011 Ed. Il Frangente I.I. 3133 (2010)” and “Ricerche idrodinamiche nello Stretto di Messina in vista dell’istituzione di un collegamento stabile viario tra Sicilia e Calabria - Osservatorio Geofisico Sperimentale di Trieste (1980), E. Acerboni, A. Michelato” (for more details and data on tide levels refer to [29][30]).

The results were validated comparing them to “CENEX Project Joule II – Tidal and Marine Currents Energy Exploitation. Detailed Current Analysis – Final Report B200 (1992)”.

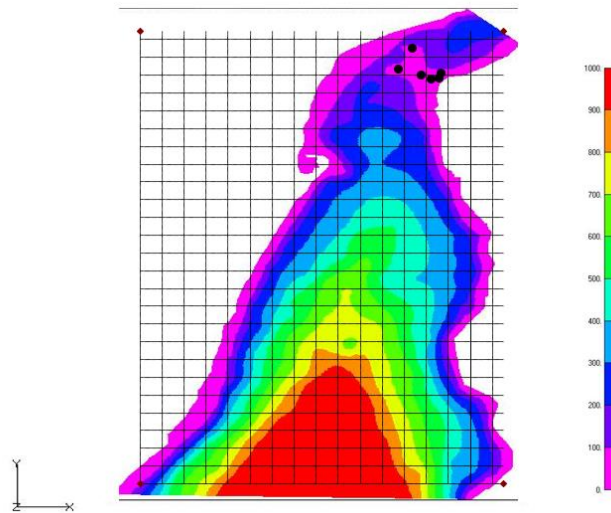


Figure 62. Bathymetry of the study area and position of monitor points [TRITONE]

The data used by RSE software are before 2011; as a reference, the mappings of the energy producibility (velocity of currents) are more recent, referring to 2019-2020. Comparing the specific power flux values of Messina Strait area with the values obtained through the calculus module just described, similar results were observed. Therefore, this data can be considered reliable for actual studies as well since they are data with a low level of variability. It was not possible to compare them directly with CMEMS because its archive does not have data prior to 2018; anyway, even with values dating back to that year, the situation is still the same.

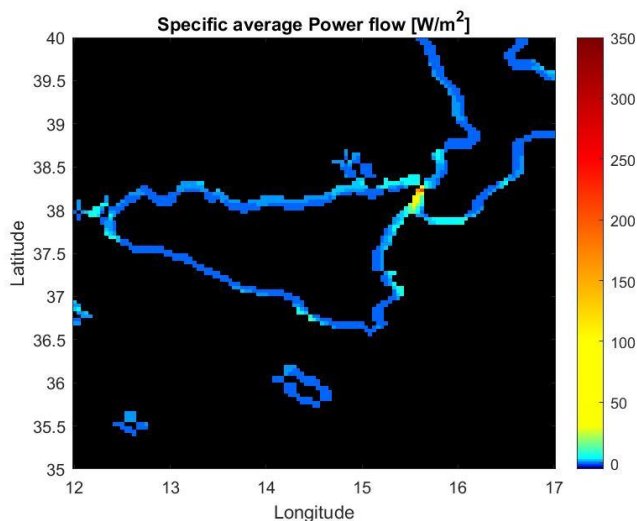


Figure 63. Average annual (2018) specific Power flow [W/m²] near the coast of Sicily (Z=10m)

Examining the characteristics of the machine considered for the study of energy producibility (a cross-flow turbine for marine currents designed by Ocean Renewable Power), it was decided to choose, among the available options, a site close to the seabed, since it is a device that needs to be anchored to it. In this area, it was placed ideally a system composed of 8 turbines in parallel, corresponding to an active equivalent section of 540 m². The area close to the seabed is known to be limiting in terms of producibility, therefore an analog theoretical study was performed considering a system of virtual turbines with the same characteristics but positioned less deeply.

Table 7: Results for the hypothetical floating system (first) and for the anchored system (second) from Web-GIS TRITONE

Assumptions	
Cut-in value (m/s)	0.8
Efficiency (%)	25
Section Area (m ²)	540

Monitor Point (X;Y node)	Depth (m)	Section Orientation (°)	Specific average Power flow (W/m²)	Annual average Power (kW)	Annual Energy produced (MWh)
1 (-2230; -4000)	10	125	1125.62	151.96	1331.16
7 (-1780; -4200)	10	145	639.03	86.27	755.72
13 (-1410; -4130)	10	140	199.79	26.97	236.27
18 (-1320; -3890)	10	115	440.97	59.53	521.50
24 (-2660; -2490)	10	115	746.26	100.75	882.53
30 (-3260; 3665)	10	125	888.58	119.96	1050.84

Monitor Point (X;Y node)	Depth (m) (seabed)	Section Orientation (°)	Specific average Power flow (W/m²)	Annual average Power (kW)	Annual Energy produced (MWh)
5 (-2230; -4000)	70 (80)	125	14.00	1.89	16.55
11 (-1780; -4200)	50 (60)	145	2.58	0.35	3.06
17 (-1410; -4130)	50 (50)	140	0.00	0.00	0.00
21 (-1320; -3890)	50 (60)	135	15.99	2.16	18.91
27 (-2660; -2490)	70 (90)	115	149.33	20.16	176.59
28 (-2660; -2490)	80 (90)	115	43.93	5.93	51.96
34 (-3260; 3665)	80 (90)	145	23.21	3.13	27.45

For the floating system of hydraulic turbines, the point optimizing the energy producibility is represented by monitor 1, placed at depth -10 m, with positioning to current direction of 125° (with respect to the x-axis). The annual energy that can be produced is 1300 MWh (about 150 kW of equivalent average power).

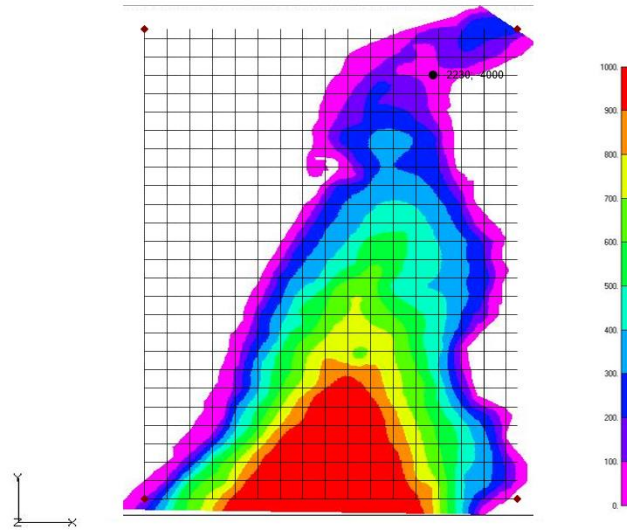


Figure 62(b). Bathymetry of the study area and position of monitor point 1 ($Z=10m$) [TRITONE]

For the anchored system of hydraulic turbines, the point optimizing the energy producibility is represented by monitor 27, positioned at depth -70 m, with positioning to current direction of 115° (with respect to x-axis). The annual energy that can be produced is 180 MWh (about 20 kW of equivalent average power).

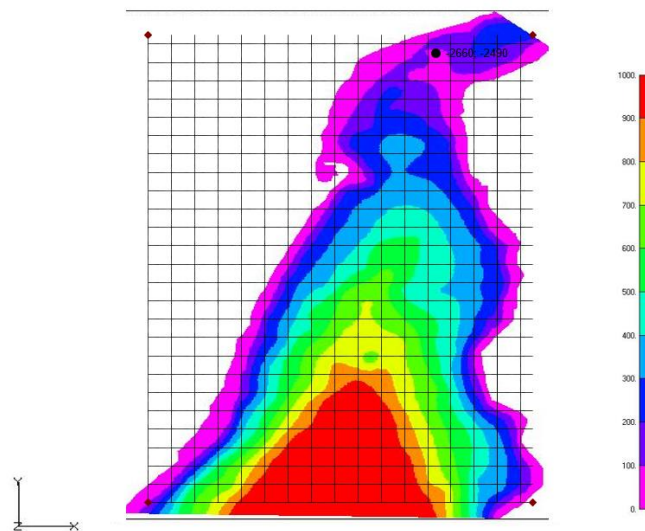


Figure 62(c). Bathymetry of the study area and position of monitor point 27 ($Z=70m$) [TRITONE]

4.2.1 Modelling and Simulation of Tidal Current Turbine System

[31] [32] [33]

Optimum points for the installation of a tidal current turbine system identified in the Strait of Messina are in the areas of Punta Pezzo and Ganzirri. Therefore, it was decided to model and simulate a potential system sited in these locations. The main components are tidal currents, tidal currents turbine, the mechanical drive train, and the generator.

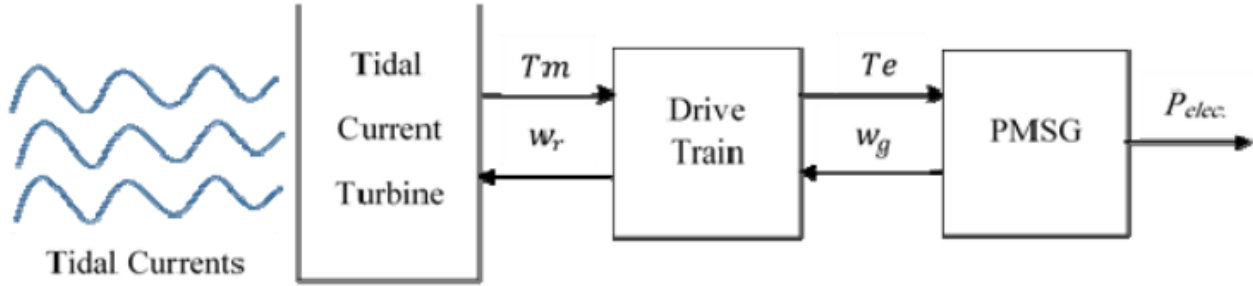


Figure 64. Tidal current energy system

The current velocity data are the same used for the energy producibility mapping created previously; obviously, not having such detailed spatial data, the maximum mean value of the Strait was considered, and it was modeled as a flow of harmonics in accordance with the following equation:

$$v(t) = \sum v_i \cdot \sin(2\pi f_i t + P_i)$$

Where, v_i is the amplitude, T is the period and P_i is the phase for i -th harmonic constituents.

The phenomena that are at the origin of the tides are linked to astronomical and meteorological components that can be easily correlated to the geographical position through coefficients of harmonic expressions known from appropriately coded tables. This method makes it possible to know the level of the tide at a given instant by adding the values of some sine curves deriving from variations in declination, parallax and other alterations produced by the motion of the Moon and the Sun. These curves are linked to various harmonic components, but normally at least five are used characterized by the abbreviations M2, S2, N2, K1, O1.

The harmonic components are described and reported in Table 8 through which the Simulink model gives the tidal turbine speed profile as in Figure 66. The latter repeats in similar way throughout the year.

Table 8. Tidal harmonic components of the main sequence in the Strait of Messina according to ENEL monitoring

		DIURNAL	DIURNAL	SEMI-DIURNAL	SEMI-DIURNAL	SEMI-DIURNAL
POINTS		O1	K1	N2	M2	S2
		(main Lunar)	(Sun-Moon Declination)	(major Lunar elliptical component)	(main Lunar)	(main Solar)
	Period (h)	25.82	23.93	12.66	12.42	12.00
PUNTA PEZZO	Phase (d°)	235	226	198	143	37
GANZIRRI	Phase (d°)	214	242	290	216	364

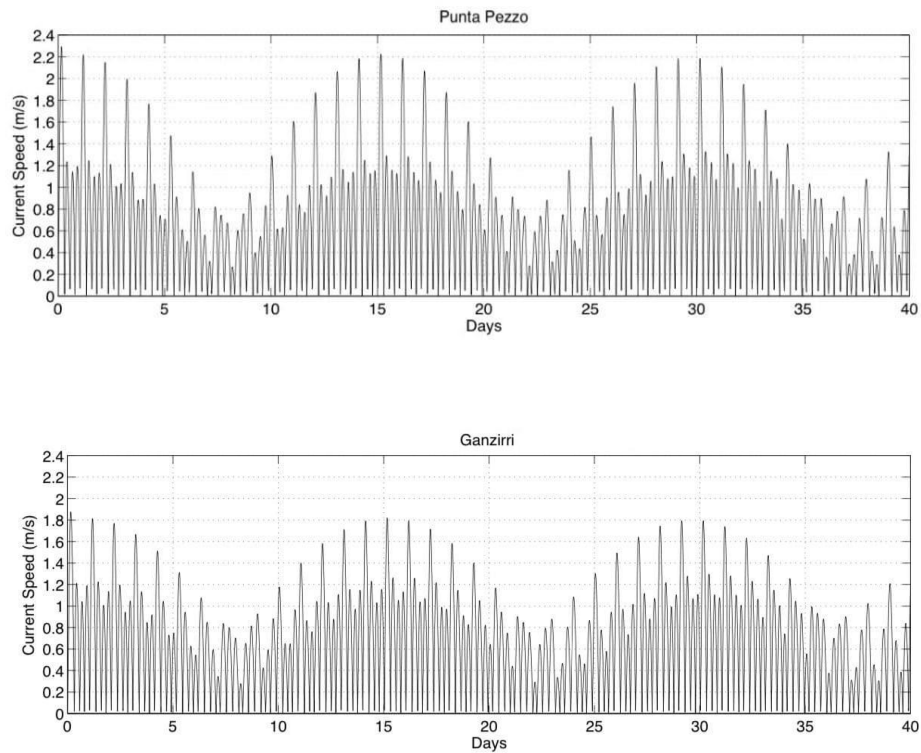


Figure 65. Tidal current speed profile for 40 days in Punta Pezzo (top) and Ganzirri (bottom)

In the previous paragraph it was found that the optimal depth in Punta Pezzo is 10 m (sea surface), while in Ganzirri is 70 m. In the first case, therefore, a floating system would be suitable, while an anchored system to the seabed would be better in the second one: they could be the already mentioned FRI-EL SEA Power and OpenHydro, respectively. Thanks to the Permanent Magnet Synchronous Generator (PMSG), suitable for low tidal current velocities, with no need for gearbox and able to provide more details, we have chosen to consider the latter for the modeling work here presented. It is also relatively easy to build since it has no depth range for installation, low maintenance requirements, and it can operate in bidirectional tidal flow. The main features are a rotor diameter of 15 m, a cut-in speed of 0.7 m / s and a rated power (at $v = 2.57$ m / s) of 1.5 MW.

As already seen in *paragraph 1.5*, the power available in tidal currents is proportional to the cube of the current speed, and the actual power is given by:

$$P_{act} = 0.5\rho C_p(\lambda, \beta) A v^3$$

$$\text{with } C_p(\lambda, \beta) = c_1 \left(\frac{c_2}{\lambda i} - c_3 \beta - c_4 \right) e^{-c_5/\lambda i} + c_6 \lambda$$

$$\text{and } \lambda i = \frac{1}{\lambda + 0.08 \beta} - \frac{0.035}{\beta^3 + 1}$$

C_p cannot exceed 0.593 according to Betz's limit, and with $c_1=0.5176$, $c_2=116$, $c_3=0.4$, $c_4=5$, $c_5=21$, $c_6=0.0068$ we obtain $C_{p,max} = 0.48$ for $\lambda=6.5$ and $\beta=0$ degree (pitch angle).

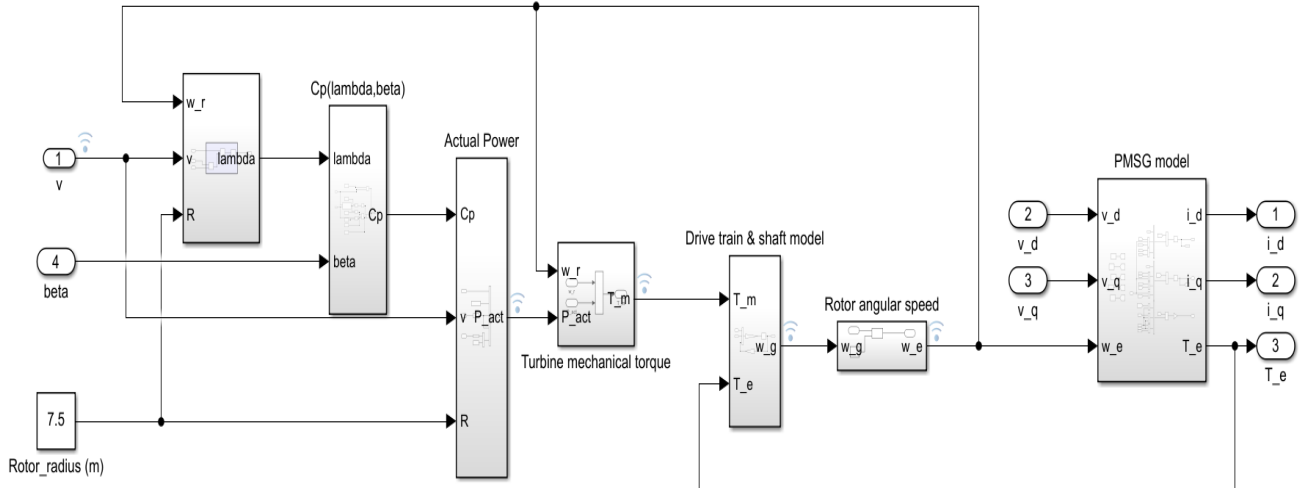


Figure 66. Simulink model of tidal current turbine

The drive train is the connector that delivers the turbine rotor mechanical motion to the generator. Direct drive transmission is used in case of multi-pole synchronous generator.

For the model, efficiency was assumed to be constant, and the effect of the construction features on its performance is neglected.

The system can be considered as a set of discrete masses, so that the drive train can be modeled by the equation:

$$j \frac{dw_g}{dt} = T_m - T_e - V_f w_g$$

$$\text{with } T_m = \frac{P_{act}}{w_r}$$

where j is the summation of rotor and generation inertia, T_m is the turbine mechanical torque, w_g is the generator angular, w_r is the rotor angular speed, T_e is the generator electromagnetic torque and V_f is the viscous friction coefficient. Below the mathematical model is presented.

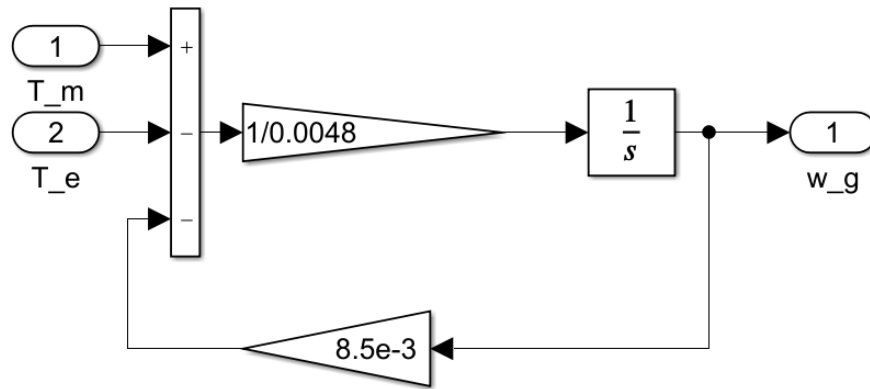


Figure 67. Simulink drive train and shaft model

PMSG has several advantages such as its simple structure, self-excitation capability leading to high power factor, high efficiency operation, and it was preferred over other types of generators because due to low speed operation there is no need for a gearbox, which often makes the system unreliable.

The mathematical model according to the synchronous d-q reference frame is given by:

$$V_d = -L_q I_q \omega_e + L_d \frac{dI_d}{dt} + R I_d \quad \text{direct stator Voltage (V), Inductance (L), Current (I)}$$

$$V_q = L_d I_d \omega_e + L_q \frac{dI_q}{dt} + R I_q + \omega_e \phi_{pm} \quad \text{quadrature stator Voltage, Inductance, Current}$$

$$\phi_d = L_d I_d + \phi_{pm} \quad \text{direct stator Flux and permanent magnet Flux}$$

$$\phi_q = L_q I_q \quad \text{quadrature stator Flux}$$

$$\omega_e = P \omega_g \quad \text{electrical (rotor) and generator (stator) angular velocity, number of poles (P)}$$

And so the electromagnetic torque:

$$T_e = \frac{3}{2} P [(L_q - L_d) I_d I_q + I_q \phi_{pm}]$$

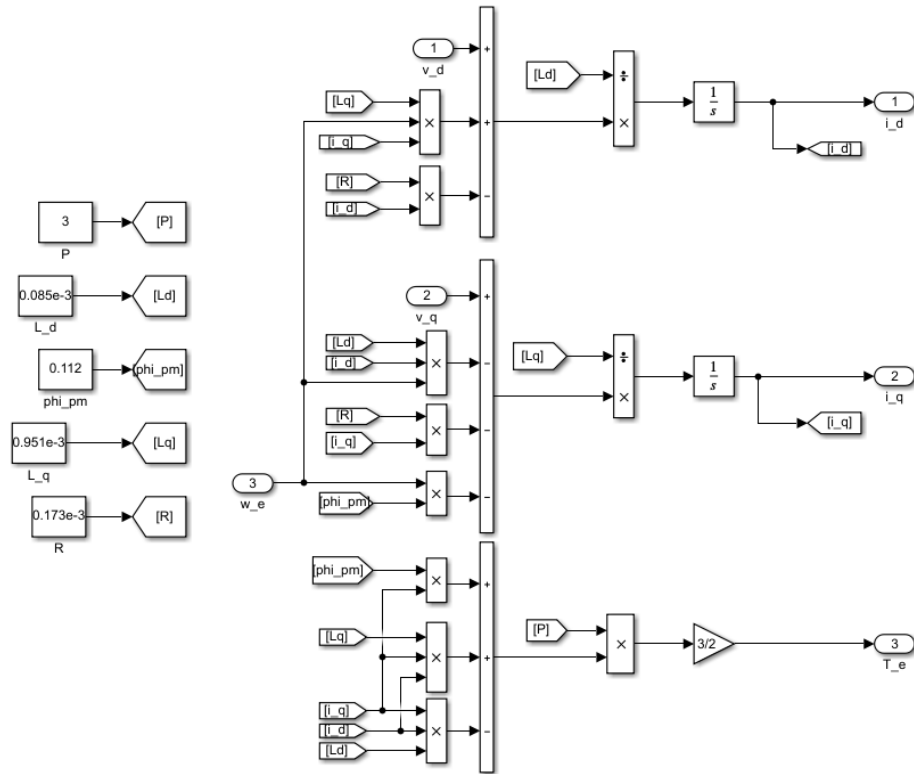


Figure 68. Simulink model for PMSG

The simulation with tidal current speed of 1 m/s shows a resulting power = 85 kW at steady state conditions (reached within a short time, 0.075 s) which corresponds to the one calculated by the equation according to turbine parameter. Therefore, the power curve verifies the validity of the model.

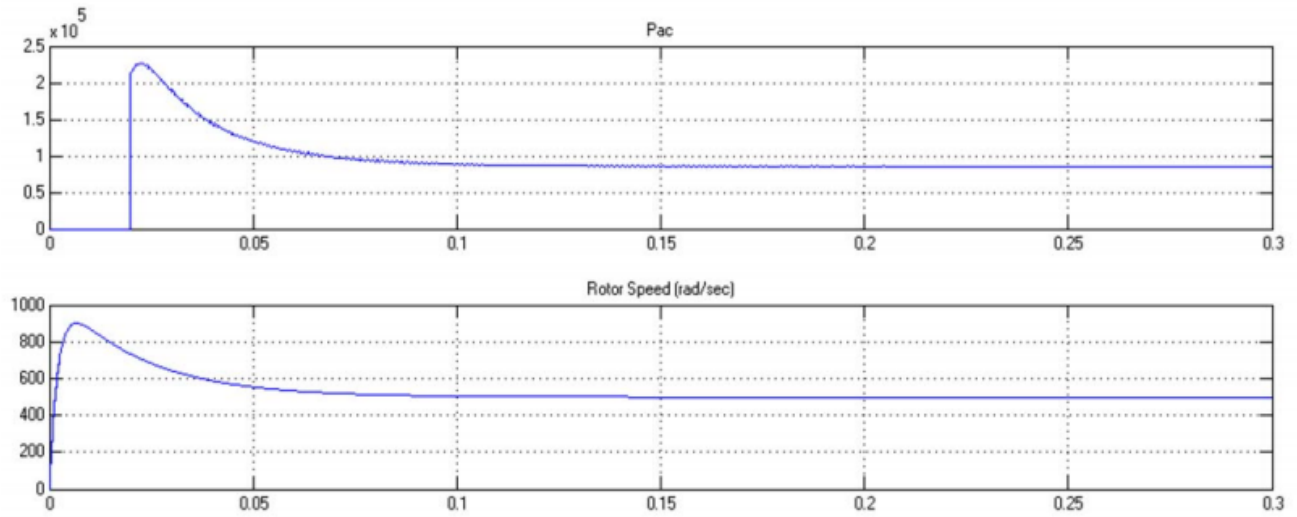


Figure 69. Power and rotor angular speed at tidal current speed $v=1$ m/s

4.3. NUMERICAL ANALYSIS PROCEDURE FOR A GENERATING MACHINE

Currently no turbine for marine currents seems to be working in Italian waters, except for some experimental devices operating in Messina Strait. The availability of a complete map of Italian seashore energy potential suggested to set up a procedure to evaluate, as a first approximation and in simple way, the capacity of a generating machine to operate in mapped conditions on a specific site.

The procedure presented that follows is the one described in *Report RSE I2000353* of 2012 [30], inclusive of results obtained. It contains characteristics to provide an evaluation of the turbine itself (at machine level) to study the power of the marine current exploited by the machine, directly estimating the fluidics efficiency, with the final goal to provide the methodological elements to verify and choose turbines for marine currents.

The necessary steps are then reposed: the assessment of possible restrictions concerning the characteristics of Italian marine currents, the building of the machine geometry, the production of a calculation grid, the definition of the fluid-dynamical model and the configuration of numerical simulations and, finally, the analysis of the results.

The study objective is to verify the assigned operational points and to identify the optimal range of machine performances. Given its general characteristics, the proposed procedure represents a simple and basic numerical tool to choose, verify, and optimize turbines for the exploitation of energy from marine currents.

- a) **Qualitative assessment of the machine characteristics** according to functional and environmental restrictions required by operational conditions.

To evaluate an electrical motor to exploit energy from marine currents specific of Italian sites, it is opportune that it satisfies a series of preliminary conditions, both of functional and environmental type. A summary of the concerning functional characteristics is shown below:

- Low current velocity operation (reference value between 0.5 m/s and 1.5 m/s). The turbines, specific for the exploitation of energy from marine currents (both vertical and horizontal axis, airfoil, propellers, crossflow type), reach, in ocean applications, maximum power of few hundreds of kW and refer to undisturbed currents with velocity of at least 2 m/s. This is quite the opposite for what concerns Italian sites, whose reference velocity reaches normally up to 1.5 m/s. Among the above-mentioned turbines, only the crossflow model, designed by Ocean Renewable Power, seems to present acceptable efficiency at lower values, down to 0.8 m/s. A proper machine for Italian sites should have an adequate efficiency at low operating velocity.
- Setting of operational depth. Usually, currents reach top speed near the surface layers or, in any case, at a depth sufficiently distant from the seabed. Generally, the depth corresponding to the maximum speed varies in time. It would be useful to have a depth adjustment system to properly adapt the operational depth, position the turbine far enough from the seabed. This characteristic would prevent problems caused by gathering of sediment inside the machine body and its erosion or abrasion.

- Multi-directional plants. Marine currents can show a predominant direction (due to geomorphologic characteristics of seabed and/or islands and tides), but it is present a substantial variation in time. Furthermore, the current driving direction is important. It is then advantageous to have a machine capable of rotating on its vertical axis in function of the instant direction of the flow.
- System maintenance. The machine should be equipped with specific corrosion and erosion prevention systems and a lubrication device, considering its peculiar site of application.

To properly evaluate the environmental impact, as previously described, it is necessary to analyze the following steps:

- Respect of land use restrictions.
- Consequences on landscape and visual impact.
- Consequences on marine ecosystem (thermal and acoustic impact). A possible preventive action could be the use of sonar systems, deactivating the turbines when marine mammals are close to the site.
- Consequences on anthropic activities (fishing, maritime transportation).
- Biocide release (anti-algae) and lubricating greases; biocide control organism growth or deposit formation on submerged structures (fouling). The best solutions could be the use of self-lubricating turbines or of biodegradable fluids.
- Consequences on possible loss of scrap material caused by damage to the plant.
- Electromagnetic consequences. Generated electromagnetic fields are not negligible in the immediate areas of the plants. Here it is possible to record values over the guideline limits for population exposure. Burial cables can reduce the issue, but they increase the cost and causes damage to the seabed during the excavation processes and possible sediment lift effect.
- Possible consequences to oxygen and nutrient recirculation, due to local currents inhibition, particularly in the event of turbine usage on a great scale.

The turbine considered as an example is a prototype machine available at RSE in the “Ricerca di Sistema” scope, originally employed in fluvial currents. The machine characteristics conflict with the above-mentioned restrictions showing some critical issues; but it is important to keep in mind that the analysis is performed regardless of the results, since it has methodological value aiming at validating the proposed procedure and not at proposing any specific machinery. ANSYS software has been employed.

b) Geometric designing of the machine

The geometry of the machine was conveniently simplified as compared to the original design, to reduce the calculus data necessary to the preliminary study; the original design was not planned to be employed in this kind of application, anyway. It was a centripetal turbine, provided of a conveyor, 4 blades rotor, and diffuser.

The geometry was found out defining the main sections of the machine and deducing the connecting surfaces: the stator, the stator-rotor interface, and the pivot (holding the blades); this is not true for the cylindrical bodies.

The geometry was divided in two lower domains: one internal to the other: the rotating one (rotor) and the static one (stator, conveyor, and diffuser).

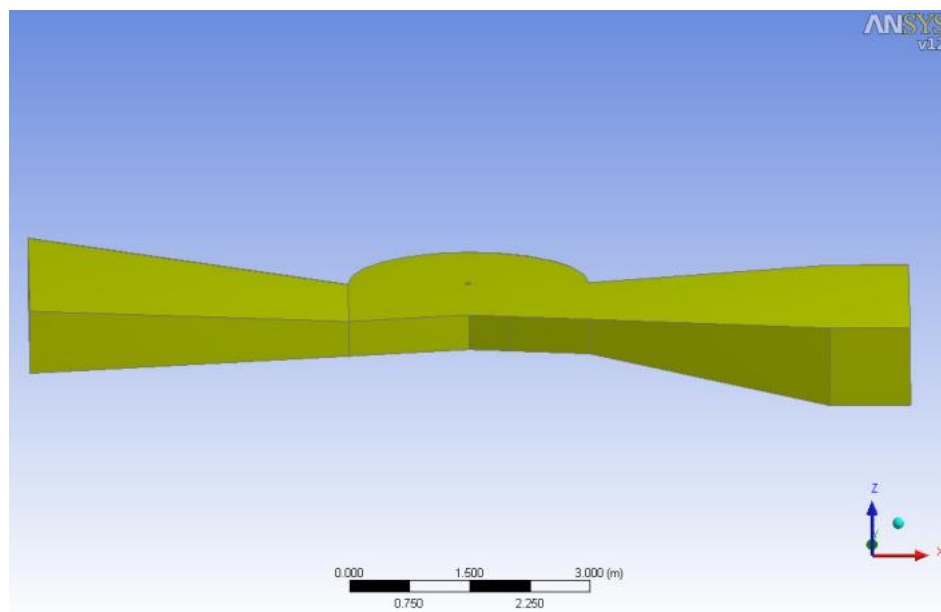


Figure 70. Reconstruction of the turbine geometry [Design Modeler, ANSYS from [30]]

c) Calculation grid development

The lower domain's geometries were utilized to develop a calculation grid. They were firstly optimized to avoid ambiguity in points, lines, surfaces, and volumes definition. Then, a tridimensional calculation grid was generated on the entire domain with tetrahedral and triangular elements; the latter were placed nearby the bordering surfaces (solid walls and stator-rotor interface). This first grid of tetrahedrons and triangles was then modified near the calculus surfaces (walls and interface) with prismatic and quadrilateral elements, so that they could accurately reproduce the limiting layers. The smoothing of the grid was then performed for the most distorted and low-quality elements.

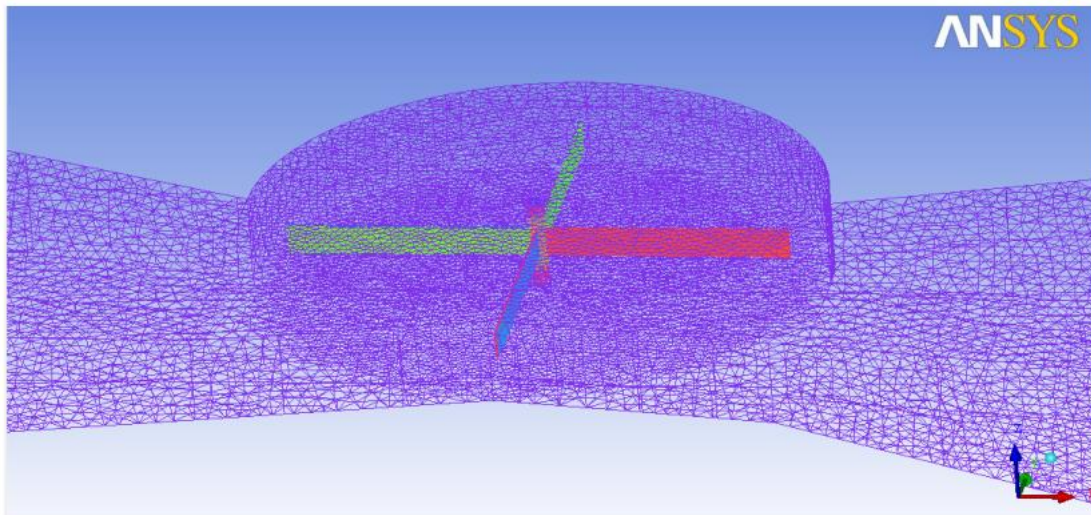


Figure 71. Representation of the computation domain surface grid [ICEM-CDF, ANSYS from [30]]

d) Definition of the fluid-dynamical model

Constituting a fluidic model concerns the choice of a system of equation to be solved, the definition of the background conditions, the monitoring variables, and the other parameters of input in the simulation.

Even if the velocities considered are relatively low (from 10^{-1} to 10^1 m/s) it was decided to solve, as default, “Reynolds Averaged Navier-Stokes” model for turbulent motion regimes. The unknown fluidic variables are then the pressure and the components of velocity (eventually the turbulent kinetic energy and its dissipation rate). The initial conditions of the reference simulation were assigned recalling a preliminary simulation. The results obtained from this type of simulation represent the input fields for the actual simulation.

As for the background conditions the flow (and so the velocity) was fixed in input section, while pressure (101300 Pa) was set by the barycenter of the output section. To relate the current input speed to the machine and the undisturbed current velocity, it was considered the machine itself as an obstacle transforming kinetic energy of the marine current to potential energy of pressure, applying as a first approximation the Bernoulli theorem. Thus, considering a point in the undisturbed current and a point of the input section, it results that the difference between the two velocities (Δv) and the differential pressure (Δp) are connected by the following relationship:

$$\Delta v = \sqrt{\Delta p / 500}$$

The power is equal to the angular velocity for the moment of the fluid on the rotor (blades and pivot). In particular, the average power (P) employed on the axle is:

$$P = \frac{1}{T} \int_T^{t+T} \left(\int_A p v dA \right) dt = \frac{\omega}{T} \int_T^{t+T} M dt$$

where T is the rotation cycle period, v velocity vector, p pressure, (A) the total area of surface of the impeller in contact with water and, finally, the impeller rotation speed ($\omega = v/r$, where r represents the vector of the relative position of a point of the impeller in respect to the barycenter of the pivot). The formula can be expressed as a function of the twisting motion M.

According to the usual calculation procedures applied for fluidic analysis of turbomachine, the time cycle is constant and defined as a function of the portion of round angle (in degrees) covered by the impeller motion in a single cycle. A value of 3.0° was chosen as cycle period (reference values 0.5° - 3.0°) and, for each cycle, a maximum of 3 interactions have been carried out (reference values: 3-5).

e) **Numeric simulations**

The fluidic modeling of each operational point of the machine is composed of two subsequent simulations.

The first, called “start-up simulation”, simulates the interaction between stator and rotor with a “frozen rotor” scheme. This type of modeling is faster, even though less precise, and can provide in shorter time fluidic fields sufficiently accurate to initialize the out-and-out simulation. A stationary solution is obtained. At this first step the simulated time can be fixed equal to the rotation cycle (T). The second simulation is a transient one and it considers an explicit and complete modeling of the interaction between stator and rotor, (“transient stator-rotor interface model”). The simulation ends when the results converge towards a cyclic stationary solution. As a first approximation the time of simulation can be fixed to about $3T$.

The first modelling analyzed consists in checking assigned operational points, while the following in defining the best operational interval, bound to respect the background conditions fixed by the undisturbed current. Velocity and pressure fields and the estimated power are then analyzed in stationary regime (cyclic). The reference flow is imposed to $Q_0=3080$ kg/s, with rotating velocity $\omega_0=8.07$ rad/s (machine data provided by the manufacturer).

- I) The evaluation of assigned operational points consists in estimating the power provided to the impeller, with flow and angular velocity of rotor fixed. It is mainly a test, provided that the point (interval) of operation is representative of working conditions, otherwise this simulation simply represents a first evaluation of the power. The fields of pressure and velocity are analyzed in detail.

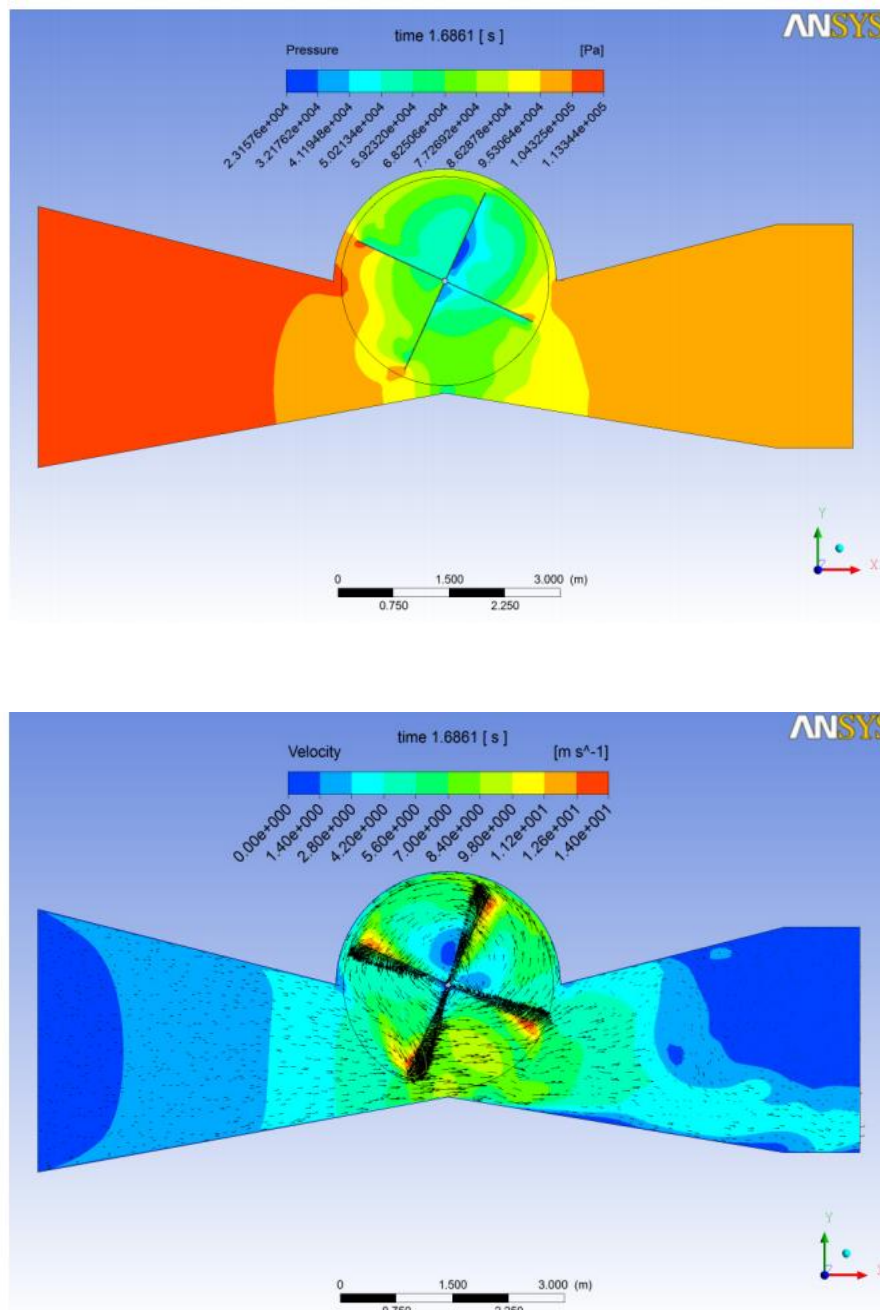


Figure 72. Example of Pressure field (top) and Velocity field (bottom) for an assigned operating point [CFX, ANSYS from [30]]

- II) The research of the optimal operational interval of the turbine consists in defining the interval of operational points whose power or efficiency reaches their maximum values. It is then a bi-dimensional process (in function of flow and angular velocity) bound to respect the background conditions, such as the differential of pressure (input-output) compatible with the velocity of the undisturbed current.

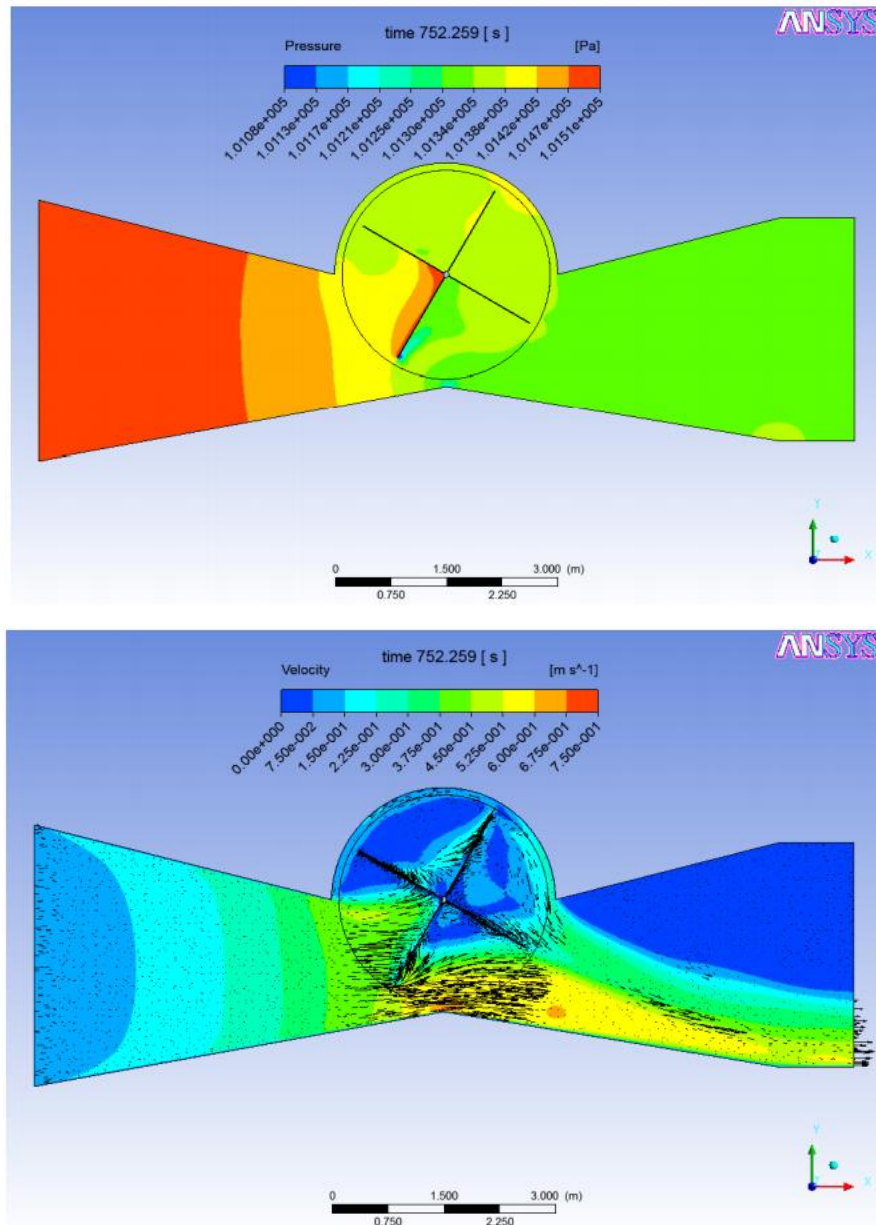


Figure 73. Example of Pressure field (top) and Velocity field (bottom) for an estimated (optimal) operating point [CFX, ANSYS from [30]]

f) Analysis of the results

The study performed could estimate the interchanged power between fluid and impeller of the machine. Given its specific operational point, the provided power presented a negative sign: the fluid absorbs power from the machine.

Because of the preliminary characteristics of this study, the search for the optimum was performed only through preliminary simulations. For a more detailed analysis, all the operational points relative to values of undisturbed current between 0.5 m/s and 1.5-2.0 m/s (reference interval) should be studied.

In this context, the estimated optimal operational point maximizing the power gathered by the axle is characterized by $\omega = \omega_0/200$ and about $Q = Q_0/5$, with velocity of undisturbed current equal to 1.5 m/s and power negligible ($P = 3$ W). However, a more detailed analysis was performed at an operational point with velocity of undisturbed current of 0.8 m/s, closer to the average of the interval of reference values ($\omega = \omega_0/400$, $Q = Q_0/10$). The power provided was even lower (about 0.4 W), and the impeller almost stopped (1 complete rotation every 300 sec).

From these data, it was clear that the configuration studied was too dissipative and not adequate to operate at such current velocities. Instead, the evolution of power in time showed interesting qualitative characteristics, those proper of operational points typical of hydraulic turbines (conceived and designed appropriately), such as reaching the cyclic stationary regime in relatively short period of time, and the low variation in time of the provided power.

5. CONCLUSIONS

[7] *“The recent climate change conference agreed global targets for climate change, and through these drivers of policy, world-wide commitment to reducing carbon emissions and sourcing renewable energies is strengthened year on year. Marine energy and specifically wave and tidal energy are a significant part of the renewable energy of the future, as a significant part of the overall energy infrastructure, and as a key clean and secure component of the energy mix.”*

Some of the main challenges remaining in tidal currents energy are the reliability of devices operating in the marine environment, their installation and maintenance and their impact on the resources. Tidal energy has seen the greatest development advance in recent years and the first large arrays of tidal stream converters are under development in the UK. The Atlantic coast presents the highest potential for oceanic energy development, but it is not the only one: very productive sites exist in the Mediterranean Sea as well (e.g., the Strait of Messina in Italy). Tidal energy technologies are generally much further advanced than wave energy technologies and they have arguably converged into a single design category, namely the horizontal-axis turbine. Current energy, though, lacks a specific procedure universally recognized to analyze the energy producibility. For this reason, a quantitative reference map of Italian seas was completed at first. Such map was completed starting with a classification of the seas as a function of the flow of power in synoptic scale based on the data provided by the European project *MyOcean*. This solution is based on verified data and easily available, but its resolution is low in space and time. Also, marine-weather data unavailability was a major critical issue; in particular, detailed data of currents in low and medium scale was necessary to perform this kind of study. Starting from the known data, which are assumed as background conditions and gathered from the reference map, an analysis procedure was developed. Placing one or more power generating turbines, with known useful working area and efficiency, in the three-dimensional directional field, it is possible to evaluate the quantity of producible energy and to estimate the optimal position and orientation of the turbines (through WebGIS Tritone software), considering the possible seasonal variations of the currents. The peculiar conditions of low intensity currents, typical of Italian coastline, limit the use of conventional turbines, as shown in the retrieved map. Anyway, even if limited to the examined sites, this study showed that the energy production from the sea is feasible even with the limiting conditions of Italian shores and can constitute an important resource of renewable energy, if advanced technologies and innovative power generating machines will be applied. Therefore, a simple numerical procedure of machine fluidic analysis was proposed: it was designed on a CFD approach and it permits the modelling of rotating bodies as well. Such procedure was utilized to study a simplified model of a turbine potentially installed in a marine environment and, despite the results of the model showed its inefficiency for what concerns the necessary requirements for marine usage, the described procedure, given its general characteristics, represents a simple basic numerical tool to verify and select turbines and innovative machinery for energy exploitation of marine currents. Hence, the need of a software specifically developed for and dedicated to turbine analysis (turbomachinery modules or numerical schemes).

It is possible to conclude that creating a map of energy potential, which can possibly be analyzed through GIS tools, and the definition of models and procedures supporting the analysis, represent a valid system support to a detailed study of the potential capacity of power generation from marine currents, also considering the impact of the machine employed.

In conclusion,

“Tidal energy is a fast moving and exciting sector, with complex unresolved research challenges and many unknown and open questions remaining. It is a fascinating sector to be involved in and what we will see in twenty years is likely to be very different from the technologies we see under development today. Despite these complex challenges, we can expect to see tidal industry move through and beyond research and into development in the next decades and be part of the future for us all.” [7]

6. MATLAB SCRIPTS

Chap. 3.4.1

```
clc
clear all
close all

% rho_w_sum = 998; % water density in summer [kg/m^3]
% rho_w_win = 1030; % water density in winter [kg/m^3]
rho_w = 1005; % average water density [kg/m^3]

ncfile='data.nc'; % enter NetCDF file name (extension *.nc)
ncinfo(ncfile);
ncdisp(ncfile);

depth = ncread(ncfile,'depth'); % [m]
time = ncread(ncfile,'time'); % [min]
uo = ncread(ncfile,'uo'); % eastward sea water velocity [m/s]
vo = ncread(ncfile,'vo'); % northward sea water velocity [m/s]
lat = ncread(ncfile,'lat');
lon = ncread(ncfile,'lon');

Fp_tot = 0;
% average annual specific power flow for each depth
for i=1:16
    for j=1:12

        uo_m = uo(:,:,i,j);
        vo_m = vo(:,:,i,j);

        UV_m = (uo_m.^2 + vo_m.^2).^(1/2); % sea water velocity [m/s]
        UV3_m = UV_m.^3;

        Fp_m = UV3_m.*(0.5*rho_w); % specific power flow [W/m^2]
        Fp_tot = Fp_tot + Fp_m;

    end
    Fp_ave(:,:,i) = Fp_tot./12;
    Fp_tot = 0;
end
```

```

% mean annual value
for k=1:16
    Fp_mean_all_part = nanmean(Fp_ave(:,:,k));
    Fp_mean_med(k,1) = nanmean(Fp_mean_all_part);
End

% max value (from annual average)
for z=1:16
    [Fp_ave_max_part, long_max] = max(Fp_ave(:,:,z));
    [Fp_ave_max(z,1), lat_max(z,1)] = max(Fp_ave_max_part);
end

% average annual specific power flow near the coast
d = 2; % depth value [1=1.018, 2=3.166, ...]
Fp_bool = isnan(Fp_ave(:,:,d));
coast_idx = zeros(1,2);
k=1;
fl=0;
Fp_coast = NaN(size(Fp_ave(:,:,d),1),size(Fp_ave(:,:,d),2));

for i=1:size(Fp_ave(:,:,d),2)
    fl=0;
    for j=1:size(Fp_ave(:,:,d),1)
        if(j==length(lon))
            fl = 1;
        end
        if(fl==0)
            if(Fp_bool(j,i) == 1 & Fp_bool(j+1,i)==0)
                coast_idx(k,:) = [j+1, i];
                Fp_coast(j+1,i) = Fp_ave(j+1,i,d);
                k=k+1;
            if(j<length(lon)-1 & Fp_bool(j+2,i)==0)
                coast_idx(k,:) = [j+2, i];
                Fp_coast(j+2,i) = Fp_ave(j+2,i,d);
                k=k+1;
            if(j<length(lon)-2 & Fp_bool(j+3,i)==0)
                coast_idx(k,:) = [j+3, i];
                Fp_coast(j+3,i) = Fp_ave(j+3,i,d);
                k=k+1;
            end
        end
    end
end
end

```

```

    if(Fp_bool(j,i) == 0 & Fp_bool(j+1,i)==1)
        coast_idx(k,:) = [j, i];
        Fp_coast(j,i) = Fp_ave(j,i,d);
        k=k+1;
    if(j>1 & Fp_bool(j-1,i)==0)
        coast_idx(k,:) = [j-1, i];
        Fp_coast(j-1,i) = Fp_ave(j-1,i,d);
        k=k+1;
    if(j>1 & Fp_bool(j-2,i)==0)
        coast_idx(k,:) = [j-2, i];
        Fp_coast(j-2,i) = Fp_ave(j-2,i,d);
        k=k+1;
    end
end
end
else
    continue
end
end
end
end

for i=1:size(Fp_ave(:, :, d),1)
    fl=0;
    for j=1:size(Fp_ave(:, :, d),2)
        if(j==length(lat))
            fl = 1;
        end
        if(fl==0)
            if(Fp_bool(i,j) == 1 & Fp_bool(i,j+1)==0)
                coast_idx(k,:) = [i, j+1];
                Fp_coast(i,j+1) = Fp_ave(i,j+1,d);
                k=k+1;
            if(j<length(lat)-1 & Fp_bool(i,j+2) == 0)
                coast_idx(k,:) = [i, j+2];
                Fp_coast(i,j+2) = Fp_ave(i,j+2,d);
                k=k+1;
            if(j<length(lat)-2 & Fp_bool(i,j+3) == 0)
                coast_idx(k,:) = [i, j+3];
                Fp_coast(i,j+3) = Fp_ave(i,j+3,d);
                k=k+1;
            end
        end
    end
end
end

```

```

if(Fp_bool(i,j) == 0 & Fp_bool(i,j+1)==1)
    coast_idx(k,:) = [i, j];
    Fp_coast(i,j) = Fp_ave(i,j,d);
    k=k+1;
if(j>1 & Fp_bool(i,j-1) == 0)
    coast_idx(k,:) = [i, j-1];
    Fp_coast(i,j-1) = Fp_ave(i,j-1,d);
    k=k+1;
if(j>1 & Fp_bool(i,j-2) == 0)
    coast_idx(k,:) = [i, j-2];
    Fp_coast(i,j-2) = Fp_ave(i,j-2,d);
    k=k+1;
end
end
end
else
    continue
end
end
end
end

```

```

figure(1)
imagesc(lon,lat,transpose(Fp_ave(:, :, d)))
axis xy tight
colormap jet
colorbar
caxis([-5 350])
xlabel ('Longitude')
ylabel ('Latitude')
title ('Specific average Power flow [W/m^2]')

```

```

figure(2)
barh(Fp_mean_med, 'blue')
xlabel ('Specific power flow [W/m^2]')
ylabel ('Depth [m]')
set (gca, 'YDir', 'reverse')
yticks([1 2 3 4 5 6 7 8 9 10 11 12 13 14 15 16]) % 16 depth levels
yticklabels({'1.018','3.166','5.465','7.920','10.537','13.318','16.271','19.398','22.706','26.201','29.886','33.768','37.852','42.145','46.652','51.380'}) % substitution of depth levels with their correspondent values in meters

```

```

figure(3)
barh(Fp_ave_max, 'red')
xlabel ('Specific power flow [W/m^2]')
ylabel ('Depth [m]')
set (gca, 'YDir', 'reverse')
yticks([1 2 3 4 5 6 7 8 9 10 11 12 13 14 15 16])
yticklabels({'1.018','3.166','5.465','7.920','10.537','13.318','16.271','19.398','22.706','26.201','29.886','33.768','37.852','42.145','46.652','51.380'})

```

```

figure(4)
imagesc(lon,lat,transpose(Fp_coast(:,:)))
axis xy tight
colormap jet
colormapeditor
colorbar
caxis([-5 350])
xlabel ('Longitude')
ylabel ('Latitude')
title ('Specific average Power flow [W/m^2]')

```

```

uo_months = squeeze(uo);
vo_months = squeeze(vo);
UV_tot = 0;

```

```

for i=1:12

```

```

    uo_month = uo_months(:,i);
    vo_month = vo_months(:,i);
    UV_month = (uo_month.^2 + vo_month.^2).^(1/2); % sea water velocity [m/s]

```

```

    NaN_idx = isnan(UV_month);
    UV_month(NaN_idx)=0;

```

```

    [r,c]= find(UV_month>0.7); % cut-in value = 0.7 m/s

```

```

    UV_tot = UV_tot + UV_month;

```

```

end

```

```

UV_ave = UV_tot./12
% row long, column lat
% Strait of Messina -> r=543, c=194 -> UV_ave(543,194)= 0.7383 m/s

```

```

% UV3_ave = UV.^3;
% Fp = UV3_ave.*(0.5*rho_w); % specific power flow [W/m^2]

```


7. REFERENCES

- [1] OES – *An international vision for Ocean Energy*, 2017
- [2] OES – *Spotlight on Ocean Energy*, 2018
- [3] E. Segura, R. Morales, J. A. Somolinos *A strategic analysis of tidal current energy conversion systems in the European Union* - Appl. Energy 212, pp. 527-551, 2018
- [4] D. Magagna, A. Uihlein *Ocean energy development in Europe: Current status and future perspectives* - International Journal of Marine Energy 11, pp. 84-104, 2015
- [5] J. Zhang, L. Moreau, M. Machmoum, P. E. Guillerme *State of the art in tidal current energy extracting technologies* - IEEE First International Conference on Green Energy, pp. 1-7, 2014
- [6] J. M. Blanco Ilzarbe, J. Amaral Teixeira *Recent Patent on Tidal Power Extraction Devices*, 2009
- [7] D. Greaves, G Iglesias *Wave and Tidal Energy* - Wiley, 2018
- [8] Spicer, Preston *Tide and Storm Surge Dynamics in Estuaries of Variable Morphology* - Electronic Theses and Dissertations 2993, 2019
- [9] S. H. E. Abdel Aleem, A. F. Zobaa, A. M. Ibrahim *Mathematical analysis of the turbine coefficient of performance for tidal stream turbines*, 2014
- [10] S. B. Elghali, M. E. H. Benbouzid, J. F. Charpentier *Marine tidal current electric power generation technology: State of the art and current status* - IEEE International Electric Machines & Drives Conference 2, pp. 1407-1412, 2007
- [11] ITPENERGISED Earth. Smart. Solutions *Tidal Stream Industry Update* - States of Jersey, 2019
- [12] *State-of-the-art of tidal projects* - TETHYS, 2019
- [13] *SR 2000 - A safe access floating tidal turbine* - Scotrenewables Tidal Power Ltd, 2017
- [14] *Operational principles* (online) - Aqua-RET Project, 2012
- [15] Handouts *Wind Power Systems* F. Spertino (Dip. Energia Politecnico di Torino), 2019
- [16] B. Whitby, S. Member, C. E. Ugalde-Loa *Performance of Pitch and Stall Regulated Tidal Stream Turbines* - IEEE Trans. Sustain. Energy 5, pp. 64-72, 2014
- [17] M. DeGraaf, J. Mather *The potential of tidal in stream energy conversion turbines* - University of Pittsburgh Swanson School of Engineering, 1-10, 2010
- [18] C. A. Douglas, G. P. Harrison, J. P. Chick *Life cycle assessment of the SeaGen marine current turbine* - Journal of Engineering for the Maritime Environment, 222, 1-12, 2008
- [19] J. A. C. Orme, I. Masters, C. Mima *Analysis and comparison of support structure concepts for tidal stream turbines*, 2006
- [20] Y. Li, H. K. Florig *Modeling the operation and maintenance costs of a large scale tidal current turbine farm* - IEEE OCEANS, pp. 1-6, 2006

- [21] D. V. Val, L. Chernin, D. V. Yurchenko *Reliability analysis of rotor blades of tidal stream turbines* - Reliability Engineering & System Safety 121, 26-33, 2014
- [22] K. Touimi, M. Benbouzid, P. Tavner *Tidal stream turbines: With or without a Gearbox?* - Ocean Engineering 170, 74-88, 2018
- [23] M. DeGraaf, J. Mather *The potential of tidal in stream energy conversion turbines* - University of Pittsburgh Swanson School of Engineering, 1-10, 2010
- [24] OES - *International Levelised Cost Of Energy for Ocean Energy Technologies*, 2015
- [25] G. L. Zupone, M. Amelio, S. Barbarelli, G. Florio, N. M. Scornaienchi, A. Cutrupi *Levelized Cost of Energy: A first evaluation for a self balancing kinetic turbine* - Energy Procedia 75, 283-293, 2015
- [26] S. Astariz, A. Vazquez, G. Iglesias *Evaluation and comparison of the levelized cost of tidal, wave, and offshore wind energy* - Journal of Renewable and Sustainable Energy 7, 2015
- [27] D. Magagna, R. Monfardini, A. Uihlein *JRC Ocean Energy Status Report*, 2016
- [28] F. Salvatore (CNR), G. Sannino & A. Carillo (ENEA), M. Peviani & L. Serri (RSE) *Energia dalle correnti marine*, 2017
- [29] R. Guandalini, G. Agate, M. Peviani, F. Carli *Valutazione del potenziale di producibilità energetica dal moto ondoso e dalle correnti marine dei mari italiani* - (Rapporto RSE n. 11000312), 2011
- [30] R. Guandalini, G. Agate, A. Amicarelli, G. Stella *Mappe di producibilità energetica dal moto ondoso e dalle correnti marine dei mari italiani* - (Rapporto RSE 12000352), 2012
- [31] S. Benelghali, R. Balme, K. Le Saux, M. Benbouzid, J. F. Charpentier, F. Hauville *A Simulation Model for the Evaluation of the Electrical Power Potential Harnessed by a Marine Current Turbine* - IEEE Journal of Oceanic Engineering, Institute of Electrical and Electronics Engineers, 32 (4), pp.786-797, 2007
- [32] M. M. Elzalabani, F. H. Fahmy, A. El-Shafy, A. Nafeh, G. Allam *Modelling and Simulation of Tidal Current Turbine with Permanent Magnet Synchronous Generator* - TELKOMNIKA Indonesian Journal of Electrical Engineering, Vol. 13 No. 1, pp. 57-64, 2015
- [33] A. Bargagli, G. Sannino (ENEA) *Modello di circolazione dello Stretto di Messina* - Report Ricerca di Sistema Elettrico, 2012

➤ Sitography

Search and analyze patents – PatentInspiration → <https://www.patentinspiration.com/>

Welcome to Aqua-RET → <https://aquaret.com/>

SIMEC Atlantis Energy | A global sustainable energy company → <https://simecatlantis.com/>

ResearchGate | Find and share research → <https://www.researchgate.net/>

ScienceDirect.com | Science, health and medical journals, full text articles and books → <https://www.sciencedirect.com/>

CMEMS → <https://marine.copernicus.eu/>

ECMWF | Advancing global NWP through international collaboration → <https://www.ecmwf.int/>

ISPRA → <https://www.isprambiente.gov.it/it>

TRITONE → <http://tritone.rse-web.it/map.phtml>

Ocean Renewable Power Company (ORPC) → <https://orpc.co/>

Engineering Simulation & 3D Design Software | Ansys → <https://www.ansys.com/>

MathWorks – MATLAB & Simulink → <https://it.mathworks.com/>

8. ACKNOWLEDGMENTS

I would like to thank my supervisor Doctor Giovanni Bracco and my co-supervisor Professor Giuliana Mattiazzo for the opportunity they have given me and Giulia for the help she has provided.

I am grateful to my family for giving me this possibility, for their support in my choices, for their love, patience and understanding.

I want to thank my friends, with whom I grew up, with whom I lived and with whom I studied, who gave me strength and sometimes even distracted me, but who have remained at my side both in good and bad times.

To myself, to where I come from, to my sacrifices and to my future...

...my work here is (almost) done!